10-28-2009

# Environment, Channel, and Interference Awareness for Next Generation Wireless Networks

Serhan Yarkan
*University of South Florida*

Environment, Channel, and Interference Awareness for Next Generation Wireless Networks

by

Serhan Yarkan

A dissertation submitted in partial fulfillment
of the requirements for the degree of
Doctor of Philosophy
Department of Electrical Engineering
College of Engineering
University of South Florida

Major Professor: Hüseyin Arslan, Ph.D.
Dmitry B. Goldgof, Ph.D.
Joseph Mitola III, Ph.D.
Chris P. Tsokos, Ph.D.
Paris H. Wiley, Ph.D.

Date of Approval:
October 28, 2009

Keywords: cellular networks, cognitive radio, line–of–sight identification, vertical handoff

**DEDICATION**

To my family.

## ACKNOWLEDGEMENTS

First of all, I would like to thank Dr. Hüseyin Arslan for his encouragement, support, and supervision throughout my study at University of South Florida (USF). I wish to thank individually Dr. Dmitry B. Goldgof, Dr. Joseph Mitola III, Dr. Chris P. Tsokos, and Dr. Paris H. Wiley for agreeing to serve in my committee; and for their valuable time, feedback, and recommendations. I am also thankful to Dr. Gangaram Ladde for chairing my defense. I would like to express my sincere appreciation to Dr. Arthur Dave Snider, Dr. James Leffew, Becky Brenner, and Irene Wiley from the Electrical Engineering Department at USF who have been always helpful and understanding.

I would like to extend my special thanks to Dr. Koon Hoo Teo at Mitsubishi Electric Research Laboratories (MERL) who supported my research financially for the majority of my Ph.D. duration. Also, I would like to thank Dr. Amine Maaref for his precious help and time during my time at MERL and thereafter. I am also grateful to my colleagues at USF and to all my friends at Wireless Communications and Signal Processing (WCSP) group whose each and every member contributed a lot to me technically. However, I would like to recognize in a special way, Dr. Hasari Çelebi, Ali Görçin, Dr. İsmail Güvenç, Dr. Hisham Abdelaziz Mahmoud, Mustafa Emin Şahin, and Dr. Tevfik Yücek who, during most of my time at USF, helped me in every aspect.

Special thanks go to Turkish community in Tampa. I would like to mention Salih Erdem, Salim Erdem, Akif Uzuner, Şener Gültekin, İsmail Bütün, Ali Emre Erçelebi, Ali Rıza Ekti, Özgür Yürür for their continuous support. Although not residing in Tampa, I would like to extend my thanks also to Dr. Halim Zaim who provided me with his support and to Dr. Celal Çeken with whom I had opportunity to meet and share many great things in a short period of time.

Last but by no means least, I would like to express my deepest gratitude to my family to whom this work is dedicated. I will be forever indebted to my parents, my grandparents, and my sister. Without their immense sacrifice, their unconditional support, and their profound wisdom I would not be here today...

## TABLE OF CONTENTS

## LIST OF TABLES

## LIST OF FIGURES

## LIST OF ACRONYMS

| | |
|---|---|
| 3GLTE | Third Generation Long Term Evolution |
| ACC | autocorrelation coefficient |
| ACI | adjacent channel interference |
| ADC | analog to digital converter |
| AI | artificial intelligence |
| AoA | angle–of–arrival |
| AP | access point |
| APCV | access point candidacy value |
| ARQ | automatic repeat request |
| AWGN | additive white Gaussian noise |
| BCCH | broadcast control channel |
| BER | bit–error–rate |
| BS | base station |
| C/I | carrier–to–interference ratio |
| CCI | co–channel interference |
| CDMA | code division multiple access |
| CINR | carrier–to–interference–plus–noise ratio |
| CMI | cross–modulation interference |
| COST | European Co–operation in the field of Scientific and Technical research |
| CP | cyclic prefix |
| CR | cognitive radio |
| CRC | cyclic redundancy check |
| CSMA | carrier sense multiple accessing |

| | |
|---|---|
| CSMA/CA | carrier sense multiple accessing/collision avoidance |
| DEM | digital elevation model |
| DSSS | direct–sequence spread–spectrum |
| ED | energy detection |
| FDD | frequency division duplexing |
| FER | frame–error–rate |
| FFT | fast Fourier transform |
| FH | frequency hopping |
| FILO | first–in–last–out |
| FMADM | fuzzy multiple attribute decision making |
| FRO | frequency reuse of one |
| GIS | Geographical Information System |
| GPS | Global Positioning System |
| GSM | Global System for Mobile |
| HDT | handoff decision table |
| HMM | hidden Markov model |
| ICI | inter–cell interference |
| IFI | inter–frame interference |
| IPI | inter–pulse interference |
| IrDA | Infra–red Data Association |
| ISI | inter–symbol interference |
| ITU–R | International Telecommunication Union – Radiocommunications |
| KRS | Knowledge Representation Space |
| LAN | local area network |
| LCR | level crossing rate |
| LOS | line–of–sight |
| MAC | medium access control |

| | |
|---|---|
| MAI | multi–access interference |
| MERL | Mitsubishi Electric Research Laboratories |
| MES | minimum $E\{\mathbf{K}\}$ scheduler |
| MIMO | multi–input multi–output |
| MOS | mean opinion score |
| MS | mobile station |
| NBI | narrow–band interference |
| NGWN | next generation wireless network |
| NLOS | non–line–of–sight |
| OFDM | orthogonal frequency division multiplexing |
| OFDMA | orthogonal frequency division multiple access |
| OLOS | obstructed line–of–sight |
| OSI | open systems interconnection reference |
| PDA | personal digital assistant |
| PDF | probability density function |
| PDP | power delay profile |
| PHY | physical layer |
| PMF | probability mass function |
| PN | pseudo noise |
| QoS | quality of service |
| RAT | radio access technology |
| RF | radio frequency |
| RKRL | Radio Knowledge Representation Language |
| RMS | root–mean–squared |
| RSRP | reference symbol received power |
| RSS | received signal strength |
| RSSI | received signal strength indicator |

| | |
|---|---|
| SDR | software–defined radio |
| SER | symbol–error–rate |
| SIM | spatial interpolation method |
| SINR | signal–to–interference–plus–noise ratio |
| SIR | signal–to–interference ratio |
| SMT | smart mobile terminal |
| SNR | signal–to–noise ratio |
| TDMA | time division multiple access |
| ToA | time–of–arrival |
| PM | proposed method |
| TTI | transmission time interval |
| UE | user equipment |
| UMTS | Universal Mobile Telecommunications System |
| USF | University of South Florida |
| UWB | ultra–wide band |
| VHDF | vertical handoff decision function |
| WBI | wide–band interference |
| WCSP | Wireless Communications and Signal Processing |
| WGN | white Gaussian noise |
| WiFi | wireless fidelity |
| WiMAX | Worldwide Interoperability for Microwave Access |
| WLAN | wireless local area network |
| WMAN | wireless metropolitan area network |
| XPD | cross polarization discrimination |

**ENVIRONMENT, CHANNEL, AND INTERFERENCE AWARENESS FOR NEXT GENERATION WIRELESS NETWORKS**

**Serhan Yarkan**

## ABSTRACT

Wireless communication systems have evolved substantially over the last two decades. The explosive growth of the wireless communications market is expected to continue in the future, as the demand for all types of wireless services is increasing. Beside providing higher data rates, next generation wireless networks (NGWN) are expected to have advanced capabilities such as interoperability, efficient spectrum utilization along with a wide variety of applications over different domains (*e.g.*, public safety and military, aeronautical networks, femtocells, and so on) to the mobile users while serving as many users as possible.

However, these advanced capabilities and services must be achieved under the constraint of limited available resources such as electromagnetic spectrum and power. In addition, NGWNs (and nodes within) need to modify themselves under rapidly changing conditions such as wireless propagation channel characteristics, traffic load, and so on. Moreover, NGWNs are expected to optimize their parameters by evaluating their experiences in the past. All of these characteristics imply that NGWNs should be equipped with *cognitive* capabilities including sensing, *awareness*, adaptation and responding to changing conditions along with learning about the past experiences.

In this dissertation, environment, channel, and interference awareness are investigated in detail for NGWN. Methods for being aware of environment, channel, and interference are provided along with some possible ways of adapting several design parameters of NGWNs. In addition, cross–layer optimization issues are addressed from the perspective of both recently emerging technology called cognitive radio (CR) and NGWN.

# CHAPTER 1

# INTRODUCTION

Wireless communication systems have evolved substantially over the last two decades. The explosive growth of the wireless communications market is expected to continue in the future, as the demand for all types of wireless services is increasing. Beside providing higher data rates, next generation wireless networks (NGWN) are expected to have advanced capabilities such as interoperability, efficient spectrum utilization along with a wide variety of applications over different domains (*e.g.*, public safety and military, aeronautical networks, femtocells, and so on) to the mobile users while serving as many users as possible.

However, these advanced capabilities and services must be achieved under the constraint of limited available resources such as electromagnetic spectrum and power. In addition, NGWNs need to modify themselves under rapidly changing conditions such as wireless propagation environment characteristics, traffic load, and so on. Moreover, NGWNs are expected to optimize their parameters by evaluating their experiences in the past. All of these characteristics imply that NGWNs should be equipped with *cognitive* capabilities including sensing, awareness, adaptation and responding to changing conditions along with learning about the past experiences. It is important to state that a recently emerging technology called cognitive radio (CR) is considered to possess the same advanced capabilities pointing out a convergence of capabilities for future wireless communications systems. Such a convergence is not a coincidence, because the evolution of wireless communications has always been toward a system that possesses comprehensive adaptation and optimization capabilities. Hence, a wireless communications system equipped with advanced cognitive capabilities can be considered to be the common purpose of all future system designs. Figure 1.1 illustrates this convergence along with desired objectives and some sample applications.

Among the aforementioned capabilities, awareness has a special place because it interprets the data/information fed by sensing and converts into knowledge for adaptation and for possible learning purposes. In other words, awareness establishes the link between observable quantities and available

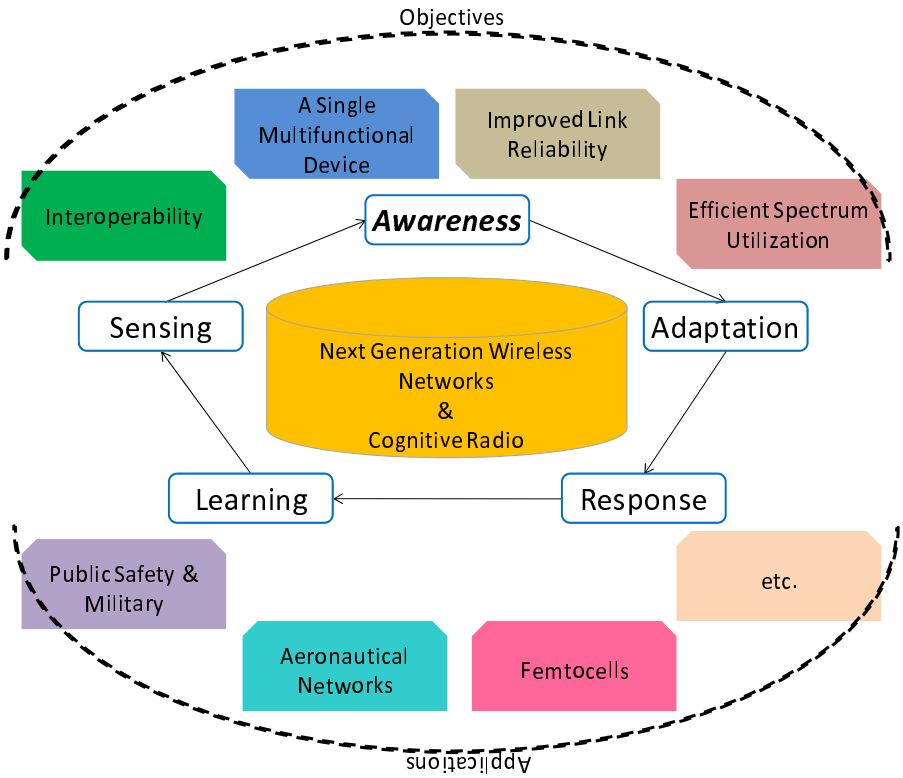


Figure 1.1 Fundamental functionalities of NGWN and CR along with main objectives and sample applications.

adaptation parameters defined in the system of interest. From the perspective of NGWNs, there are various quantities to observe and many parameters to adapt for better performance. Traditional protocol stack defined by open systems interconnection reference (OSI) layers provides a formal way of defining quantities to observe and parameters to adapt, and gives an insight into the connection between them. In OSI, physical layer (PHY) is the interface between physical propagation environment and radios themselves within NGWNs. From this point of view, PHY can be considered to be the place in which major awareness functionalities are held.

When a wireless signal is transmitted, it is altered by the wireless channel and reaches at receiver after being exposed to several other impairments such as noise and interference. The impact of wireless channel on the signal transmitted depends on several characteristics of physical propagation environment such as its topographical structure, having line–of–sight (LOS), and so on. Note that environment, channel, and other ambient impairments such as interference and noise are concepts which cannot be directly controlled by radios since all of them reside between the transmitter and receiver PHY layers. Therefore, in NGWNs, being aware of the operating environment, of wireless

channel, and of interference (along with noise) lie in the heart of a successful design and are key to improved performance.

In this dissertation, environment, channel, and interference awareness are investigated in detail for NGWN. Methods for being aware of environment, channel, and interference are provided along with some possible ways of adapting several design parameters of NGWNs. Since there is an obvious convergence in the characteristics of NGWN and of recently emerging technology CR in terms of awareness, CR perspective is also investigated in detail.

### 1.1 Dissertation Outline

In this dissertation, a detailed investigation on environment, channel, and interference awareness for NGWNs is established; critical issues and challenges are identified and addressed. Considering the technological convergence in the evolution of wireless systems, awareness is also considered from the perspective of CR. Following the introduction (Chapter 1), the outline of this dissertation consists of the following elements:

- An outline of environment awareness concept and propagation environment classification (Chapter 2)
- A detailed study of channel awareness for NGWNs and CR (Chapters 3 – 4),
- Examination of interference awareness including its identification and use in different OSI layers (Chapters 5 – 8)

The conceptual relationship between these elements are given in Figure 1.2. It is worth mentioning that even though the physical impact of both wireless channel and interference takes place in the propagation environment, each individual element has its own unique conceptual characteristics and properties. Many of the propagation characteristics of wireless channel are determined by the physical environment. However, for the same physical propagation environment, wireless channel treats signals differently depending on the transmitted waveforms. For instance, multipath characteristics of a physical propagation environment for ultra–wide band (UWB) systems differ from those for narrow–band systems because of the difference in time resolutions of transmitted waveforms. The same argument holds for interfering signals as well since different interfering waveforms yield different effects. For instance, an interfering signal of a different type from that of the desired signal can be interpreted either as wide–band interference (WBI) or as narrow–band interference

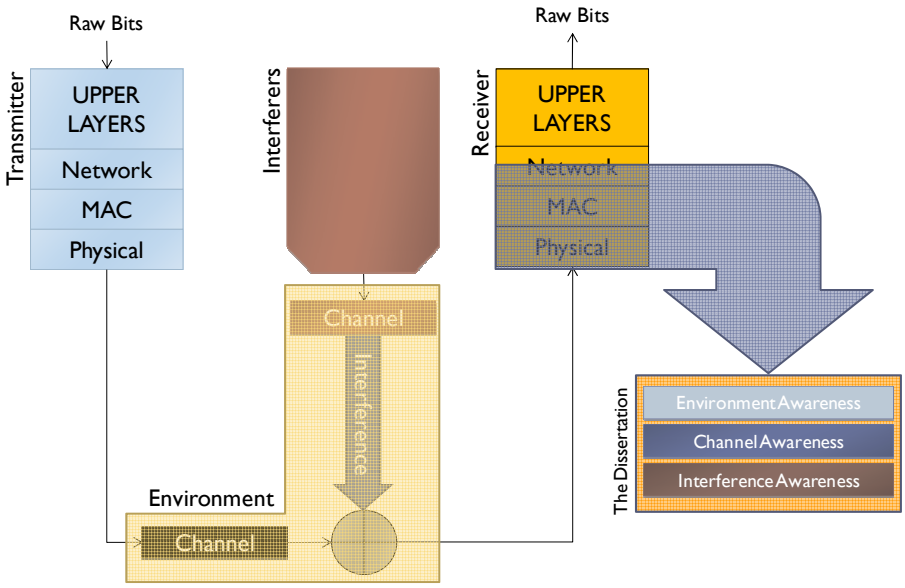


Figure 1.2 The conceptual relationships between the elements along with the relevant notions studied in this dissertation.

(NBI) depending also on the bandwidth of the desired signal. This reasoning flavors the idea of investigating the awareness for each individual elements listed above.

Considering the fact that wireless communications takes place in physical propagation environment, first the environment awareness is investigated in Chapter 2. The relationship between wireless channel parameters and physical environments along with vastly used propagation environment classes in wireless community are discussed. Several ways of being aware of environment and of their possible use are also provided. A conceptual model both for NGWNs and for CR is given along with an environment/location awareness algorithm in which environmental classes introduced within the same chapter are exploited.

Second, channel awareness is investigated in detail in Chapter 3, since the transmitter–receiver pair is connected to each other via the wireless channel. Critical wireless channel parameters are identified and listed in detail along with several measurement methods. In addition, a new method on identifying and being aware of one of the critical wireless channel parameters, namely LOS, is given in Chapter 4.

Received signal accommodates the impact not only of the wireless channel, but also of other disturbances such as interference and noise present in the propagation environment. Therefore, subsequently, interference awareness is investigated and its use is exemplified. In Chapter 5 the fun-

damental issues regarding the interference awareness in wireless communications are outlined and discussed. Next, a new method for identifying interference is given Chapter 6. In order to exemplify the use of interference awareness on different OSI layers, performance of orthogonal frequency division multiple access (OFDMA)–based voice schedulers for NGWNs in the presence of interference is investigated in detail in Chapter 7. Another example of the use of interference awareness which takes into account parameters of another OSI layer is given in Chapter 8 by considering the expected heterogeneous structure of NGWNs.

In the remainder of this chapter, a more detailed outline of the following chapters in this dissertation are introduced.

### 1.1.1 Chapter 2: Environment Awareness Toward Improved Wireless System Design for NGWN

In this chapter,[1] environment/location awareness is exploited to improve the wireless communication system design for both NGWNs and CR. It is shown that several crucial wireless channel parameters are environment dependent. In order for both the NGWNs and CR to relate a corresponding empirical model with an environment, the classification of propagation environments is outlined as well. The methods of characterizing the propagation environment are also discussed. In addition, how NGWNs and CR can carry out all these steps with the aid of a Knowledge Representation Space (KRS) along with Radio Knowledge Representation Language (RKRL) and complete its adaptation cycle are described. In the light of NGWNs, CR networks are also discussed from the perspective of disseminating the environment/location awareness information and of propagation characteristics including the effects on the network itself.

### 1.1.2 Chapter 3: Channel Awareness for Next Generation Wireless Networks

In this chapter,[2] the ability to measure, sense, learn about, and be aware of parameters related to the radio channel characteristics along with many other related aspects such as, availability of spectrum and power are investigated in detail for NGWNs. Beside the relationships between these parameters and measurements, effects on the performance including relevant challenges are given as well.

[1] Certain parts of the content of this chapter are published in [1, 2], and a patent application is filed [3].
[2] Certain parts of the content of this chapter are published in [2, 4].

### 1.1.3 Chapter 4: Identification of LOS in Time–Varying, Frequency Selective Radio Channels

In this chapter,[3] a method is proposed to identify the existence of one of the critical wireless channel parameters, namely LOS, for time–varying, frequency selective radio channels. The proposed method considers the second–order statistical characteristics of underlying process in the channel taps. Identification is established by comparing the autocorrelation coefficients of the first tap with that of any other tap when the other tap reaches its coherence time. Numerical results and related discussions are presented considering several practical scenarios.

### 1.1.4 Chapter 5: Real Time Measurements for Adaptive and CR Systems

In this chapter,[4] the importance of ability to measure, sense, learn about, and be aware of parameters related to interference are investigated in detail for NGWNs. Important measurement parameters for NGWNs and for enabling adaptive radio and CR systems along with their relationships and impacts on the performance including relevant challenges are discussed.

### 1.1.5 Chapter 6: Identification of Shadowed Fast Fading Interference in Cellular Mobile Radio Systems

In this chapter,[5] a method that identifies shadowed fast fading interference is proposed on downlink transmission for frequency division duplexing (FDD)–based cellular mobile radio communications systems. The independence of shadowing and fast fading processes is exploited along with the difference between their occurrence scales in space, and a second–order statistical approach is employed to identify the interference.

### 1.1.6 Chapter 7: Upper and Lower Bounds on Subcarrier Collision for Inter–cell Interference Scheduler in OFDMA–Based Systems: Voice Traffic

This chapter[6] investigates upper and lower bounds on subcarrier collision for inter–cell interference (ICI) schedulers in OFDMA–based wireless systems carrying voice traffic. It is shown that the amount of knowledge regarding the reserved resources in neighboring cell plays a crucial role on the performance of ICI schedulers. Also, it is proven that upper bound of subcarrier collision

[3] Certain parts of the content of this chapter are published in [5, 6].
[4] Certain parts of the content of this chapter are published in [4, 7], and a patent application is filed [8].
[5] Certain parts of the content of this chapter are published in [9] and a patent application is filed [10].
[6] Certain parts of the content of this chapter are submitted to [11] and a patent application is filed [12].

for ICI schedulers corresponds to the case which is driven by the absence of knowledge about the reserved resources in neighboring cell. On the other hand, lower bound of subcarrier collision for ICI schedulers corresponds to the case which is driven by the perfect knowledge about the reserved resources in neighboring cell. Based on the lower bound analysis, minimum expected number of collision scheduler is developed and its performance is investigated as well. Moreover, impact of scheduling period on performance of schedulers is examined. Numerical results are presented along with related discussions.

### 1.1.7 Chapter 8: Interference Aware Vertical Handoff Decision Algorithm for Quality of Service Support in Wireless Heterogeneous Networks

It is known that NGWN concept aims at collaboration of various radio access technologies in order to provide quality of service (QoS) supported and cost efficient connections at anywhere and anytime. Since the next generation wireless systems are expected to be of heterogeneous topology, traditional handoff (horizontal handoff/handover) mechanisms are not sufficient to meet the requirements of these types of networks. More intelligent vertical handoff algorithms which consider user profiles, application requirements, and network conditions must be employed in order to provide enhanced performance results for both user and network. Moreover, frequency reuse of one (FRO) seems to be the strongest candidate of deployment options for next generation wireless networks; therefore, interference conditions gains a significant attention in vertical handoff decision making process. Hence, in this chapter,[7] a fuzzy logic–based handoff decision algorithm is introduced for wireless heterogeneous networks. The parameters; data rate, received signal strength indicator (RSSI), and mobile speed are considered as inputs of the proposed fuzzy–based system in order to decide handoff initialization process and select the best candidate access point around a smart mobile terminal. Also, in contrast to the traditional fuzzy–based algorithms, the method proposed takes ambient interference power, which is referred to as interference rate, as another input to the decision process. The results show that the performance is significantly enhanced for both user and network by the method proposed.

[7] Certain parts of the content of this chapter are published in [13].

### 1.1.8 Other Works Done

Apart from the work discussed above, there are some other works that did not get into this dissertation. Although most of them are related to the elements given in Chapter 1.1, in order to keep the integrity of the text and flow, these works are not included in this dissertation. In what follows, some of them are briefly outlined.

In the frame of environmental classification discussed in Chapter 2.3, radio propagation characteristics in extreme environments such as underground mines are investigated in [14–17]. As mentioned in Chapter 3, time selectivity caused by motion in the propagation environment must be understood very well in terms of channel awareness for NGWN. An experimental study related to characterizing the impact of motion in wireless channels is established as well [18]. Similarly, electromagnetic spectrum aspect of wireless channel is studied from the perspective of opportunistic spectrum usage concept which is believed to be one of the key concepts in NGWNs [19]. In the light of interference awareness concept, reporting period for interference status is also examined in order to optimize the over–the–air signaling in NGWNs [20].

# CHAPTER 2

# ENVIRONMENT AWARENESS TOWARD IMPROVED WIRELESS SYSTEM DESIGN

## 2.1 Introduction

With the advances in digital technology, sizes of the digital devices decrease while their processing power increases. As a consequence, the newer digital devices are more powerful and even smaller compared to the older ones. By taking advantage of this shrinkage in size and exploiting the increase in processing power, communications companies are able to design a single mobile device which has several add–on functions for different purposes. For instance, currently, it is very easy to find a personal digital assistant (PDA) that has wireless communication capability beside its main purpose, which is computation. In parallel, almost all contemporary mobile phones have non–wireless applications (such as a digital camera). Currently, there are mobile devices in which Infra–red Data Association (IrDA), Bluetooth, local area network (LAN) wireless connectivity options, digital camera, and Global Positioning System (GPS) are embedded together.

In spite of this vast variety of wireless and other applications embedded in a single device, it is striking that the functions, which have the ability to provide extremely important information to each other, operate independently. This lack of cooperation stems from the fact that there is no unit which can control, coordinate, and interpret the data obtained from different functions. However, with the emergence of cognitive radio (CR), this lack of cooperation can be removed.

As an emerging technology, CR receives significant attention from both academia and industry. Nevertheless, there is no formal definition of CR on which everybody agrees. However, distinct features of CR, which are sensing, being aware of, learning, and adapting to its surrounding environment [21], allow us to describe it coarsely. Built on software–defined radio (SDR), CR is able to employ these features in its adaptation cycle with the aid of several sensors (*e.g.* GPS, light, and temperature sensors) and tools used in artificial intelligence (AI) applications (*e.g.* neural networks, hidden Markov models (HMM), genetic algorithms). Naturally, the adaptation cycle requires a com-

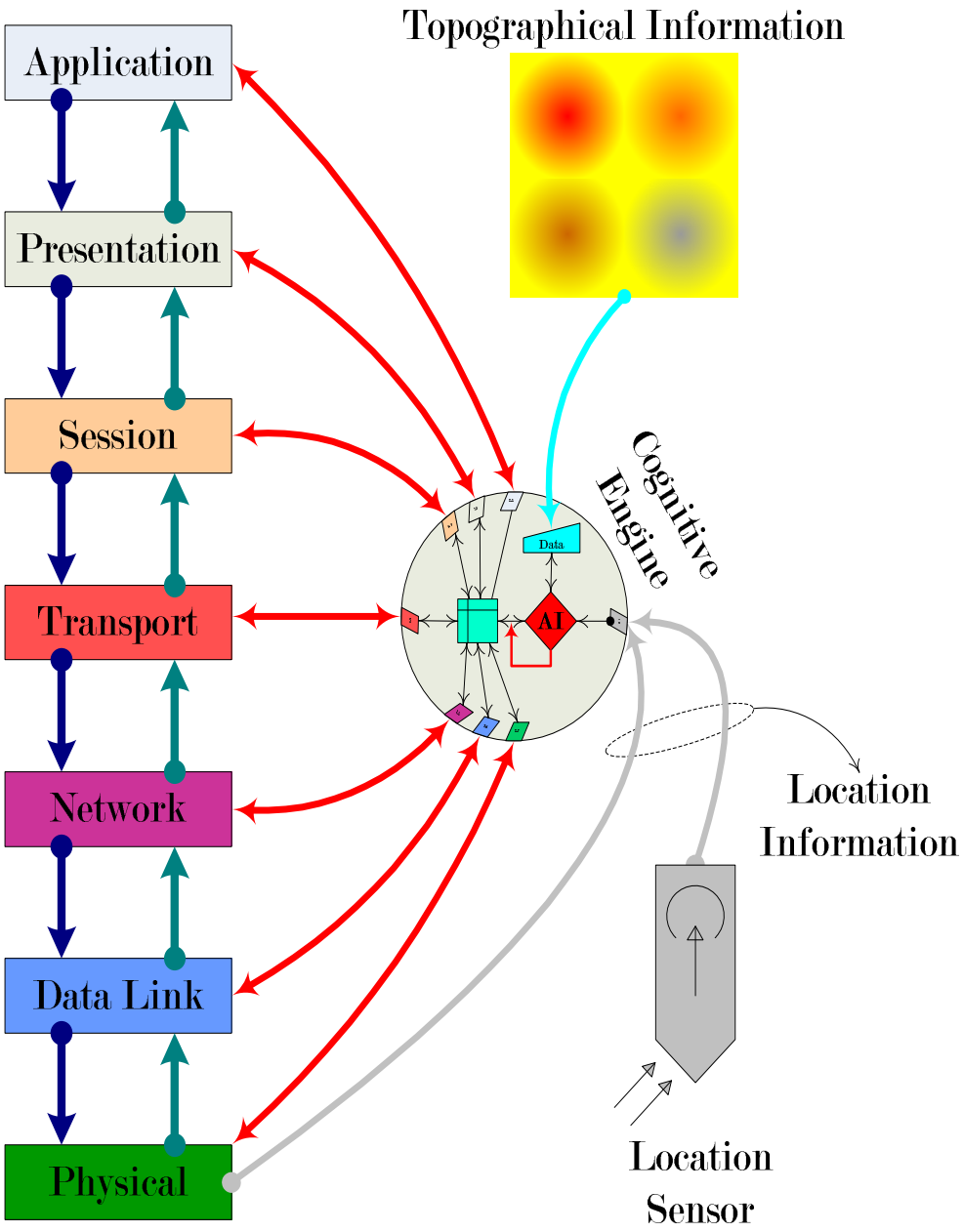


Figure 2.1 Conceptual model of CR in connection with the traditional protocol stack and a location sensor.

plete control and coordination of these features. Hence, a special unit, which is called "cognitive engine," is considered to take on these control and coordination tasks. Cognitive engine carries out these tasks by obtaining all the available information from the sources such as sensors, protocol layers, a policy engine, and its own hardware. Then, it interprets, reasons, and makes the optimum decision to adapt. Figure 2.1 illustrates a conceptual model for CR within this context.

In this chapter, environment/location[1] awareness is exploited to improve the wireless communication system design in CR. More explicitly, it is emphasized that given the environmental knowledge, a CR that has only an absolute location determination capability (by means of GPS or cellular) improves the performance of its communication via optimizing the system parameters and controlling the interference. The organization of this chapter is as follows: Chapter 2.2 outlines several wireless channel parameters from the environmental dependency perspective; Chapter 2.3 investigates what sort of propagation environments exist and how they can be classified; Chapter 2.4 discusses the concept Knowledge Representation Space (KRS) along with Radio Knowledge Representation Language (RKRL), which enables cognitive engine to deal with location awareness, interpreting the collected information, and adapting it accordingly; Chapter 2.5 explains location awareness from the perspective of CR networks.

## 2.2 Wireless Channel Parameters

The most important aspects of improving the wireless transmission are to be aware of the radio channel and change the parameters of the system accordingly. A transmitted signal reaches the receiver after passing through various distortions depending on the transmitted waveform structure and the environment because of the propagation characteristics of the electromagnetic waves. Traditionally, the effects of the wireless channel on the transmitted signal are classified as: (I) large–scale and (II) small–scale. Large–scale effects determine path–loss. Small–scale effects focus on the drastic variations of the received signal strength for short displacements, which are on the order of few wavelengths. These drastic changes in the signal are caused by the multipath phenomenon and variation of the wireless channel in time, due to mobility. Small–scale effects manifest themselves with three different parameters: (I) delay spread, (II) Doppler spread, and (III) angular spread. Delay spread arises from the arrivals of different multipaths at different delays at the receiver. Doppler spread occurs when the wireless channel changes in time because of the mobility of the user and/or transmitter and/or relative motions of the objects within the environment. Angular spread is a measure of how multipaths concentrate about a specific direction [22].

Each form of the small–scale effects introduces a different aspect of the wireless channel. Delay spread is used to describe the time dispersion of the channel. In connection with coherence bandwidth, it is related to the frequency selectivity of the channel. Typical values of delay spread of

[1]From this point on, the terms environment and location will be used interchangeably throughout the text.

indoor mobile radio channels differ from those of outdoor radio channels. Furthermore, outdoor environments that have different terrain and building structures exhibit different delay spread characteristics. In order to see this, the delay spread characteristics of urban and suburban areas can be considered. The typical root–mean–squared (RMS) delay spread values for urban areas are on the order of microseconds, whereas those of suburban areas are on the order of nanoseconds [23]. The channel shapes (power delay profiles) of these environments differ from each other too.

Doppler spread is the measure of the broadening of the signal in frequency domain due to temporal variation of the channel. The temporal variation of the channel is quantified by coherence time and it is inversely proportional to the Doppler spread. Thus, the larger the Doppler spread, the narrower the coherence time interval, and the faster the channel changes. It is also known that the slower the mobile, the narrower the Doppler spectrum. Therefore, it is easily deduced that for the environments in which the mobility is limited (*e.g.* inside the buildings), the Doppler spectrum is more likely to be narrow. Conversely, for the environments in which the mobility is not limited (*e.g.* rural areas), it is expected that the Doppler spectrum is wide.

For angular spread, the effect of multipaths is examined from the perspective of their angles of arrival. The amount of spreading is directly related to the amount of scattering in the environment. The richer the scattering environment is, the more the spread is experienced in the angle domain. Besides, the larger the angular spread is, the lower the correlation becomes between antenna elements. For indoor communications, one might anticipate that the angular spread is larger than that for outdoor because of the presence of numerous scatterers. With the same reasoning, it is possible to find different angular spread behaviors within different scenarios among outdoor radio environment sub–classes. For instance, in an environment which is identified as open rural area, the angular spread is expected to be narrower than that in an area which is identified as urban.

The impact of environmental characteristics on small–scale parameters discussed up until this point is presented in Table 2.1.

Apart from small–scale parameters; there are some crucial parameters for further description of the wireless channel. In almost every wireless radio technology standard, the relevant channel models are classified based on a very important distinction: being in line–of–sight (LOS) or non–line–of–sight (NLOS). It is known that for every kind of radio transmission, LOS channels differ from NLOS channels because of the presence of the direct path. This fact along with several other

Table 2.1 The impact of environmental characteristics on small–scale parameters

| Parameter | Description | Illustration |
|---|---|---|
| Delay spread | Delay spread characteristics depend on physical environment. Some standards classify the environments and assign explicit statistical power delay profile (PDP) for each of them. In the figure next cell, the four major categories of PDPs for typical urban, bad urban, rural area, and hilly terrain in European Co–operation in the field of Scientific and Technical research (COST) 231 (and even in COST 259) is shown [24]. In each category, the corresponding PDP has some distinct features such as number of clusters and arrival times beside a common property, which is exponentially decaying power. | 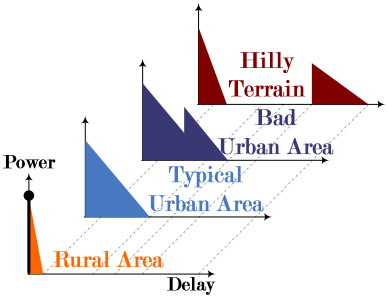 |
| Doppler spread | Doppler spread characteristics differ from each other for different propagation environments. According to International Telecommunication Union – Radiocommunications (ITU–R) model, for outdoor, classical Jakes' type Doppler spectrum is recommended, whereas for indoor, flat Doppler spectrum is recommended [25]. | 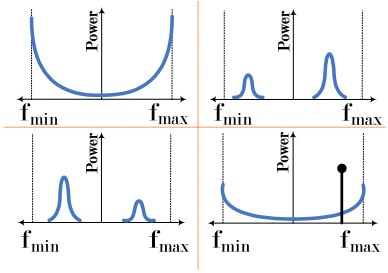 |
| Angular spread | Depending on the richness of the scatterers in an environment, angles of arrival of multipath components vary [22]. | 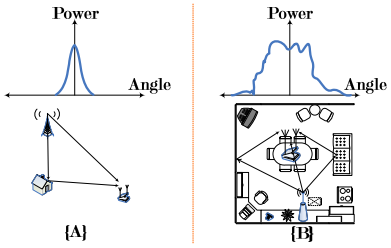 |

effects sometimes requires a special design structure in wireless communication systems such as in 10–66GHz portion of the physical layer part of IEEE 802.16.

Noise also must be taken into account in realistic wireless channel models, since its impact on the communication systems is obvious [26]. Generally, because of its mathematical tractability, noise is assumed white and chosen as Gaussian distributed, which has a flat power spectrum. However, it has been reported that offices, factories, and hospitals have impulsive noise rather than white and Gaussian distributed [27] as well as some outdoor environments, due to man–made noise sources.

Table 2.2 Some crucial wireless transmission parameters, their effects, and related adaptation options

| **Parameter** | **Effect** | **How to use** |
|---|---|---|
| Path–loss | RSS | Link adaptation via adaptive coding/modulation<br>Handoff (handover)<br>Channel allocation<br>Interference management<br>Simple distant–based power control algorithm |
| Delay Spread | Frequency selectivity | Number of equalizer taps for single carrier systems<br>Number of pilots and spacing for multi carrier systems<br>fast Fourier transform (FFT) size for multi carrier systems<br>Carrier spacing for multi carrier systems<br>Adaptive filtering for channel estimation<br>Cyclic prefix length for multi carrier systems |
| Doppler spread | Time selectivity | Channel tracker step size<br>Interleaving schemes<br>Handoff management<br>Frequency allocation |
| Angular spread | Spatial selectivity | Beamforming<br>Smart antenna<br>Adaptive multi–input multi–output (MIMO)<br>Interference management<br>Frequency allocation |
| LOS/NLOS | Overall channel behavior | Transmission frequency<br>Power adjustment |
| Noise | Capacity | Transmission frequency<br>Link adaptation (Adaptive coding/modulation) |

Furthermore, it is shown that maximal ratio combining, equal gain combining, and selection diversity are not effective in impulsive noise environments [28]. Hence, being aware of the type of the noise is of crucial importance in adjusting some of the system parameters such as coding requirements [27].

Aforementioned propagation related parameters, their effects, and adaptation options (in case of having *a priori* knowledge about them) are tabulated in Table 2.2.

### 2.3 Classification of Propagation Environments

In the literature, there are two methods to model the radio propagation: (I) stochastic and (II) deterministic method. In (I), field measurements are made with extensive amount of work to characterize the wireless channel. Fields in which the measurements are made are classified based

on their topographical properties. In (II), numerical calculations (such as ray–tracing methods) are employed to attain the desired wireless channel parameters with ultimate pinpoint accuracy. The major differences between (I) and (II) are that, (I) allows use of simple formulas which are valid for general cases (due to stochastic structure), whereas (II) provides pinpoint accuracy for a specific case at the expense of computationally complex processes [29].

Considering the fact that (I) is faster and can provide solutions for general scenarios compared to (II), (I) is more appropriate for CR at this stage. However, employing (I) requires a CR to have the topographical information about the geographical area. Some of the basic topographical databases such as digital elevation models (DEM) (*i.e.* digital representations of topographic surfaces, which are used for determining properties of terrain in terms of elevation at any point, slope, aspect and extracting features of it, such as peaks and pits and other landforms) have already been used in wireless communications for similar purposes such as checking whether LOS exists between a transmitter–receiver pair [23]. DEMs are easy to be processed digital data which can give some hints to a CR about the attributes of the surrounding environment via spatial interpolation methods (SIM). Also, a Geographical Information System (GIS) provides comprehensive topographical information which can be queried by GPS. Thus, when the cognitive engine is provided with a sort of topographical information such as DEM or GIS, it can recognize the pattern of the aerial information, locate the appropriate class, and match the most appropriate statistics out of its memory. In Figure 2.2, the flow of the environmental classification algorithm is shown.

## 2.4 Knowledge Space, Environmental Characterization, and Adaptation

This chapter focuses on the following goals of CR: (I) to recognize and classify its environment, (II) to match it with corresponding statistical propagation model parameters, and (III) to employ the relevant adjustments in hardware and software. Up to this point, these goals have been discussed from an algorithmic perspective. This section, particularly, focuses on how CR can achieve these goals in a more formal way in connection with SDR.

In Chapter 2.2, it has been explained that radio propagation behaves differently in each type of environment. Establishing a universal model, which works in every kind of environment, is extremely difficult because of the nature of radio propagation. As introduced in Chapter 2.3, a stochastic approach simplifies the modeling process with the aid of some tools such as delay power spectra, amplitude distribution, and correlation function. It is also known that these tools can be described

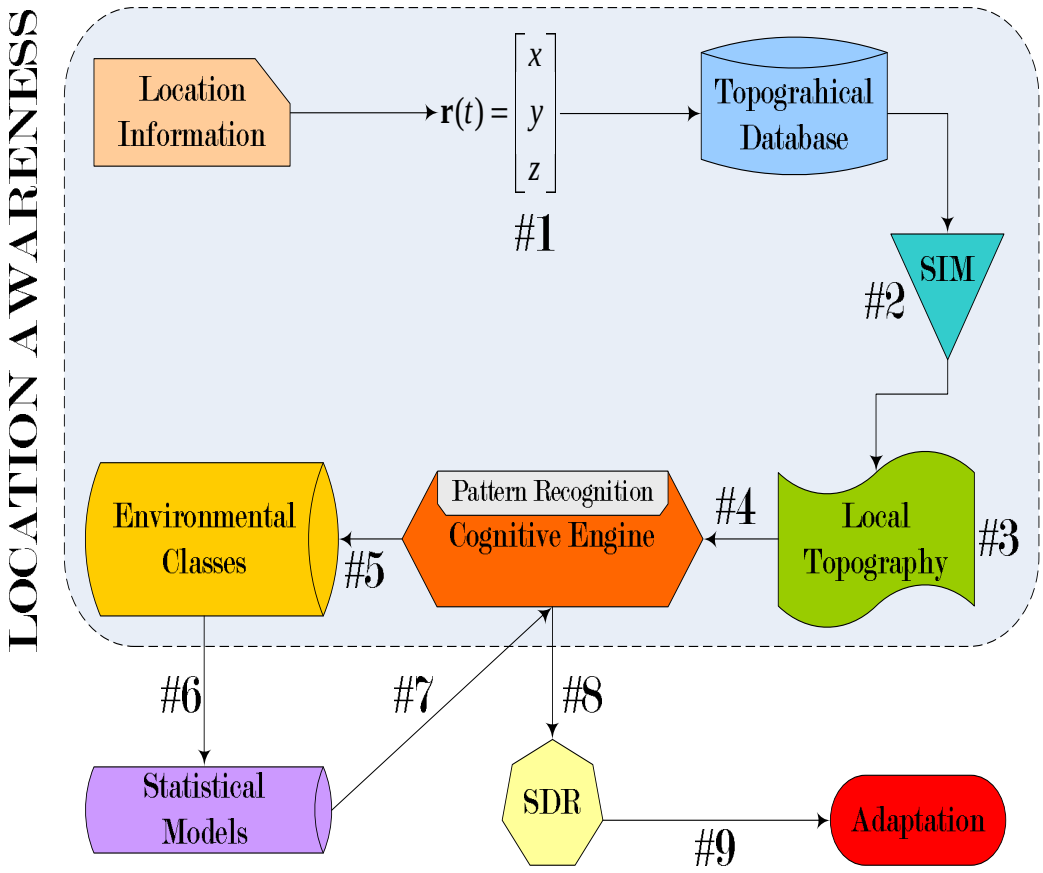


Figure 2.2 The flow of the environmental classification algorithm for CR.

via a few parameters whose values change from one environment to another [30]. Hence, the first step for CR in exploiting the location awareness is to classify its environment according to a chart which is similar to the one presented in Table 2.3. This is very important, since classification facilitates storing and searching for appropriate statistical models that correspond to the environments in which CR operates. Moreover, a structure such as presented in Table 2.3 can easily be expanded for new environments that might be defined in the future. In order to attain the organized structure mentioned here, having the ability to represent the data in a hierarchical way is essential.

In addition to representing the data in a hierarchical way, CR also gets information from various sources (as shown in Figure 2.1) such as sensors, protocol layers, external devices, and even its own hardware. Even though the pieces of information obtained are coming from independent sources, some of them can be related. Consider the case in which CR has light and temperature sensor along with GPS. If a contextual connection can be established between the bits of information provided

Table 2.3 Frequently used environmental classifications for wireless propagation with some related parameters

| Main | Subcl. I | Subcl. II | Characteristics | $\tau_{RMS}$ | Mobil. |
|---|---|---|---|---|---|
| OUTDOOR | ***Urban*** | *Typical* | Large buildings, closely & homogeneously placed houses, thick–tall trees | 0.5–2$\mu$s | High |
| | | *Bad* | Inhomogeneous placed buildings | $\geq$ 20$\mu$s | High |
| | ***Suburban*** | *Commer. Resid.* | Relatively short buildings, scattered trees & obstacles | 0.3–2$\mu$s | High |
| | | *Suburb. Resid.* | Short and closely spaced buildings | 0.3–2$\mu$s | High |
| | ***Rural*** | *Open* | Flat, few & separated buildings | 0.08-0.14$\mu$s | High |
| | | *Forest* | Flat, few & separated buildings, dense tree texture | 0.08-0.14$\mu$s | High |
| | ***H. Terr.*** | *Hilly terrain* | Moderate–to–heavy tree densities | 2.8–5.2$\mu$s | High |
| | | *Mostly Flat* | Moderate–to–heavy or hilly terrain with light tree densities | 0.26–1.25$\mu$s | High |
| | | *Flat* | Flat terrain with light tree density | 0.11–0.2$\mu$s | High |
| | ***Open*** | | No obstacles, buildings like farm–lands, fields, etc. | $\leq$ 0.2$\mu$s | High |
| | ***Street Microcell*** | | Linear streets, stadiums, parking lots, etc. | 10–100ns | Low |
| | ***Suburb. Microcell*** | | Last connection step to wired network | 10–100ns | Low |
| INDOOR | ***Dense*** | | Small rooms; typically an office mostly NLOS | 30–60ns | Low |
| | ***Open*** | | Large rooms; typically an office with several people; mostly LOS or obstructed line–of–sight (OLOS) | 100–200ns | Low |
| | ***Large*** | | Very large rooms; typically a factory hall, shopping center or airport building; mostly LOS or obstructed line–of–sight (OLOS) | 100–200ns | Low |
| | ***Corridor*** | | Tx & Rx along the same corridor; LOS | Up to 300ns | Low |

by these sources in a combined fashion such that "all of them provide information related to the surrounding environment," CR can make use of them in exploiting the location awareness. It is clear that the contextual relation is not limited to the sensors. Relationships between sensors and other types of sources may exist too. For instance, GPS information is related to location–aware routing application over network layer. However, this sort of connection is not possible unless the context of the information is included. This requirement leads to an abstraction, which is known as KRS.

In order for a CR to represent the data in a hierarchical and contextual form, the "KRS" concept has been put forward [21]. A KRS represents the universe of a CR and consists of numerous subspaces such as space, time, user, the radio itself, spectrum, network, and their subspaces such as environment, air interfaces, protocol layers, and so on. It is very difficult to document all possible subspaces in the universe of CR. Although this looks discouraging, fortunately, a KRS can be expanded when it is necessary. With the same reasoning, –even though it is not favorable since a radio, which is able to interpret as many things as possible, is desired– when it is needed (for instance, due to insufficient memory, the necessity of deletion of some subspaces such as old standards which have never been used), it can be shrunk as well. As a matter of fact, this flexibility is a requirement, since a CR is considered to have a dynamic library that can be updated easily when environments, policies, needs, etc. change.

Solely the construction of KRS will not be enough for a CR to exploit location awareness. Beside KRS, a tool for processing KRS must be present as well. RKRL has been proposed filling the gap in processing KRS [21]. Therefore, RKRL can be defined as "a formal structure that helps CR to process the hierarchical and contextual construction, which is KRS."

RKRL consists of statements and each statement forms a special structure called "frame." Frames express the relationship between their contents in a particular context. The ontological structure of the universe of a CR, the hardware in a CR, and the environment in which a CR operates are only a few examples that can be defined and described by the frame structure. For instance, the ontological structure of the universe of a CR might be of the form:

$$
\begin{aligned}
&\bullet\langle Universe\rangle \\
&\quad \blacktriangleright \langle Solar\ system\rangle \\
&\qquad \blacktriangleright \langle Earth\rangle \\
&\qquad\quad \blacktriangleright \{\langle Space\rangle, \langle Time\rangle, \langle User\rangle, \langle Radio\rangle, \dots\},
\end{aligned}
\tag{2.1}
$$

where $\langle\cdot\rangle$ denotes a contextual set that might contain several subsets; $\bullet$ represents the set of everything; $\blacktriangleright$ denotes one of the subsets of its superset.

Following the same pattern in (2.1), CR can represent the "space" in detail as:

$$
\begin{aligned}
&\ddots \\
&\quad \blacktriangleright \langle Space\rangle \\
&\qquad \blacktriangleright \{\langle Position\rangle, \langle Temperature\rangle, \dots\}.
\end{aligned}
$$

Peculiar to our interest, CR can easily represent the "sensors" as:

$$
\begin{aligned}
&\ddots \\
&\quad \blacktriangleright \langle Radio\rangle \\
&\qquad \blacktriangleright \langle Sensors\rangle \\
&\qquad\quad \blacktriangleright \{\langle GPS\rangle, \langle Heat\rangle, \langle Light\rangle, \dots\}.
\end{aligned}
$$

Similarly, the "position," which is denoted with $\langle Position\rangle$ in KRS, can be represented with the following subset:

$$\{\langle \mathbf{r}\rangle, \langle Environment\rangle, \langle Direction\rangle, \dots\},$$

where $\langle \mathbf{r}\rangle$ denotes the coordinate triple, which is of the form $\langle \mathbf{r}\rangle = \langle [x, y, z]\rangle$.

Note that, this hierarchical representation quantifies what a CR can be aware. For example, a CR, which solely has GPS, will shrink its $\langle Sensors\rangle$ subset and define it by only $\{\langle GPS\rangle\}$.

Once the hierarchical structure is formed, attaching the corresponding contexts to the sources can be investigated. For example, the context of a sensor, say GPS, can be defined in the following

mapping manner:

$$[\langle GPS\rangle \doteqdot \langle Space\rangle \times \langle Time\rangle \mapsto \langle \mathbf{s}\rangle],$$

where $\langle Space\rangle \times \langle Time\rangle$ represents the notion "space–time" and $\langle \mathbf{s}\rangle$ is the space–time quadruple of the form $\langle [\mathbf{r}, t]\rangle$. With the same reasoning, in case of using a heat sensor, the context of the sensor can be shown in the following form:

$$[\langle Heat\rangle \doteqdot \langle Space\rangle \times \langle Time\rangle \mapsto T],$$

where $T$ denotes the temperature.

As can be seen, CR is able to recognize each piece of information fed by each sensor with the aid of the context. Furthermore, CR can even find the connection with other $\langle Space\rangle$ and/or $\langle Time\rangle$ related entities in its universe by just looking at the context of the sensor of interest. For instance, the domains of both $\langle GPS\rangle$ and $\langle Heat\rangle$ (*i.e.* the left hand side of $\mapsto$) contain $\langle Space\rangle$ and $\langle Time\rangle$ together. Therefore, it is deduced that $\langle GPS\rangle$ and $\langle Heat\rangle$ produce related information. Note that once the contexts and rules are established, as in Prolog, –which is a logic programming language, – in RKRL, the reasoning depends solely on querying the relationship. Thus, with the aid of RKRL, CR can find every context that is related to another one in its KRS.

In Chapter 2.3, it has been discussed that environmental classification carries a crucial importance for CR. Having a classification such as in Table 2.3 in hand, representing the classification is straightforward by following the pattern in (2.1). As an example, CR can express "open rural area," which will be a subset of $\langle Environment\rangle$, as follows:

$$\ddots$$
$$\blacktriangleright \langle OUTDOOR\rangle$$
$$\blacktriangleright \langle Rural\rangle$$
$$\blacktriangleright \langle Open\rangle.$$

In this sequel, relating empirical models with corresponding environmental classes can be considered. Recall that RKRL can process every entity that belongs to the universe of CR with the aid of frames. Hence, propagation models are nothing but collection of frames for CR. Because differ-

ent environmental classes require different path–loss models, it is appropriate to represent relevant models as subsets of the classes to which they belong. For instance, path–loss for a rural area can be of the form:

$$\ddots$$

$$\blacktriangleright \langle Rural \rangle$$

$$\blacktriangleright \langle Path - Loss\ Model \rangle$$

$$\blacktriangleright \langle Hata's\ Model \rangle,$$

which is based on already settled down and widely used models such as in [24]. Similar to path–loss, other important propagation statistics such as power delay profile (PDP), Doppler spread, etc. can also be represented in this manner. For example, PDP can be represented in such a way that it includes number of clusters, number of taps in each cluster, relative power, RMS delay spread, and so on.

As a final step, after matching operation, it is sufficient for CR only to read the values from statistical model "frame" and apply them to relevant transmission parameters accordingly. Some of the options that CR can adapt after adjusting its parameters in connection with the propagation characteristics of the environment are presented in Table 2.2.

## 2.5 Cognitive Radio Networks and Location Awareness

Up to this point, the use of information about propagation environment from the perspective of individual CRs has been discussed. However, the dissemination of this information in a network that consists of multiple CRs is very important as well. The main urge behind disseminating this information is to make other CRs, –which do not have the capability of obtaining this information on their own because of lack of necessary sensors and/or insufficient resources, – be aware of the characteristics. For the sake of brevity, $CR_0$ is used for representing CRs which do not have the capability of obtaining the information on their own and $CR_1$ is used for the capable ones. As will be seen subsequently, sharing this information improves several aspects of network while it helps CRs to adjust their parameters in an optimum manner for individual adaptation.

- Information Dissemination in CR Networks. The dissemination of the information can be considered in two ways depending on the architecture of the network: (I) Centralized and (II) decentralized. In I), first, $CR_0$ requests the propagation characteristics from the center. If the center is of type $CR_1$, it forms the data with the aid of RKRL and forwards it to $CR_0$. $CR_0$ interprets this structural data and employs the necessary changes accordingly. In case the center is not of type $CR_1$, then, it broadcasts the location information of $CR_0$ to other nodes (which may be established by using a pre–defined control channel) and an available $CR_1$ sends the relevant information back to the center to be dispatched to $CR_0$. On the other hand, in II), $CR_0$ solely broadcasts its location information and waits for $CR_1$s to respond back with the data processed by RKRL.

- CR Networks and Exploiting the Location Awareness. Once CR obtains the propagation characteristics, it adapts its parameters accordingly. Of course, this individual adaptation of CR leads to several improvements in the network as well. Path–loss adaptation can be used in power–control algorithms in code division multiple access (CDMA) based networks. Hence, the average amount of interference experienced by other users is reduced, which increases the network capacity. In an orthogonal frequency division multiplexing (OFDM) based network, adjusting cyclic prefix (CP) size accordingly rather than setting it to the worst–case scenario will improve the spectral efficiency. In case CP size is lower than that for the worst–case, the overall data rate will increase as well. There are numerous ways of exploiting the propagation characteristics in terms of adaptation apart from the ones mentioned here. Some of the crucial parameters and corresponding adaptation options are presented in Table 2.2. For a more detailed discussion of adaptation options, [22] can be referred.

Because some of the adaptation options mentioned here have already been used by the contemporary wireless communication systems, it is appropriate to discuss the differences between CR and contemporary wireless communication systems. In order to stress the differences, how contemporary wireless communication systems quantify important propagation characteristics can be reviewed. In contemporary wireless communication systems, path–loss is measured from the samples of received signal strength (RSS). Based on the RSS measured and a threshold value, the link quality is evaluated and adaptation is established. In order to estimate the delay spread, contemporary communication systems employ channel frequency correlation estimates as well as level crossing rate

(LCR) of the channel in frequency domain. Depending on the estimated value, adaptive channel equalization is applied. Doppler spread estimation is carried out in current wireless communication systems too. Correlation and variation of the channel estimates (or signal envelope) are prominent methods in estimating the Doppler spread. Doppler spread information is used in radio network control algorithms such as cell assignment and channel allocation in cellular systems.

Even though current wireless communication systems are able to measure the major propagation parameters and use it for adaptation, they do not have any other option except for the received signal, which can be called as "internal sensing." However, CR systems are not limited to internal sensing, since, –as discussed in Chapter 2, – there are new sensing capabilities emerging. Therefore, CR systems are capable of taking advantage of these recently emerging sensing opportunities to better estimate the propagation parameters with the aid of cognitive engine, which leads to improvement in overall system performance. Besides, these recently emerging sensing opportunities can provide CRs with novel awareness and adaptation options that cannot be achieved by internal sensing. For instance, being aware of the user is one of the prominent awareness and adaptation options, which includes the user's identity, perception, and preferences as well as the characteristics of the user's surrounding environment (*e.g.* physical location, illumination, ambient acoustic noise, and so on). The information that is obtained by this sort of sensing can be very useful to improve the network and service performance [21]. However, the use of this type of information is only possible when the sensing data is processed by RKRL. Cognitive engine cannot determine the context of the sensing data unless RKRL forms it, as discussed in Chapter 2.4.

One must keep in mind that the traditional strictly layered protocol architecture causes the contemporary wireless devices (and therefore the systems) to perform in a sub–optimal range. On the other hand, the presence of cognitive engine along with external sensing capabilities allows CR systems to achieve cross–layer adaptation and optimization as shown in Figure 2.1. CR systems are able to perform in the optimum range by incorporating the bits of information coming from external sensing into the cognition cycle with the aid of RKRL, as explained before.

## 2.6 Conclusion

CR can be aware of many concepts via internal and/or external sensing defined in Chapter 2.5. Especially for location, each concept to be aware of has different projections or impact on different layers in the protocol stack. These projections define two very important relationships. The first

relationship is between the layers and each other, since the projections are caused by the same concept. Peculiar to this part, it is seen that the concept of "location" has impact on almost each layer. This relationship between layers allows a CR to consider the projections jointly and leads to cross–layer adaptation and optimization. The second relationship is between the concept itself and its projections. Again, here, it has been discussed that specific locations cause specific effects. This second relationship provides a sort of mapping or function in a mathematical perspective so that CR can either examine (or evaluate, or measure) the projections to be aware of the concept, or be aware of the concept first and then exploit the corresponding projections in terms of cross–layer adaptation and optimization. Considering the increasing trend that allows people to define more relationships through having more sensors on devices along with high processing power, the cognition cycle can be extended to attain the ultimate CR.

# CHAPTER 3

# CHANNEL AWARENESS FOR NEXT GENERATION WIRELESS NETWORKS

## 3.1 Introduction

Wireless communication systems have evolved substantially over the last two decades. The explosive growth of the wireless communications market is expected to continue in the future, as the demand for all types of wireless services is increasing. New generations of mobile radio systems aim to provide higher data rates and a wide variety of applications (such as video, data, positioning, and so on) to the mobile users while serving as many users as possible. However, this goal must be achieved under the constraint of limited available resources such as spectrum and power. Given the high price of spectrum and its underutilized use, the systems must provide higher capacity and performance through a better exploitation of all available resources. Therefore, *adaptive* and cognitive radio (CR) have been becoming popular for optimizing mobile radio system transmission and reception at the physical layer as well as at the higher layers of the protocol stack. Traditional system architectures focus on allocating fixed resources to the mobile users, since the fundamental goal is simplicity in the design. Adaptive design methodologies, on the other hand, typically identify the users' requirements, and then allocate just enough resources; thus, enabling more efficient utilization of system resources and consequently increasing the capacity.

Considering the escalating demand in use of wireless communications along with the fact that radio spectrum is finite, a straightforward conclusion, which is called as "spectrum scarcity," can be drawn. Contrary to this common reasoning, recent measurements revealed that radio spectrum is actually underutilized rather than being scarce. CR that is based on software–defined radio (SDR) is brought forward to remedy this underutilization problem. Through cognition cycle and SDR, CR is capable of pushing the traditional and limited adaptation concept towards the global adaptation by introducing multi–dimensional awareness, sensing, and learning from its experiences to reason, plan, and decide future actions to meet user needs. Even though there is no consensus on the formal

definition of CR as of now, the concept has evolved recently to include various meanings in several contexts. Interoperability across several networks; roaming across borders while being able to stay in compliance with local regulations; adapting the system, transmission, and reception parameters without user intervention; and having the ability to understand and follow actions and choices taken by their users, and learn to become more responsive over time can be considered just to name few. Since these parameters and notions might tinker over time and over multitude of other dimensions, the radios need to be equipped with proper mechanisms to react these changes.

Including contemporary communication systems, it is not difficult to see that a global adaptation covering the entire protocol stack has not been achieved yet. This stems from the architecture of the protocol stack, which is based on strictly defined individual layers. Furthermore, a global adaptation requires all of the layers to be examined in a combined way leading to a multi–dimensional problem. However, CR cannot come true without having such a global adaptation which comes at the expense of very challenging trade–offs in terms of contending goals defined in layers. Hence, by its very definition, being aware of the situation, environment, and many other aforementioned issues will compel CR to find a compromise between many contending objectives. Moreover, it is important to note that CR is also responsible for observing the consequences of its actions to be able to improve the quality of its decisions in the future through its learning ability. Although the contemporary strictly layered protocol structure solves some of the problems to some extent, a conceptual model of CR is required.

In this chapter, some of the important parameters for enabling the adaptive radio and CR systems will be discussed along with measurement and estimation techniques including relevant challenges and some sample applications. Desired user's radio channel parameters will be studied in detail. The channel parameters will be grouped under two categories, namely, channel selectivity measurements and channel quality measurements. Interference parameters, which could have also been interpreted as part of the channel parameters, will be treated separately, since for CR, the definition of interference includes concepts beyond what has been interpreted in the past. In addition to the channel and interference parameters, many other parameters that can be useful for CR will be discussed under the concept of external sensing. Based on the traditional channel parameter measurements along with externally obtained ones, a conceptual model of CR is presented, as well.

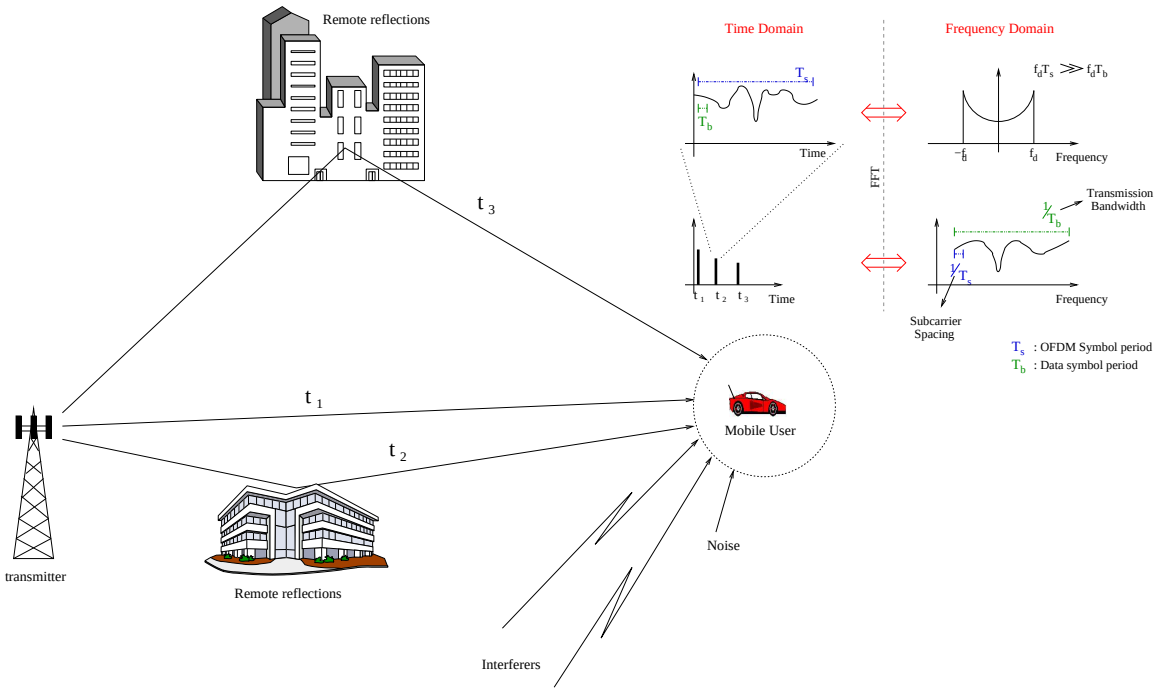


Figure 3.1 Illustration of some of the effects of radio channel.

### 3.2 Channel Parameters

In wireless radio communication systems, information is transmitted to the receiver through a radio propagation environment. Transmitted signals are typically reflected, diffracted, and scattered, arriving at the receiver along multiple paths with different delays, amplitudes, and phases (*see* Figure 3.1). Multipath propagation affects the signal significantly, corrupting the signal, and often placing limitations on the performance of the system.

Depending on the transmission bandwidth (or symbol duration) and the type of environment in which the communication takes place, multipath can cause various problems. When the relative delays are small compared to the transmitted symbol period, different "images" of the *same* symbol arrive at the same time, adding either constructively or destructively. The overall effect is a random fading channel response. When the relative path delays are on the order of a symbol period or more, then images of *different symbols* arrive at the same time causing inter–symbol interference (ISI).

In addition, in wireless mobile radio systems mobility, which includes the mobility of the transmitter, the receiver, and the scattering objects within the propagation environment, causes the channel response to change rapidly in time leading to spectral broadening, which is also referred

to as Doppler spread. Impact of Doppler spread depends on the transmission bandwidth. As the transmission bandwidth increases, the relative broadening of the channel with respect to the transmission bandwidth will be insignificant. In other words, the time variation of the channel within the transmission of a symbol will be negligible, since wider transmission bandwidths imply shorter symbol duration. This gives rise to a common trade–off between high mobility and high data rate.

Finally, the interference conditions in wireless systems change rapidly. Many of the wireless communication systems are interference limited, affecting the performance, capacity, range, data rate, and so on. Since the radio channels of the desired and interfering users are highly random, and the statistical characteristics of the channel are environment dependent, the effect of interference also varies in time, frequency, and space. As will be discussed subsequently, behavior of interference is also influenced by some other notions such as traffic type and mobility patterns within the propagation environment.

In the following sections, the important measurements related to the radio channel will be discussed. First, channel selectivity measures in different dimensions will be reviewed. Then, various channel quality measures will be studied in detail.

### 3.2.1 Channel Selectivity Measurement

Multipath propagation causes the signal to spread in time, frequency, angle, and other possible dimensions (*see* Table 3.1). These spreads, which are related to the selectivity of the channel, have significant implications on the received signal. The information about the variation of the channel in multiple dimensions is very crucial in adaptation of wireless communication systems.

The first phenomenon is known as time selectivity measure/Doppler spread. Doppler shift is the frequency shift experienced by the radio signal when there is a relative motion in the propagation environment, and Doppler spread is a measure of the spectral broadening caused by the temporal rate of change of the mobile radio channel. Therefore, time–selective fading and Doppler spread are directly related. The coherence time of the channel can be used for characterizing the time variation of the time–selective channel. It represents the statistical measure of the time window over which the two signal components have strong correlation, and it is inversely proportional to the Doppler spread.

In CR, Doppler spread information can be used for improving performance or reduce complexity. For example, in channel estimation algorithms, whether using channel trackers or channel interpo-

Table 3.1 Dimensions★ of channel selectivity and their importance with sample applications

| ★ | Importance | Sample Applications | Illustrations |
|---|---|---|---|
| TIME | Indicates how fast the channel is varying in time, and Doppler spread | Receiver optimization (such as channel estimation), adaptation of transmitter and system parameters (such as interleaving length, channel and cell assignment, hand–off optimization) | 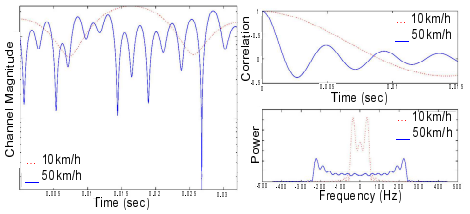  |
| FREQUENCY | Indicates how fast the channel frequency response is changing, and Delay spread | Adaptive equalizer design, adaptive receiver design, adaptive cyclic prefix design for OFDM systems, and so on | 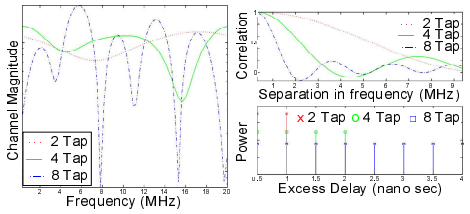  |
| SPACE | Determines how rich the scattering environment and how wide angle spread are | Adaptive multi–antenna system design | 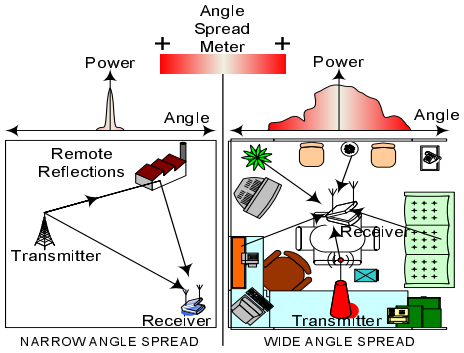  |
| INTERFERENCE | Indicates how interfering sources affect the desired signal in time (as in frequency hopping (FH)), in frequency (as in narrow–band interference (NBI)) | Intelligent interference cancellation and avoidance mechanisms | 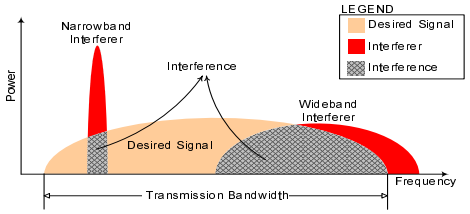  |

lators, instead of fixing the tracker or interpolation parameters for the worst case Doppler spread value (as commonly done in practice), the parameters can be optimized adaptively based on the Doppler spread information [31–33]. Similarly, Doppler information could be used for controlling the receiver or the transmitter adaptively under different mobile speeds as in variable coding and interleaving schemes [34].[1] Also, radio network control algorithms, such as hand–off, cell assignment,

[1]The direct relationship between mobile speed and Doppler phenomenon is studied broadly in the literature as well [35–38].

and channel allocation in cellular systems, can utilize the Doppler information [39, 40]. For example, in a hierarchical cell structure, the users are assigned to cells based on their speeds (mobility); fast–moving mobiles can be assigned to larger umbrella cells (to reduce the number of hand–offs), while slow–moving mobiles are assigned micro–cells (to increase capacity).

Doppler spread estimation has been studied for several applications in wireless mobile radio systems. Correlation and variation of channel estimates [41] as well as correlation [42, 43] and variation of the signal envelope have been used extensively [35, 40]. Multiple antennas can also be exploited for Doppler spread estimation [44], where a linear relation between the switching rate of the antenna branches and Doppler frequency can be obtained.

Although the estimation of the Doppler spread information is very useful for adaptive systems, one might wonder if the estimation process brings a heavy burden onto the system. If we consider contemporary wireless receivers, we see that most of them are already accessorized with channel estimation ability. Although the Doppler spread estimation requires additional effort after the channel estimation process, the gain to be obtained in the long term is encouraging. However, considering the desire of having a mobile device as small as possible such as a cell phone, the use of multiple antennas for this purpose becomes questionable.

Delay spread is one of the most commonly used parameters that describes the time dispersiveness of the channel, and it is related to frequency selectivity. Frequency selectivity can be described in terms of coherence bandwidth, which is a measure of range of frequencies over which the two frequency components have a strong correlation. The coherence bandwidth is inversely proportional to the delay spread [23, 45].

Such as time selectivity, the information about frequency selectivity of the channel can be very useful for improving the performance of all types of adaptive wireless radio systems including CR. For example, in a time division multiple access (TDMA) based Global System for Mobile (GSM), the number of channel taps needed for equalization might vary depending on the dispersion of the channel. Instead of fixing the number of equalizer taps for the worst case condition, they can be changed adaptively, allowing simpler receivers with reduced battery consumption and improved performance [46, 47]. Dispersion estimation can also be used for other parts of transmitters and receivers. For example, in channel estimation using channel interpolators, instead of fixing the interpolation parameters for the worst expected channel dispersion, the parameters can be changed adaptively depending on the dispersion information [48].

Although dispersion estimation can be very useful for many wireless communication systems, it is particularly crucial for orthogonal frequency division multiplexing (OFDM)–based wireless communication systems. OFDM, which is a multi–carrier modulation technique, handles the ISI problem due to the high bit rate communication by splitting the high rate symbol stream into several lower rate streams, and transmitting them on different orthogonal carriers. The OFDM symbols with increased duration might still be affected by the previous OFDM symbols due to the multipath dispersion. cyclic prefix (CP) extension of the OFDM symbol avoids ISI from the previous OFDM symbols if the CP length is greater than the maximum excess delay of the channel. Since the maximum excess delay depends on the radio environment, the CP length needs to be designed for the worst case channel condition. This makes CP as a significant portion of the transmitted data, resulting in reduced spectral efficiency. One way to increase spectral efficiency is to adapt the length of the CP depending on the radio environment [49]. The adaptation requires estimation of maximum excess delay of the radio channel, which is also related to the frequency selectivity. A very important statistical parameter that is used to characterize the time dispersiveness of the wireless channel is the root–mean–squared (RMS) delay spread. RMS delay spread is the square root of the second central moment of the power delay profile (PDP) of the channel, and it is generally less than one–fourth of the maximum excess delay. In HIPERLAN/2, which is a wireless local area network (WLAN) standard, a CP duration of 800ns, which is sufficient to allow good performance for channels with RMS delay spread up to 250ns, is used. Optionally, a short CP with 400ns duration may be used for short range indoor applications. Similarly, the broadband wireless metropolitan area network (WMAN) standard, IEEE 802.16, defines several CP options that can be used in different environments. Delay spread estimation allows adaptation of these various options to optimize the spectral efficiency. Other OFDM parameters that could be changed adaptively using the knowledge of the dispersion are the OFDM symbol duration and OFDM sub–carrier bandwidth.

Characterization of the frequency selectivity of the radio channel is studied extensively using level crossing rate (LCR) of the channel in frequency domain [50–52]. Frequency domain LCR gives the average number of crossings per Hz at which the measured amplitude crosses a threshold level. An analytical expression between LCR and the time domain parameters corresponding to a specific multipath PDP can be easily obtained. LCR is very sensitive to noise, which increases the number of level crossing and severely deteriorates the performance of the LCR measurement. Filtering the channel frequency response reduces the noise effect, but finding the appropriate filter parameters is

a challenge. If the filter is not designed properly, one might end up smoothing the actual variation of frequency domain channel response. Channel frequency selectivity and delay spread information can also be calculated using the channel frequency correlation estimates, and analytical expressions between delay spread and coherence bandwidth can be obtained easily [45, 53].

Angle spread is a measure of how multipath signals are arriving (or departing) with respect to the mean arrival (departure) angle. Therefore, angle spread refers to the spread of angles of arrival (or departure) of the multipaths at the receiving (transmitting) antenna array [54]. Angle spread is related to the spatial selectivity of the channel, which is measured by coherence distance. Such as coherence time and frequency, coherence distance provides the measure of the maximum spatial separation over which the signal amplitudes have strong correlation, and it is inversely proportional to angular spread, i.e. the larger the angle spread, the shorter the coherence distance. For a given receiver antenna spacing, large angle spread leads to weaker antenna correlations between the signals received by different antenna elements. Note that although the angular spread is described independent of the other channel selectivity values for the sake of simplicity, in reality, the angle of arrival can be related to the path delay. The multipath components that are arriving to the receiver earlier (with shorter delays) are expected have similar angle of arrivals (lower angle spread values).

Compared to time and frequency selectivity, spatial selectivity has not been studied widely in the past. However, recently, there has been a significant amount of work in multi–antenna systems. With the widespread application of multi–antenna systems, it is expected that the need for understanding spatial selectivity and related parameter estimation techniques will gain momentum. Spatial selectivity will especially be useful when the requirement for placing antennas close to each other increases, as in the case of multiple antennas in mobile units.

Spatial correlation between multiple antenna elements is related to the spatial selectivity, antenna distance, mutual coupling between antenna elements, antenna patterns and so on [55, 56]. Spatial correlation has significant effects on multi–antenna systems. Full capacity and performance gains of multi–antenna systems can only be achieved with low antenna correlation values. However, when this is not possible, maximum capacity can be achieved by employing efficient adaptation techniques. Adaptive power allocation is one way to exploit the knowledge of the spatial correlation to improve the performance of multi–antenna systems [57]. Similarly, adaptive modulation and coding, which employ different modulation and coding schemes across multi–antenna elements depending on the channel correlation, are possible [58, 59]. Different antenna systems such as multi–input multi–

output (MIMO) employ adaptive power allocation by exploiting the knowledge of channel matrix estimate and by employing eigenvalue analysis, as well [60, 61].

Researchers need to explore ways to adaptively access all dimensions associated with the electromagnetic spectrum. The three fundamental dimensions of the channel selectivity (time, frequency, and angle) are well understood in the wireless community (see Table 3.1). There are other possible dimensions that can be considered as part of channel selectivity. Even though they might not be directly associated with the actual wireless medium, it is possible to consider them within this context. Power, polarization, interference, and coding are some of these dimensions that are really part of the signal space rather than the actual channel space. However, they have strong ties with the channel space.

Code selectivity, like pseudo noise (PN) codes in direct–sequence spread–spectrum (DSSS) or time hopping codes in ultra–wide band (UWB) or frequency hopping (FH) codes in FH systems, could be a strong measure for adaptive system design for future CR systems. Many of the wireless systems are interference limited. Therefore, the capacity is determined by how much interference the system can tolerate. For example, the self interference (such as ISI) which is caused by the non–zero auto-correlation side lobes, and multi–access interference (MAI) due to the non–zero cross–correlations are major interference sources that are related to the code design. The effect of interference and near–far problem can be minimized by employing power control [62]. Alternatively, decreasing side lobes of the auto– and cross–correlation also reduces interference and increases spectral efficiency. Therefore, it is desirable to have sequences with ideal auto– and cross–correlation properties. However, it is proven that "perfect" sequences do not exists. Also, it is well known that there is a trade–off between obtaining good auto– and cross–correlation properties, (*i.e.*, smaller ISI) leads to larger MAI or vice-versa. In addition, the number of possible codes (and hence the capacity) can be increased by allowing some correlation (or interference) in code domain. Being aware of that the number of codes that have good correlation properties is limited, by allowing some correlation adaptively depending on the other system, channel, and transceiver parameters, the overall capacity of the system can be increased. The correlation properties can also be changed adaptively to provide desired properties over a zone depending on other channel selectivity parameters.

Interference selectivity can be considered how the interfering sources (such as co–channel interference (CCI) and adjacent channel interference (ACI)) are affecting the desired signal in different dimensions of electrospace. For example, interference can be a strong narrowband interference or

wideband interference indicating the selectivity of the interference in spectrum, as presented in Table 3.1. Similarly, interference can hop across the spectrum over time which might correspond the time selectivity of interference. Interference might also be selective over other dimensions such as space or code as discussed earlier.

### 3.2.2 Channel Quality (link quality) Measurement

Channel quality estimation, by far, is the most important measure that can be used in adaptive receivers and transmitters [63]. Different ways of measuring quality of the radio channel exist and many of them are done in the physical layer using baseband signal processing techniques. In most of the adaptation algorithms, the target quality measure is either frame–error–rate (FER) or bit–error–rate (BER), where FER (or BER) is the ratio of the erroneous frames (or bits) relative to the total number of frames (or bits) received during the transmission. FER and BER are closely related to higher level quality of service parameters such as speech and video quality. However, reliable estimation of these qualities requires numerous measurements and this causes delays in the adaptation as the process can be very long. Therefore, other types of channel quality measurements, which are related to FER and BER, might be preferred. When the received signal is impaired only by white Gaussian noise, analytical expressions can be found relating the BER to other measurements. For other impairments such as colored interferers, numerical calculations and computer simulations that relate these measurements to BER can be performed. Hence, depending on the system, the channel quality is related to the BER. Then, for a target BER (or FER), a required signal quality threshold can be calculated to use it with the adaptation algorithm.

The measurements can be performed at various points of a receiver or protocol stack, depending on the complexity, reliability, and delay requirements. There are trade–offs in achieving these requirements simultaneously. Figure 3.2 shows a simple example where some of these measurements can take place. In the following sections, these measurements will be discussed briefly.

The received signal strength (RSS) estimation provides a simple indication of the fading and path loss, and provides the information about how strong the signal is at the receiver front end. If the RSS exceeds a threshold, then the link is considered as "good." Measuring the signal strength of the available radio channels can be used as a part of the scanning and intelligent roaming process in cellular systems. Also, other adaptation algorithms, such as power control and hand–off can use this information. The RSS measurement is simply done by reading samples from a channel and averaging

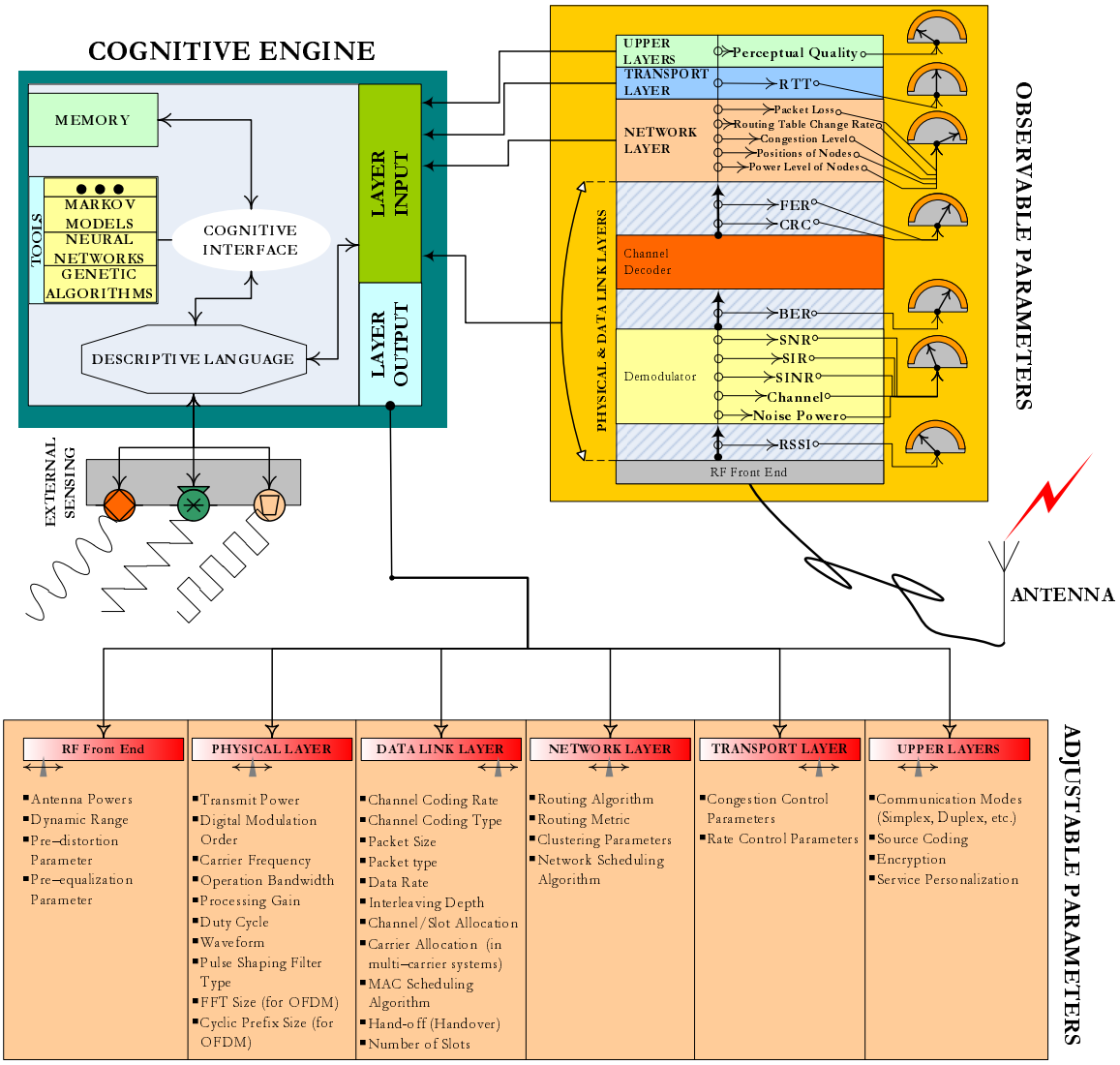


Figure 3.2 A conceptual model of CR including external sensing capabilities to improve estimations and to attain global adaptation along with observable and adjustable parameters across the protocol stack.

these samples [64]. Compared to other measurements, RSS estimation is simple and computationally less complex, as it does not require processing and demodulation of the received samples. However, the received signal includes noise, interference, and other sorts of channel impairment. Therefore, observing a good signal strength does not tell much about the channel and signal quality. Instead, it indicates whether a strong signal is present or not in the channel of interest.

The signal–to–interference ratio (SIR), signal–to–noise ratio (SNR), and signal–to–interference–plus–noise ratio (SINR) are the most common ways of measuring the channel quality during (or just after) the demodulation of the received signal. SIR (or SNR, or SINR) provides information about how strong the desired signal is compared to the interferer (or noise, or interference plus noise). Most wireless communication systems are interference limited; therefore, SIR and SINR are more prevalent. Compared to RSS, these measurements provide more accurate and reliable estimates at the expense of computational complexity and additional delay.

There are many adaptation schemes where these measurements can be exploited. Link adaptation (adaptive modulation and coding, rate adaptation, and so forth), adaptive channel assignment, power control, adaptive channel estimation, and adaptive demodulation are only a few from countless applications [63, 65–67].

SIR estimation can be employed by estimating the signal power and the interference power separately, and then by taking the ratio of these two. In many new generation wireless communication systems, coherent detection, which requires estimation of channel parameters, is used. These channel parameter estimates can also be used to calculate the signal power. The training (or pilot) sequences can be used to obtain the estimate of SIR. Instead of using a training sequence, the data symbols can also be used for this purpose. For example, in [63, 68], where SNR information is used as a channel quality indicator for rate adaptation, the cumulative Euclidean metric corresponding to the decoded trellis path is exploited for channel quality information. There are several other SNR measurement techniques available in the literature, which can be found in [69, and references therein].

Note that since both channel of the desired signal and conditions of the interferer change rapidly, depending on the application, both short– and long–term estimates would be desirable. Long–term estimates provide information on long–term fading statistics due to shadowing and log–normal fading as well as average interference conditions. Short–term measurements, on the other hand, provide measurements of instantaneous channel and interference conditions. Applications such as adaptive channel assignment and hand–off prefer long–term statistics, whereas applications such as adaptive demodulation and adaptive interference cancellation prefer short–term statistics.

For some applications, a direct measure of the channel quality from channel estimates would be sufficient for adaptation. As mentioned above, channel estimates only provide information about the power of the desired signal. It is a much more reliable estimate than RSS information, as it does not include the other sorts of impairment as part of the desired signal power. However, it is

less reliable than SNR (or SINR) estimates, since it does not provide information about the levels of noise and/or interference power with respect to the power level of the desired signal.

Channel estimation for wireless communication systems has a very rich history. Significant amount of work has been done for various systems. For the details of channel estimation for wireless communication systems, the readers may refer to [70, 71, and references therein].

Channel quality measurements can also be based on post–processing of the data (after demodulation and decoding). BER, symbol–error–rate (SER), FER, and cyclic redundancy check (CRC) information are some of the examples of the measurements falling in this category. CRC indicates the quality of a frame, which can be calculated using parity check bits through the use of a known cyclic generator polynomial. FER can be obtained by averaging the CRC information over a number of frames. In order to calculate the BER, the receiver needs to know the actual transmitted bits, which is not possible in practice. Instead, BER can be calculated by comparing the bits before and after the decoder. Assuming that the decoder corrects the bit errors that appear before decoding, this difference can be related to BER. Note that the comparison makes sense only if the frame is error–free (good frame), which is obtained from the CRC information.

Although these estimates provide excellent link quality measures, reliable estimates of these parameters require observations over a large number of frames. Especially, for low BER and FER measurements, extremely long transmission intervals will be needed. Therefore, for some applications these measures might not be appropriate. Note also that these measurements provide information about the actual operating condition of the receiver. For example, for a given RSS or SINR measure, two different receivers which have different performances will have different BER or FER measurements. Therefore, BER and FER measurements also provide information on the receiver capability as well as the link quality.

Measures after speech or video decoding: The speech and video quality, the delays on data reception, and network congestion are some of the parameters that are related to user's perception. Essentially, these are the ultimate quality measures that need to be used for adaptive algorithms. However, these parameters are not easy to measure, and in many cases, measurements in real–time might not be possible. On the other hand, these measures are often related to the other measures mentioned in the previous subsections. For example, speech quality for a given speech coder can be related to FER of a specific system under certain assumptions [72]. However, as discussed in [72], some frame errors cause more audible damage than others. Therefore, it is still desired to find

ways to measure the speech quality more reliably (and timely), and to adapt the system parameters accordingly. Speech (or video) quality measures that take the human perception of the speech (or video) into account would be highly desirable.

Perceptual speech quality measurements have been studied in the past. Both subjective and objective measurements are available [73]. Subjective measurements are obtained from a group of people who rate the quality of the speech after listening to the original and received speech. Then, a mean opinion score (MOS) is obtained from these feedbacks. Although these measurements reflect the exact human perception that is desired for adaptation, they are not suitable for adaptation purposes as the measurements are not obtained in real–time. On the other hand, the objective measurements can be implemented at the receiver in real–time [74]. However, these measurements require sample of the original speech at the receiver to compare the received voice with the undistorted original voice. Therefore, they are not applicable for many scenarios either.

### 3.3 Other Parameters

The parameters that have been discussed so far are measured using the received signal and in many cases, these parameters are obtained using baseband signal processing techniques of the signal over the transmission bandwidth. Therefore, from the CR perspective, we can classify the methods to evaluate the parameters mentioned up to this point as "internal sensing." However, the sensing and measurement capabilities should not be limited to the internal sensing, or in other words, to the parameters that can be obtained from the received signal. Because, there are some other parameters that cannot be quantified solely by internal sensing such as measuring the light intensity and the temperature of the environment to understand if the device is inside or outside a building [75]. For these sorts of measurements, CR needs "external sensing" capabilities as well. Recently, we see that many wireless devices come along with some stand alone sensing capabilities embedded. Therefore, the devices such as camera/video phones, voice recognition capable wireless units, geolocation capable terminals can be used to obtain additional information about the users' perception and even about the environment on which the device is operating. In other words, through external sensing, CR takes advantage of the additional capabilities to improve its adaptation.

In this sequel, we must state that there are some types of measurements that can be counted in both internal and external sensing. For instance, estimation of the location of a mobile device can be established through base stations depending on internal sensing parameters such as RSS. On the

other hand, a Global Positioning System (GPS) embedded device can do the same thing, which is counted in external sensing.

One of the prominent adaptation parameters of CR is the characteristics of the environment, which can be obtained through external sensing. It is known that the wireless channel is highly dependent on the environment. Environmental dependency manifests itself in terms of previously discussed statistical parameters of the wireless channel. Under different geographical environments, delay spread statistics change drastically such as in hilly terrain area and rural area. Also, some of the environments inherently have less mobility as compared to the others, which determines the crucial factor for Doppler spread. It is not very likely to have users with very high speed mobility in an indoor environment. On the contrary, in rural areas, the mobility of the users can be much more than that in indoor. Similarly, angle spread highly depends on the surrounding environment of the wireless device in connection with the number of scatterers around. Considering that there are numerous statistical models related to almost every sort of environment in the literature, CR can take advantage of these models by choosing the one which fits the best. However, selecting the best model includes a major challenge: classification of the propagation environment. This challenge stems from the following two facts: (I) Obtaining the topographical characteristics of the surrounding environment and (II) absence of the formal descriptions of the environments presented in the literature. (I) can be overcome through the use of digital elevation models (DEM) (and recently Geographical Information System (GIS)) of the geographical area of interest. These are easy to be processed data and when combined with spatial interpolation methods, they can provide CR with some hints about the topographic characteristics of its surrounding environment.

In (I), CR faces a sort of pattern recognition problem. Because, CR needs to match the characteristics of the environment with the environmental classification. Unfortunately, there is not any formal definition for propagation environments in the literature. However, there are some properties peculiar to each environment to some extent. For instance, as stated in [75], distinguishing indoor from outdoor is possible, through light and temperature. Similarly, for outdoor environments, the topographical characteristics of a hilly terrain can be used to distinguish it from rural area.

Another challenge hidden in both (I) and (II) is to represent the raw data obtained through external sensing and to classify them in a formal way for matching operation, respectively. This is established with the aid of a special descriptive language that allows CR to represent entire universe through semantics [75]. With the aid of this language, CR is able to not only deduct information in

the presence of several external data source such as GPS and DEMs, but also adjust its parameters through SDR.

Since CR can represent the raw data and characteristics in a semantic way, by using its formal tools such as neural network and hidden Markov models, the characteristics of the environment can be selected appropriately [1]. In this sequel, it must be mentioned that, the additional sensing capabilities come at the expense of additional hardware and processing, which also means power consumption as well. Besides, the tools with which CR is equipped and cognition cycle bring additional burden onto the system in terms of delay, power consumption, and overhead.

As a final remark, we can state that it is possible for CR to combine internal and external sensing to improve the reliability of the estimates. In light of these pieces of information, a conceptual model of CR including external sensing capabilities is shown in Figure 3.2.

In accordance with the discussion above, some of the important measurements for future CR applications are briefly discussed below:

- Geolocation information for CR: Geolocationing and GPS are becoming popular due to the low power and low complexity implementation of these services, which can be embedded into other wireless devices. Beside providing the physical coordinates of the mobile user (or terminal), the geolocationing (or GPS) information can also be used to improve the wireless communication systems in many layers. Even though the use of the GPS in improving the communication functionalities does not have a long and rich history, recently many researchers started integrating the GPS information to enhance other various aspects of wireless systems. For example, some studies for GPS–aided services in cellular networks (such as the traffic and navigation services, improved hand–off, channel, and cell assignment techniques); improved MAC layer protocols in an ad–hoc networks, which eliminates the hidden terminal and exposed terminal problems; efficient multi–hopping scheme in ad–hoc cellular networks by broadening the coverage area of the base station by means of exploiting the location information of mobile devices are some samples from the previous studies that show how the GPS information can be incorporated into the wireless systems.

- LOS and non–line–of–sight (NLOS) measure of the channel: line–of–sight (LOS) and NLOS measures can be very useful for the future wireless communication systems. The radio signal transmission for LOS and NLOS is different. For example, radio transmission over millimeter

waves (above 10GHz) requires LOS. However, in microwave bands LOS is not necessary. Similarly, radio channel model will be different in both LOS/NLOS scenarios, which affects the performance of the overall network [23, 76–78]. Therefore, the transceiver performances will be highly dependent on the knowledge about the existence of LOS.

The LOS measurement can be obtained from the received signal by looking at the first–order channel statistics and finding the likelihood of whether these statistics fit the LOS or NLOS channel [79, 80] as well as examining the second–order statistics of the channel [5, 6]. Also, this information can be obtained by using additional sensing capabilities that are discussed above. As mentioned earlier, the estimation of LOS/NLOS needs a great deal of research.

- Network measurements: There are several measures in the network layer that can be used for improved adaptive systems design and cross–layer adaptation. automatic repeat request (ARQ) rate for non–real time data communication, mean and peak packet delay, routing table and routing path change rate for wireless ad–hoc and sensor networks, absolute and relative locations of nodes (location awareness), velocity of nodes, and direction of movement are some of the important measurements that can be used for improving the network performance.

  Note that the parameters that are measured in different layers can affect the adaptation parameters across several layers. This can be considered part of the cross–layer adaptation. For example, physical layer estimated parameters are often related to the adaptation parameters in physical, medium access control (MAC), and other layers of the protocol stack. Therefore, the network layer measurements discussed above should not be perceived as the measurements to improve only the network performance. They can also be used to improve the performance across many layers.

  Note also that, often one parameter, say about the channel, can affect more than one adaptation parameter. For example, SNR (or link quality) measure can be used for adapting the modulation, coding, transmitted power, or other adaptation parameters such as the packet delay in networking layer. Therefore, several adaptation parameters should not be changed independently based on the (single) quality measure, as the change of one adaptation parameter might effect the measured value. Hence, the adaptation of the system parameters should be done in a global manner by considering the relation among them, leading to the cross–layer

design approaches. In this regard, some of the adjustable parameters according to the layers in which they are defined are presented in Figure 3.2.

Another important issue related to the network measurements is the awareness of the user's terminal about the possible networks and other wireless terminals around it. This is very critical for many applications, especially for emergency, disaster relief, and rescue operations. The transmission of other possible devices can be observed by sensing the spectrum, extracting the data from the other users transmission, processing it, comparing it with some *a priori* information (such as standard information), and making a decision about the existence of a possible network. Currently, high–end signal analyzers designed by measurement companies are capable of doing this kind of measurements, but, with extremely expensive, power hungry, and bulky measurement devices. However, the goal is to implement such capabilities in wireless terminals with reasonable hardware and signal processing complexities. Hence, this area needs a significant amount of research, as well.

- Situation (context) awareness: This includes determining (measuring) the user's needs, preferences, activity, circumstances, and user's behavior (*e.g.*, tasks, habits). The previously discussed user's perception of the services can also be included into user's awareness. Even the user mobility, geographical location, and some other measurements discussed earlier can be considered within this context, as well. These measures often can not be obtained from the received signal. Therefore, additional sensing and learning capabilities are needed. As mentioned earlier, the evolution of mobile devices and networks will allow additional sensing capabilities that will make estimation of physical environment (*e.g.*, geographical location, ambient conditions) as well as other possible user contexts possible. Various sensor technologies can be included in the mobile terminal that can sense things like who the user is, where he/she is, what the environmental conditions (such as the temperature, the noise level, or the illumination conditions) are, and what the user is doing, what the mood of the user is, and so on and so forth. All these estimates would be very useful to improve the network and service performance. The wireless networks and services can use these measures to adapt themselves to the user's needs, preferences and circumstances, and cooperate with their environment to provide an optimal user experience.

### 3.4 Discussion and Future Directions

In this chapter, several measurement approaches for adapting and improving the radio network and transceiver performances are presented. These measurements and possible future extensions of the list will allow the CR concept to become a reality. The wireless communications community has already started seeing some partial adaptive and cognitive features integrated into the current generation wireless standards. There is no doubt that the future standards will include more cognitive capabilities.

In many wireless standards, some of the parameters discussed here are measured by the network terminals. For instance, received signal strength indicator (RSSI), CPICH Ec/No, and CPICH RCSP are some of the items to be measured by user equipments (UE) in Universal Mobile Telecommunications System (UMTS), whereas Ec/Io is one of the parameters to be measured in 1×EV-DO. In Worldwide Interoperability for Microwave Access (WiMAX), carrier–to–interference–plus–noise ratio (CINR)/SINR is measured for the same purpose by mobile stations (MS). In Third Generation Long Term Evolution (3GLTE), reference symbol received power (RSRP) is measured by UEs as a counterpart of RSSI measurements in some other standards [81, and references therein]. Also, SINR sort of measurements are available in 3GLTE for the purpose of network management [9]. The recent 802.11k standard defines some radio resource measurement parameters to facilitate network management and performance enhancement. Several parameters are listed and defined as mandatory and optional radio measurements within all of these standards. However, these defined parameters are still very limited, and only aimed for a specific standard, even though the list is more enhanced compared to the other earlier standards [82, and references therein]. It is expected that as wireless standards evolve further, some other parameters that need to be measured will emerge and such lists need to be extended accordingly.

In parallel to these measurement parameters and relations between them, relevant challenges from the perspective of adaptive radio systems pushes the research towards the realization of CR. In this aspect, there is a strong urge in the wireless community toward the cooperative sensing that facilitates nodes which have CR capabilities [83]. For instance, CR capability nodes are employed in [84] in order to establish cognitive sensing tasks. Furthermore, in [85], the evaluation of the pieces of information gathered through sensing operation is established by the manager nodes (peculiar

to [85], these manager nodes are assumed to be base stations (BS)) with a certain protocol.[2] Thus, it is easy to conclude that some of the promising research topics regarding measurements of CR include cooperative sensing using multiple devices that communicate each other via networks which could be assisted by a manager node in the network side and opportunistic spectrum usage in the presence of primary users in orthogonal frequency division multiple access (OFDMA)–based technologies.

[2] A detailed discussion pertaining cooperative sensing with CRs is given in [86], whereas a survey that is devoted to cognitive sensing can be found in [87].

# CHAPTER 4

# IDENTIFICATION OF LOS IN TIME–VARYING, FREQUENCY SELECTIVE RADIO CHANNELS

## 4.1 Introduction

One of the most important properties of propagation channels for wireless communications is the presence of line–of–sight (LOS) between the transmitter and receiver. Having LOS affects some of the crucial parameters of both the transmission system design and the applications. Transmission frequency (or wavelength) is one of the parameters exemplifying the impact of LOS on the system design. Radio transmissions over millimeter waves (above 10 GHz) require LOS, whereas LOS is not necessary in microwave bands. This stems from the fact that significant transmission losses occur while millimeter waves travelling through environment. In millimeter wave bands, atmospheric absorption caused by gases and water vapor leads to very high signal attenuation. Similarly, rain drops cause scattering since the size of drops are on the order of millimeters. Apart from that, foliage losses are also very significant for millimeter wave bands. In addition, it is known that diffusion provides less power at the receiver than specular reflected power and shorter wavelengths suffer from greater diffusion compared to longer wavelengths [88]. Considering all these aspects together, special standards are established for LOS transmission such as 10–66 GHz portion of the physical layer part of IEEE 802.16. Another design parameter on which LOS has a considerable impact is the transmission bandwidth of the system. Measurements show that power delay profiles (PDP) of ultra–wide band (UWB) transmission are affected drastically by the presence/absence of LOS compared to those of non–UWB systems [89–91].

Ranging and positioning are two prominent examples of wireless communication applications on which LOS has significant effects. Currently, there are numerous ranging and positioning applications such as enhanced 911 emergency calling systems (E–911) [92], criminal tracking, and lost patient locators [93]. In ranging and positioning applications, it is extremely important to know the status of the multipaths received at the receiver. Assume that there is LOS between transmitter and receiver

and this is identified by the ranging system of interest. Since the system knows that LOS exists, the time–of–arrival (ToA) estimate can easily be used for calculating the distance between transmitter and receiver by simply multiplying the speed of the wave used (in radio transmission, of course, it is assumed to be speed of light, $c = 3 \times 10^8$m/s) with it. However, this is not true for non–line–of–sight (NLOS) cases, since there is no direct path between transmitter and receiver. Therefore, ToA estimates introduce estimation bias into the calculations under NLOS [94]. Moreover, knowledge of being in LOS determines also the method to be used in estimating ToA. Maximum likelihood based estimators are employed for LOS cases, whereas maximum *a posteriori* based estimators are employed for NLOS cases. Note that maximum *a posteriori* based estimators are computationally more complex than maximum likelihood based estimators. Hence, indirectly, LOS status of the transmission has an impact on the ranging and positioning applications [95].

In conjunction with ranging and positioning, knowledge of being in LOS or NLOS can be used in adjusting some parameters of wireless networks as well. For instance, some specific types of networks such as ad–hoc networks, need the geometric characteristics of the environment to improve their communication performances. Due to their dynamic structures, determining the ranges between network nodes as accurately as possible is extremely important to optimize the routing scheme. This is known as "location awareness" [96].

Since identification of LOS provides wireless networks with some sort of awareness, it is worth mentioning a recently emerging technology which depends heavily on "awareness": cognitive radio. Cognitive radio is defined as an adaptive radio system that can sense, be aware of its surrounding environment, and change the transmission parameters according to its observations and past "experiences" [97]. Having these capabilities in hand, a cognitive device that can identify the LOS status of the transmission can easily switch to a higher order modulation, or even to a higher frequency band to obtain more data rate [5]. In parallel to transmission parameters adaptation for cognitive radio [1], cognitive positioning systems also benefit from LOS status of the transmission in terms of accuracy adaptation that they provide [98].

Due to mutually exclusive relationship between LOS and NLOS, the identification procedure is generally regarded as a composite hypothesis test in which ToA information and ranging measurements are employed [80, 95, 99, 100]. Considering that fading channel amplitudes of narrowband systems exhibit Ricean distribution under LOS transmission, the comparison of the theoretical distribution with the observed one gives an idea about LOS/NLOS status of the transmission [101].

Hypothesis testing based on distribution comparison for LOS/NLOS identification has several drawbacks in terms of time consumption and computational complexity. In order to make a reliable decision, *a priori* knowledge of the noise level of the system is essential [95]. Another method that, again, depends on the comparison of the probability distributions is examining the samples of the first tap [102]. This method has the following main drawbacks: (a) in order to obtain a reliable statistics about the distribution, observing time must be large enough; (b) the transmissions that have relatively weaker LOS component cannot be easily distinguished from other theoretical distributions like Rayleigh fading, which leads to miss–detections.[1] In order to compensate for the drawback mentioned in (a), the use of estimation of Ricean factor ($K$) has been proposed [102]. After estimating $K$, depending on the value estimated, say $\tilde{K}$, the LOS status is weighted according to a pre–defined scale. The pre–defined scale is defined over $\mathbb{R}$ and has three sections separated from each other by two $K$ levels, say $K_{min}$ and $K_{max}$, which depend on the noise level of the system. Any $\tilde{K}$ lower than $K_{min}$, namely $K \in (-\infty, K_{min})$, is regarded as Rayleigh fading (or, in other words, NLOS); any $\tilde{K}$ greater than $K_{max}$, namely $K \in (K_{max}, \infty)$, is regarded as obvious Ricean (or, in other words, LOS); for the values in between, namely for $K \in [K_{min}, K_{max}]$, a linearly changing probability value that depends on the distance to the border $K_{min}$ is assigned to the status. It is obvious that this method requires the estimation of Ricean factor ($K$).

In this chapter, a method is proposed to identify LOS for time–varying, frequency selective radio channels for coherent receivers. Given that channel and delay acquisition estimation are provided by means of coherent reception algorithms [103–107], LOS identification is performed by comparing second–order statistical characteristics of underlying processes in channel taps. Assuming that the LOS path is in the first tap, a comparison is established via coherence time and by investigating the relationship between underlying processes forming the channel taps. The contributions of this chapter can be listed as follows:

1. It is shown that in the presence of LOS, for a time–varying, frequency selective radio channel, there is a lower bound of $K$ for which the autocorrelation coefficient of the first tap always greater than those of subsequent taps when they reach their coherence time,

2. Based on the proposition above, a LOS identification method is proposed and evaluated under practical scenarios.

[1] To compare the statistics obtained to a reference one is accomplished by statistical tests, such as Pearson's test statistics [102] or Kolmogorov–Smirnov test [79].

Rest of the chapter is organized as follows: Chapter 4.2.1 introduces the channel model to be used and its second–order statistical properties. Chapter 4.2.2 provides a theoretical lower bound of $K$ for LOS identification in connection with coherence time. In Chapter 4.2.3, a method is proposed to identify LOS based on the lower bound found in Chapter 4.2.2. Chapter 4.3 presents the numerical results considering both theoretical and practical cases. In Chapter 4.4, concluding remarks are given including UWB transmission.

## 4.2 The Proposed Approach

### 4.2.1 The Channel Model

Time–varying, frequency selective radio channels can be represented at baseband in the form of:

$$h(t,\tau) = \sum_{k=0}^{L-1} h_k(t)\delta(\tau - \tau_k(t)) \tag{4.1}$$

where $L$ is the total number of multipaths, $h_k(t)$ denotes the complex, time-varying path gain corresponding to $k$–th multipath, $\delta(\cdot)$ is the Dirac delta function, $\tau$ denotes the delay axis, and $\tau_k(t)$ denotes the path arrival times [23]. At a time instant $t$, $k$–th channel tap gain $h_k(t)$ is obtained by sum of a diffuse component and a specular component as follows [33]:

$$h_k(t) = s_k(t) + d_k(t) \tag{4.2}$$

where

$$s_k(t) \quad = \sigma_{s_k} e^{j(\omega_D \cos(\theta_0^{(k)})t + \phi_0^{(k)})} \tag{4.3a}$$

$$d_k(t) = \sigma_{d_k} \frac{1}{\sqrt{M_k}} \sum_{m=1}^{M_k} b_m e^{j(\omega_D \cos(\theta_m^{(k)})t + \phi_m^{(k)})} \tag{4.3b}$$

In (4.3a), $\sigma_{s_k}$ denotes the magnitude of the specular component, $j = \sqrt{-1}$, $\omega_D$ is the maximum Doppler frequency in radian, $\theta_0^{(k)}$ is the angle–of–arrival (AoA), and $\phi_0^{(k)}$ is the phase shift for $s_k(t)$.[2]

[2]Even though $\theta_0^{(k)}$ and $\phi_0^{(k)}$ belong to specular component in $k$–th tap, in actual propagation environments, it is very unlikely to have a strong specular component in each tap. However, there are some cases in which there is specular component in both first and second taps. Nevertheless, as will be discussed in this section subsequently, this can still be treated with the aid of the concept of "underlying process."

Here, $\omega_D$ is equal to $(2\pi f_c v/c)$, where $f_c$ is the transmission frequency, $v$ represents speed of the mobile, and $c$ is speed of the propagation. In (4.3b), $\sigma_{d_k}$ denotes the magnitude of the diffused component, $M_k$ represents the number of incoming waves, $b_m$ is the amplitude and $\phi_m^{(k)}$ is the phase shift for $m$–th diffused component coming with the angle $\theta_m^{(k)}$, respectively.[3] However, it must be stated that in the method proposed, there is only one condition for (4.3b): $M_k \geq 1$. This is essential, because when $M_k = 0$, $d_k(t)$ does not exist. However, the method proposed is not limited to any other condition such as narrow–band channels, $M_k \to \infty$, or uniformly distributed $\theta_m^{(k)}$.

For the sake of completeness, the characteristics of path arrival times, namely $\tau_k(t)$, can be investigated. Since multipath effect is caused by objects in the surrounding environment, it can be concluded that path arrival times are affected by the locations of these objects. Assuming that the surrounding objects within an environment are randomly located, the path arrival statistics can be considered as Poisson process as suggested in [108]. However, the assumption that allows for randomly located objects might not be valid for urban environments, since the residential areas and buildings in urban environments have some sort of geometric structures rather than random, irregular structures. Hence, path arrival times need to be modeled in a different manner in order for the model to be realistic. One of the very well–known models for path arrival times is known as modified Poisson process [109]. Note that, $\tau_0(t)$ is deterministic rather than random in LOS cases, due to the distance–delay relationship in ranging and positioning applications mentioned earlier in Chapter 4.1.

When the autocorrelation function of (4.2) is considered assuming that uncorrelated scattering is satisfied (*i.e.*, uncorrelated attenuation and phase shift with paths of different delays exist) and the specular and diffused components are independent, the autocorrelation of $k$–th tap can be calculated as:

$$\begin{aligned} R_{h_k}(\Delta t) &= E\{h_k(t)h_k^*(t+\Delta t)\} \\ &= E\{(s_k(t)+d_k(t))(s_k(t+\Delta t)+d_k(t+\Delta t))^*\} \\ &= R_{s_k}(\Delta t) + R_{d_k}(\Delta t) \end{aligned} \tag{4.4}$$

where $E\{\cdot\}$ is the expected value operator and $(\cdot)^*$ represents the complex conjugate of its argument. For the sake of brevity, autocorrelation *coefficients* can be used in analysis instead of autocorrelation

[3] In the literature, instead of speaking of individual statistics of $b_m$s, generally, the statistics of their superposition is discussed. For instance, when narrow–band channels are considered, central limit theorem is generally applied when $M_k \to \infty$ leading to a Rayleigh amplitude distribution for $k$–th tap in the absence of LOS.

values. Autocorrelation coefficients are obtained as follows:

$$\rho_x(\Delta t) = R_x(\Delta t)/R_x(0) \tag{4.5}$$

for any random process $x(t)$. Since the specular and diffused components are previously assumed to be independent of each other, then, (4.4) can be re–organized in terms of autocorrelation coefficients as follows:

$$\begin{aligned}\rho_{h_k}(\Delta t) &= \frac{R_{h_k}(\Delta t)}{R_{h_k}(0)} \\ &= \frac{R_{s_k}(\Delta t) + R_{d_k}(\Delta t)}{\sigma_{s_k}^2 + \sigma_{d_k}^2} \\ &= \frac{K_k}{K_k+1}\rho_{s_k}(\Delta t) + \frac{1}{K_k+1}\rho_{d_k}(\Delta t)\end{aligned} \tag{4.6}$$

where $K_k = \sigma_{s_k}^2/\sigma_{d_k}^2$, which defines the power ratio between specular and diffused components and is known as Ricean factor. In the rest of the chapter, the subscript $k$ is dropped from $K_k$ for the sake of brevity. Hence, from this point on when $K$ is used, it must be understood that the Ricean factor for $k$–th tap is referred unless otherwise stated.

### 4.2.2 Bound for $K$ Parameter

Note that, (4.6) is a complex–valued function in general. Therefore, the squared envelope of (4.6) can be calculated as well:

$$\begin{aligned}|\rho_{h_k}(\Delta t)|^2 &= (\rho_{h_k}(\Delta t)\rho_{h_k}^*(\Delta t)) \\ &= \left(\frac{K}{K+1}\right)^2 |\rho_{s_k}(\Delta t)|^2 + \frac{2K\Re(\rho_{s_k}(\Delta t)\rho_{d_k}^*(\Delta t))}{(K+1)^2} + \left(\frac{1}{K+1}\right)^2 |\rho_{d_k}(\Delta t)|^2\end{aligned} \tag{4.7}$$

where $\Re(\cdot)$ denotes the real part of its argument.

In (4.7), $|\rho_{s_k}(\Delta t)|^2$ becomes unity in connection with (4.3a) and (4.5). After some mathematical manipulations (4.7) can be re–written in the following form in order to have an easier analysis in further steps:

$$|\rho_{h_k}(\Delta t)|^2 = \left(\frac{K}{K+1}\right)^2 + \frac{2K|\rho_{d_k}(\Delta t)|\cos\left(\omega_D \cos\left(\theta_0^{(k)}\right)\Delta t + \Psi(\Delta t)\right)}{(K+1)^2} + \left(\frac{1}{K+1}\right)^2 |\rho_{d_k}(\Delta t)|^2 \tag{4.8}$$

where

$$\Psi(\Delta t) = \arccos\left(\frac{\Re(\rho_{d_k}(\Delta t))}{|\rho_{d_k}(\Delta t)|}\right)$$

Note that (4.8) is composed of two parts: the part which is solely a function of $K$ (the first term to the right of equality in (4.8)) and the part which is a function of $|\rho_{d_k}(\Delta t)|$ (last two terms to the right of equality in (4.8)). From this perspective, $|\rho_{d_k}(\Delta t)|$ actually corresponds to the *underlying process* part of $|\rho_{h_k}(\Delta t)|$. An illustration of the concept of underlying processes including its relationship with the tapped delay line model is shown in Figure 4.1. Width of bins represents the resolution of the receiver over delay axis. Assume that a receiver is capable of operating on infinite transmission bandwidth. This receiver can distinguish each multipath delay, since the width of bins converges to zero. However, in reality, no receiver is capable of operating on infinite transmission bandwidth. Therefore, in reality, receivers "see" sum of multipaths falling into the same bin leading to multipath fading channel as shown in Figure 4.1. Hence, the model in (4.1) represents the observed channel. Comparing UWB receivers with traditional narrow–band receivers sheds light on this situation. In narrow–band channels fading channel amplitudes can be modeled as Rayleigh (or depending on having a dominant specular component, Ricean) process. However, this does not hold for UWB, since the time resolution of the UWB receiver (*i.e.*, width of bins) is extremely small compared to that for narrow–band systems. Therefore, even though there might be many distinct multipaths present, due to the limited capability of the receiver, "observed channel" consists of superimposed multipath components falling into the same bin. Currently, channel estimation is an essential part of coherent receivers. Receivers observe the channel through the use of several channel estimation techniques.

Peculiar to LOS scenarios, first bin includes the LOS component beside some other paths which form the diffused component defined in (4.3b). Therefore, in LOS scenarios, $h_0$ corresponds to the tap $(k = 0)$ that contains LOS component. When the taps are considered for $\bar{k}$ which defined as the set of subsequent taps $\left(i.e., \bar{k} = \{k|\ k > 0\}\right)$, the LOS component will not be present anymore. However, some measurements show that for $\bar{k}$, there may still be a relatively weaker specular component compared to the first tap [110]. Nevertheless, as will be explained in the subsequent sections, having such a component causes to have different underlying processes for the subsequent taps $\left(\bar{k}\right)$; but, it can still be treated with the method proposed. Despite it is outside the scope of this chapter, it is worth mentioning the impact of UWB transmission on the concept of underlying process as

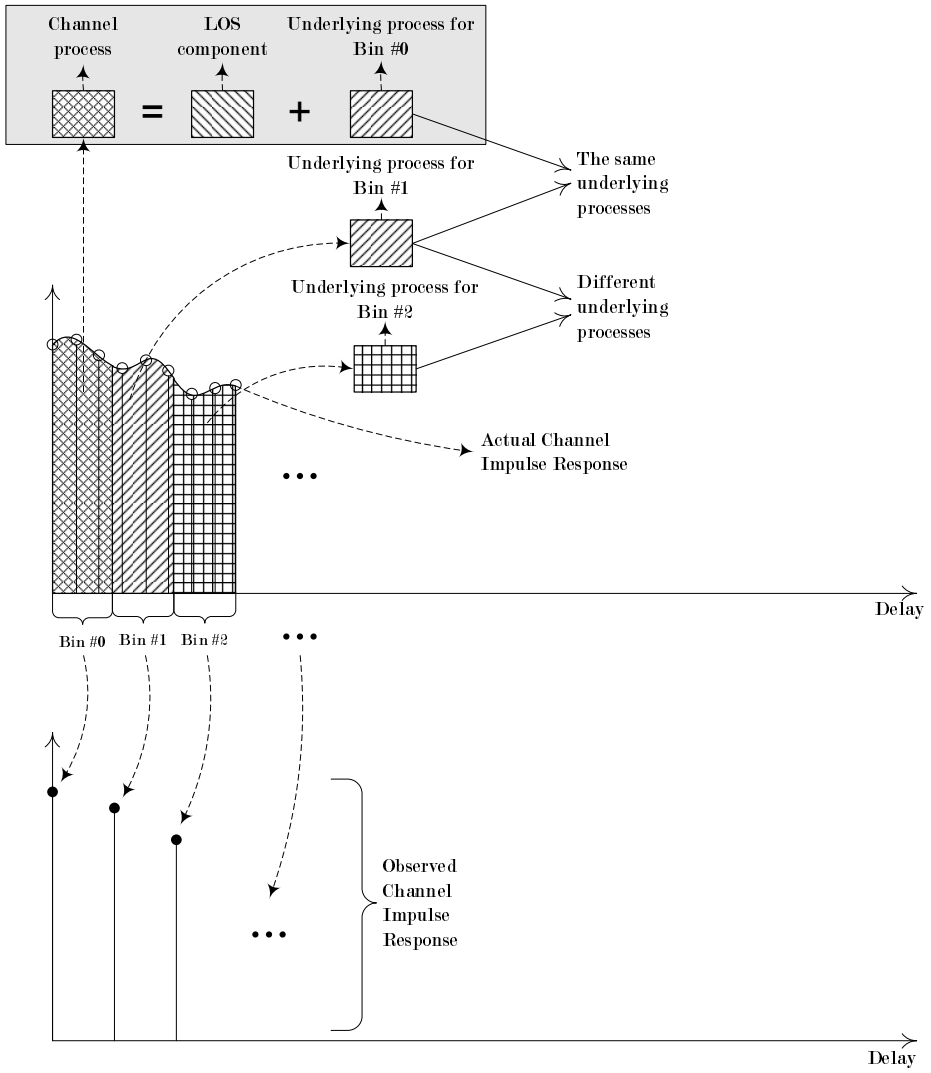


Figure 4.1 Illustration of the concept of "underlying process" and its relationship with CIR.

well. Since the increase in transmission bandwidth leads to a finer resolution in time, the width of the bins shrinks. This clearly affects the concept of underlying process, since the receiver is able to distinguish each individual path. Hence, it might not be possible for the receiver to have both specular and diffused component simultaneously within the same bin or tap. Identification of LOS in UWB cases will be discussed in Chapter 4.4.

Before proceeding into the further details of the method proposed, it is appropriate to give the definition of coherence time of a channel.

**Definition 1** (Coherence Time of A Channel [23]). *"Coherence time is the time duration over which two received signals have a strong potential for amplitude correlation." For practical purposes, the coherence time can be defined as the time duration over which the autocorrelation coefficients are above* 0.5 .

In order to establish the connection between LOS identification and statistics of the channel process, the following proposition is defined:

**Proposition 1.** *In a time–varying, frequency selective radio channel, if the first channel tap contains a specular component with $K > 3$, it will always have a higher autocorrelation coefficient compared to that of any one of the subsequent taps at the moment where any one of the subsequent taps reaches its coherence time.*

Proposition 1 includes at least two taps and their autocorrelation coefficients. Therefore, it is appropriate to consider the statistical characteristics of the processes that form these taps. In (4.8), in terms of underlying processes, there are only two possibilities for the channel that contains both specular and diffused components. The temporal statistics of the underlying process of $h_k$, namely $|\rho_{d_k}(\Delta t)|$, can be in either of the following cases:

- Case 1): the same in each tap,
- Case 2): different in each tap (or in some of the taps as illustrated in Figure 4.1).

In fact, Case 1) is a special case of Case 2). In order to see this relationship, assume that one of the subsequent taps $\bar{k}$ reaches its coherence time at $\Delta t_1$, that is $|\rho_{h_{\bar{k}}}(\Delta t_1)| = 0.5$. Let the difference between the autocorrelation coefficients of underlying processes, namely $|\rho_{d_0}(\Delta t_1)|$ and $|\rho_{d_{\bar{k}}}(\Delta t_1)|$, be defined in terms of $e(\Delta t_1)$ in a general way as follows:

$$|\rho_{d_0}(\Delta t_1)| = |\rho_{d_{\bar{k}}}(\Delta t_1)| \pm e(\Delta t_1) \tag{4.9}$$

In (4.9), note that Case 2) is identical to Case 1) for $e(\Delta t_1) = 0$. Note also that since $0 \leq |\rho_x(\Delta t_1)| \leq 1$ for any random process $x(t)$, Definition 1 requires $e(\Delta t_1) \in [0, 0.5)$ in light of (4.9). Therefore, proving solely Case 2) will be sufficient to investigate Proposition 1. However, due to the sign of

difference term in (4.9), Case 2) can be broken into two parts for $\Delta t_1$ as:

$$\text{Case 2)} := \begin{cases} \text{Case 2A),} \ |\rho_{d_{\bar{k}}}(\Delta t_1)| - e(\Delta t_1) & \text{(4.10a)} \\ \text{Case 2B),} \ |\rho_{d_{\bar{k}}}(\Delta t_1)| + e(\Delta t_1) & \text{(4.10b)} \end{cases}$$

Note that in (4.10), $e(\Delta t_1)$ is considered as an additive term. One might ask why $e(\Delta t_1)$ is modeled as an additive term instead of a multiplicative term. There are analytical reasons for $e(\Delta t_1)$ to be chosen as additive. First and foremost, multiplication is a special case of multiple addition. Second, if $e(\Delta t_1)$ were to be chosen as a multiplicative term, the result would not change; however, because of the scaling factor the domain of $e(\Delta t_1)$ would be different. Bearing in mind that $|\rho_{d_0}(\Delta t_1)|$ and $|\rho_{d_{\bar{k}}}(\Delta t_1)|$ are defined as $0 \leq |\rho_{d_0}(\Delta t_1)|, |\rho_{d_{\bar{k}}}(\Delta t_1)| \leq 1$, and $|\rho_{d_0}(\Delta t_1)| = e(\Delta t_1)|\rho_{d_{\bar{k}}}(\Delta t_1)|$; it can be concluded that $e(\Delta t_1) \in [0, 2]$ because of Definition 1 ($|\rho_{d_{\bar{k}}}(\Delta t_1)| = 0.5$). Note that the interval $[0, 1)$ corresponds to Case 2A) since $|\rho_{d_0}(\Delta t_1)| < |\rho_{d_{\bar{k}}}(\Delta t_1)|$, whereas the interval $(1, 2]$ corresponds to Case 2B) since $|\rho_{d_0}(\Delta t_1)| > |\rho_{d_{\bar{k}}}(\Delta t_1)|$. Clearly, Case 1), which is a special case of Case 2), occurs when $e(\Delta t_1) = 1$.

Now, one can proceed to investigate the two possible situations in (4.10) along with the corresponding proofs for Case 2). Therefore, first the squared–envelope of autocorrelation coefficients of $h_0$ and $h_{\bar{k}}$ must be calculated:

$$\begin{aligned} |\rho_{h_0}(\Delta t)|^2 &= \left(\frac{K_0}{K_0+1}\right)^2 + \frac{2K_0|\rho_{d_0}(\Delta t)|\cos\left(\omega_D \cos(\theta_0^{(0)})\Delta t + \Psi(\Delta t)\right)}{(K_0+1)^2} + \left(\frac{1}{K_0+1}\right)^2 |\rho_{d_0}(\Delta t)|^2 \\ |\rho_{h_{\bar{k}}}(\Delta t)|^2 &= |\rho_{d_{\bar{k}}}(\Delta t)|^2 \end{aligned} \tag{4.11}$$

Now, it will be shown that there is a lower boundary of $K_0$ ($K$ factor for the first tap) for which $h_0$ always has a higher autocorrelation coefficient value compared to those of the subsequent taps ($h_{\bar{k}}$) when they reach their coherence time.

*Proof of Proposition 1 for Case 2A).* If (4.10a) is embedded into (4.8) along with:

$$f(\Delta t_1) = \omega_D \cos(\theta_0^{(0)})\Delta t_1 + \Psi(\Delta t_1)$$

and $|\rho_{d_{\bar{k}}}(\Delta t_1)| = 0.5$, it yields:

$$\begin{aligned}|\rho_{h_0}(\Delta t_1)|^2 &= \left(\frac{K_0}{K_0+1}\right)^2 + \frac{2K_0(|\rho_{d_{\bar{k}}}(\Delta t_1)| - e(\Delta t_1))\cos\left(f(\Delta t_1)\right)}{(K_0+1)^2} + \left(\frac{|\rho_{d_{\bar{k}}}(\Delta t_1)| - e(\Delta t_1)}{K_0+1}\right)^2 \\ &= \left(\frac{K_0^2 + K_0\cos\left(f(\Delta t_1)\right) + 0.25}{(K_0+1)^2}\right) \\ &\quad + \left(\frac{e^2(\Delta t_1) - 2e(\Delta t_1)K_0\cos\left(f(\Delta t_1)\right) - e(\Delta t_1)}{(K_0+1)^2}\right)\end{aligned} \tag{4.12}$$

If (4.12) is re–written, then:

$$|\rho_{h_0}(\Delta t_1)|^2 = \underbrace{\left(\frac{K_0^2 + e^2(\Delta t_1) + 0.25}{(K_0+1)^2}\right)}_{>0\ \forall K_0,\ \Delta t_1} + \left(\frac{K_0\cos\left(f(\Delta t_1)\right)(1 - 2e(\Delta t_1)) - e(\Delta t_1)}{(K_0+1)^2}\right) \tag{4.13}$$

Recall that it is assumed that $\bar{k}$–th tap reaches its coherence time at $\Delta t_1$ (*i.e.*, $|\rho_{d_{\bar{k}}}(\Delta t_1)| = 0.5$). In this case, the lowest value of (4.13) for that specific $\Delta t_1$ is obtained if

$$\omega_D \cos\left(\theta_0^{(0)}\right)\Delta t_1 + \Psi(\Delta t_1) = (2l+1)\pi \tag{4.14}$$

is satisfied where $l \in \mathbb{Z}^+$, since $e(\Delta t_1) \in (0, 0.5)$ and the first term in (4.13) is positive for all $\Delta t_1$ and $K_0$ values.[4] Therefore, it can be re–organized as follows yielding:

$$\begin{aligned}|\rho_{h_0}(\Delta t_1)|^2 &= \left(\frac{K_0^2 - K_0 + 0.25}{(K_0+1)^2}\right) + \left(\frac{e^2(\Delta t_1) + 2e(\Delta t_1)K_0 - e(\Delta t_1)}{(K_0+1)^2}\right) \\ &= \frac{(K_0 - 0.5)^2}{(K_0+1)^2} + \frac{e^2(\Delta t_1) + (2K_0 - 1)e(\Delta t_1)}{(K_0+1)^2}\end{aligned} \tag{4.15}$$

If a change of variable is applied with $(K_0 - 0.5) = u$, then:

$$|\rho_{h_0}(\Delta t_1)|^2 = \underbrace{\left(\frac{u + e(\Delta t_1)}{u + \frac{3}{2}}\right)^2}_{\mathcal{M}_1} \tag{4.16}$$

[4]Here, note that $e(\Delta t_1)$ is defined within the open interval $(0, 0.5)$, although it is $e(\Delta t_1) \in [0, 0.5)$ in (4.9). This is because (4.9) refers to the general case including both Case 1) and Case 2), whereas the proof considers only Case 2), which excludes $e(\Delta t_1) = 0$.

is obtained. Since the condition $|\rho_{h_{\bar{k}}}(\Delta t_1)| < |\rho_{h_0}(\Delta t_1)|$ $\left(\text{or equivalently } |\rho_{h_{\bar{k}}}(\Delta t_1)|^2 < |\rho_{h_0}(\Delta t_1)|^2\right)$ is investigated:

$$\begin{aligned} |\rho_{h_{\bar{k}}}(\Delta t_1)| &< \left(\frac{u + e(\Delta t_1)}{u + \frac{3}{2}}\right) \\ 0.5 &< \left(\frac{u + e(\Delta t_1)}{u + \frac{3}{2}}\right) \\ \frac{3}{2} - 2e(\Delta t_1) &< u \end{aligned} \tag{4.17}$$

is obtained and if the change of variable is applied back while recalling $e(\Delta t_1) \in (0, 0.5)$, then:

$$2 < K_0 \tag{4.18}$$

which completes the first part of the proof of Case 2). □

*Proof of Proposition 1 for Case 2B).* Similar to Case 2A), if (4.10b) is embedded into (4.8) and the same steps between (4.12)–(4.16) are followed, it is found that:

$$\mathcal{M}_2 = \left(\frac{u - e(\Delta t_1)}{u + \frac{3}{2}}\right)^2 \tag{4.19}$$

which reads

$$3 < K_0 \tag{4.20}$$

□

Finally, proof of Proposition 1 can be unified, since all possible cases have been examined:

*Proof of Proposition 1.* Considering (4.18) and (4.20) together:

$$K \in ((K_0 > 3) \cap (K_0 > 2)) \equiv K_0 > 3 \tag{4.21}$$

is obtained and this completes the proof of Proposition 1. □

Note that, the worst case condition which is stated in (4.14) is considered in deriving both (4.16) and (4.19). Although theoretically it is possible, in order for the worst case scenario to take its place, several independent parameters must satisfy a unique condition. Assume that all the correlation properties ($|\rho_{h_k}(\Delta t)|$) of underlying processes are the same for each tap (*i.e.*, $e(\Delta t_1) = 0$). For the

sake of brevity, assume also that $\rho_{h_k}(\Delta t_1)$ is real.[5] Therefore, $\Psi(\Delta t_1) = 0$, which yields:

$$\begin{aligned} \omega_D \cos(\theta_0^{(0)})\Delta t_1 &= (2l+1)\pi \\ \Delta t_1 &= \frac{(2l+1)c}{2f_c v \cos(\theta_0^{(0)})} \end{aligned} \tag{4.22}$$

In (4.22), because $\theta_0^{(0)}$ and $v$ are two independent parameters, it is very unlikely that the worst case scenario takes its place in practical cases. As will be shown in Chapter 4.3, the condition $K_0 > 3$ can be relaxed for most of the practical cases. However, it requires further investigations to see how much relaxation can be allowed in $K_0$.

### 4.2.3 LOS Identification

Combining Definition 1 and Proposition 1, identification of LOS can be established by comparing the difference $|\rho_{h_0}(\Delta t_1)|^2 - |\rho_{h_{\bar{k}}}(\Delta t_1)|^2$ with a non–negative threshold where $\Delta t_1$ is the coherence time for $h_{\bar{k}}$, namely $|\rho_{h_{\bar{k}}}(\Delta t_1)| = 0.5$. In this regard, the identification process can formally be stated as:

$$\mathcal{T} := \begin{cases} \text{LOS}, & \text{if } \left(|\rho_{h_0}(\Delta t_1)|^2 - |\rho_{h_{\bar{k}}}(\Delta t_1)|^2\right) > z \\ \text{NLOS}, & \text{otherwise}, \end{cases} \tag{4.23}$$

where $\mathcal{T}$ denotes the status of the transmission and $z$ denotes the threshold. Note that, if the autocorrelation coefficients are known, in other words, if they can perfectly be estimated, (4.23) can detect LOS for $K_0 > 3$ with $z = 0$ as shown in (4.21). However, in practical cases, receiver deals with limited number of channel samples. Moreover, these samples might have errors due to the channel estimation process. Limited number of samples with possible errors forces the receiver to use estimations instead of the actual autocorrelation coefficients. Hence, a non–zero threshold $z$ is required in practical cases. A numerical method is applied in Chapter 4.3 in order to obtain a proper value for $z$.

In this sequel, two issues must be investigated regarding the identification procedure. First, one might want to know what happens when coherence time is reached at different time shifts. More formally, one needs to know whether the identification holds if $|\rho_{h_{\bar{k}}}(\Delta t_2)| = 0.5$ where $\Delta t_1 < \Delta t_2$. As shown in proof of Proposition 1, the identification does not depend on time shifts $\Delta t$. Identification

[5] A very well–known example set of channel models that satisfy these properties can be found in International Telecommunication Union – Radiocommunications (ITU–R) Channel Models [25].

holds as long as $|\rho_{h_{\bar{k}}}(\cdot)| = 0.5$ is satisfied, which does not consider when and how many times $|\rho_{h_{\bar{k}}}(\cdot)| = 0.5$ occurs. Second, one might want to know whether it is better to use squared–envelope $\left(i.e., |\cdot|^2\right)$ instead of magnitude $(i.e., |\cdot|)$ notation. From the analysis perspective, there is no difference between using squared–envelopes and magnitudes, because in terms of inequality, for any two arbitrary complex numbers, say $c_i$ and $c_j$, $\left(|c_i|^2 > |c_j|^2\right) \Leftrightarrow (|c_i| > |c_j|)$. However, for complex numbers, squared–envelope is obtained simply by multiplying a complex number with its complex conjugate, whereas magnitude includes one extra square–root operation in addition to complex conjugate multiplication. Squared–envelope notation is preferred regarding this fact.

### 4.3 Numerical Results

In order to test the proposed method, several simulations have been performed. Simulations can be categorized as: (i) testing the validity of the method proposed for Case 1) and Case 2) based on the assumption that channel estimation is perfect and (ii) testing the performance of the method proposed under practical scenarios. For the category (i), two different Doppler spectrum shapes are considered for the underlying processes:[6] (I) Jakes' (classical) type and (II) GAUS1 type.[7] (I) is employed in the majority of the simulation scenarios, since it is very widely used in the literature. However, (II) is used for simulating the cases in which the underlying processes are different. The following two reasons are considered in selecting GAUS1: (R1) GAUS1 type of Doppler spectrum creates one of the most challenging situations for the method proposed, since it forms an underlying process for the subsequent taps $(h_{\bar{k}})$ in which there are two strong distant scatterers; (R2) GAUS1 type of Doppler spectrum causes the autocorrelation function of the tap of interest to be a complex–valued function, whereas (I) yields a real–valued function. Three prominent Doppler spectra including the ones used in the simulations are presented in Figure 4.2.

Common parameters which are used in simulations are given in Table 4.1. Note that, in Table 4.1, the AoAs are only chosen from the interval $[0,\ \pi/2]$. This is due to the fact that $\cos(\cdot)$ is an even function and there are two nested $\cos(\cdot)$ functions in (4.8). The following main parameter subset

[6] The autocorrelation function and Doppler spectrum of a channel are dual of each other via Fourier transform. Therefore, time–varying nature of the channel can be given in either temporal (*coherence time*) or spectral domain (*Doppler spread*). In the literature, generally, time–varying nature of the channel is described by the shape of its Doppler spectrum. Hence, in this section, spectral domain name convention is adopted to emphasize the characteristics of different underlying processes.

[7] This Doppler spectrum is one of the four Doppler spectra defined in European Co–operation in the field of Scientific and Technical research (COST) 207. It is the sum of two Gaussian functions (*see* (4.24) and (4.25)). However, it is used for the taps whose delays are in $[0.5\mu s,\ 2\mu s]$ [111].

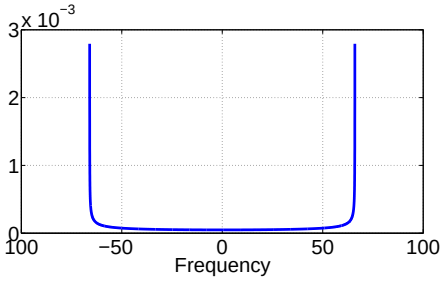


(a) Jakes' type Doppler spectrum.

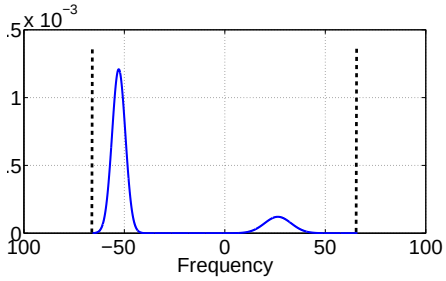


(b) GAUS1 type Doppler spectrum.

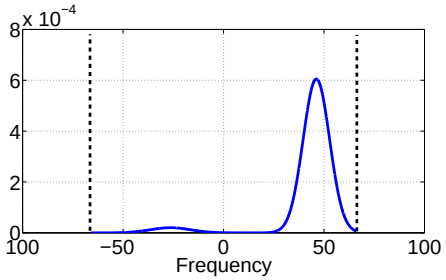


(c) GAUS2 type Doppler spectrum.

Figure 4.2 Different Doppler spectra that are encountered in different environments for 900MHz carrier frequency and a mobile speed of 22m/s.

Table 4.1 General parameter set for the simulations

| **Simulation Parameter** | **Values Used** |
|---|---|
| Transmission Frequency ($f_c$): | 900 MHz |
| Mobile Speed ($v$): | $\{1,\ 3,\ 10,\ 20\}$ m/s |
| Channel Sampling Frequency ($f_s$): | 1 KHz |
| AoA $\left(\theta_0^{(0)}\right)$: | $\{0,\ \pi/10,\ \pi/5,\ \pi/2\}$ radian |
| $K_0$ values: | $\{1, 3, 5, 10\}$ |

is used for presenting the simulation results: $K_0 = 10$, $v = 20$m/s, $\theta_0^{(0)} = \pi/5$. In addition to this subset, signal–to–noise ratio (SNR)= 10dB is employed in presenting the results for the category (ii). Here, noise is complex–valued and assumed to be white and its amplitudes are Gaussian distributed with $\mathcal{N}(0, \sigma_N^2)$. In order to reflect the influence of each parameter, results will be presented by allowing one of the variables to change while keeping the rest fixed.

For the category (i), first Case 1) is considered. In Case 1), the underlying processes are assumed to be the same, that is, of Jakes' type in both first and second taps. The results are presented in

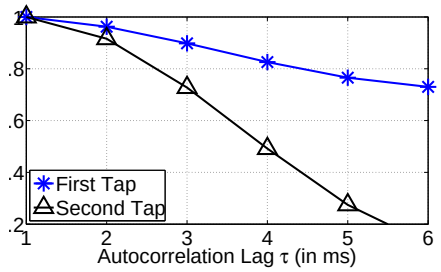


(a) $\theta_0^{(0)} = 0$

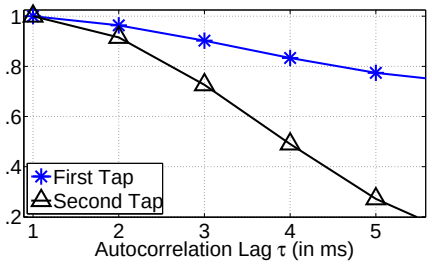


(b) $\theta_0^{(0)} = \pi/10$

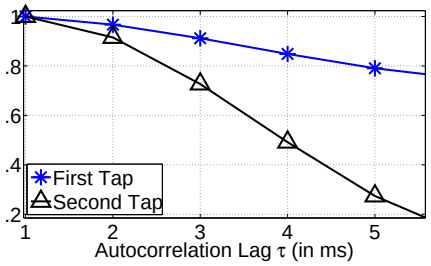


(c) $\theta_0^{(0)} = \pi/5$

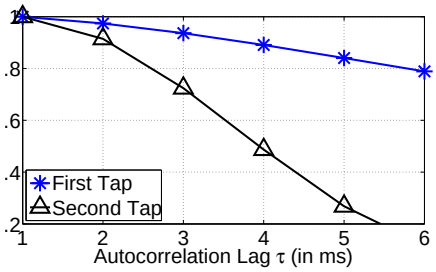


(d) $\theta_0^{(0)} = \pi/2$

Figure 4.3 Squared–envelope of the autocorrelations of first and second tap for common parameters $K_0 = 10$, $v = 20$m/s, and the set of AoA $\{\theta_0^{(0)}\}$.

Figure 4.3–Figure 4.4. In Figure 4.3, the impact of AoA is shown while $K_0$ and $v$ are fixed. When $h_{\bar{k}}$ reaches its coherence time, that is $|\rho_{h_{\bar{k}}}(\Delta t_1)| = 0.5$ (or equivalently $|\rho_{h_{\bar{k}}}(\Delta t_1)|^2 = 0.25$), the difference between $|\rho_{h_0}(\Delta t_1)|^2$ and $|\rho_{h_{\bar{k}}}(\Delta t_1)|^2$ is significant for all values of AoA. Therefore, it can be concluded that the impact of AoA, namely $\theta_0^{(0)}$, is not significant for the method proposed.

In order to evaluate the impact of $K_0$, Figure 4.5 can be investigated. It is seen that the difference between $|\rho_{h_0}(\Delta t_1)|^2$ and $|\rho_{h_{\bar{k}}}(\Delta t_1)|^2$ is very significant in Figure 4.5(b), Figure 4.5(c), and Figure 4.5(d), as expected because of Proposition 1. However, this difference is insignificant in Figure 4.5(a) compared to the cases where $K_0 > 3$.

Similar to $\{\theta_0^{(0)}\}$ and $\{K_0\}$ sets, Figure 4.4 can be investigated to determine the impact of set $\{v\}$ upon the method proposed. In Figure 4.4(a), it is seen that when speed of the mobile is close to zero, the difference between $|\rho_{h_0}(\Delta t_1)|^2$ and $|\rho_{h_{\bar{k}}}(\Delta t_1)|^2$ is not significant. However, as $v$ increases, the difference between $|\rho_{h_0}(\Delta t_1)|^2$ and $|\rho_{h_{\bar{k}}}(\Delta t_1)|^2$ increases drastically as can be seen in Figure 4.4(b),

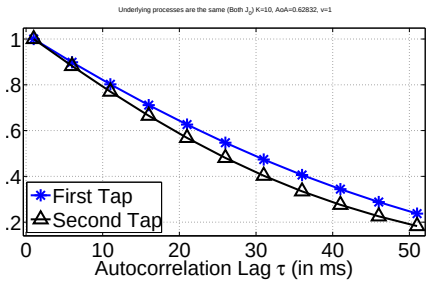


(a) $v = 1$m/s

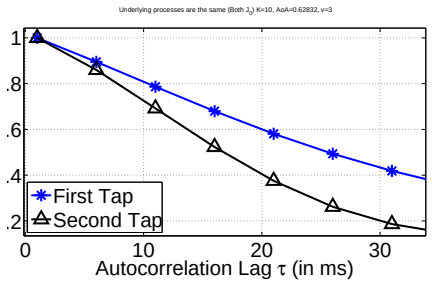


(b) $v = 3$m/s

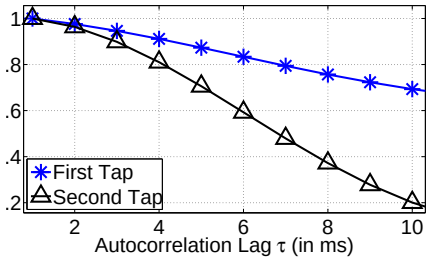


(c) $v = 10$m/s

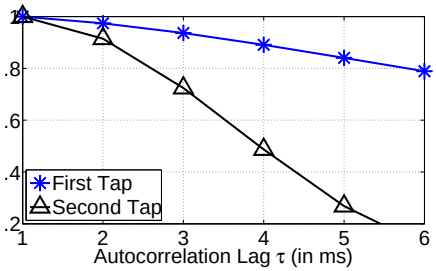


(d) $v = 20$m/s (Note that this plot is the same as Figure 4.3(c))

Figure 4.4 Squared–envelope of the autocorrelations of the first and second tap for common parameters $\theta_0^{(0)} = \pi/5$, $K_0 = 10$, and the set of $\{v\}$.

Figure 4.4(c), and Figure 4.4(d). This drastic effect of $v$ can be explained in the following way: For $v = 0$, the channel taps become time–invariant according to (4.3a) and (4.3b). Since the channel taps do not change in time, their autocorrelation coefficients become unity. This implies that the difference which is used in LOS identification gets weaker while $v \to 0$ and totally vanishes at $v = 0$ (*i.e.*, "time–invariant channel"). Conversely, for $v > 0$, the autocorrelation coefficients of the channels will differ as shown in Figure 4.4. Note also that the effect of $v$ is independent of any type of Doppler spectrum, because shape of the spectrum is determined by AoAs not by $v$.

In this sequel, it will be useful to see the cases when $K_0 \in (0, 3)$. In order to investigate this, Case 1) is considered along with (I), since it is very widely used in wireless mobile radio channel models. In these simulations, all the parameter settings and sets are maintained except for $K_0$. In addition to the one presented in Table 4.1, two more values, namely $K_{new} = \{0.5, 2\}$, are added to better see the impact when $K_0 < 3$. As can be seen from Figure 4.6, as soon as the power of specular

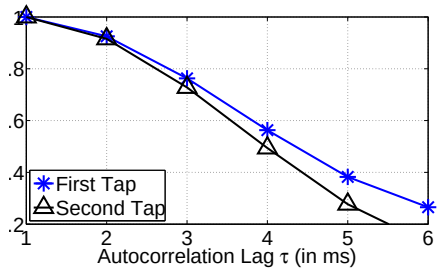


(a) $K_0 = 1$

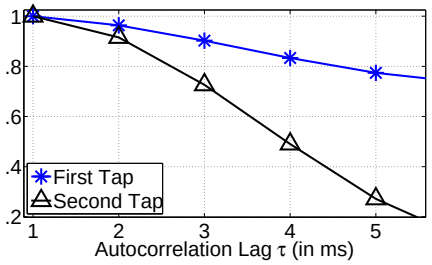


(b) $K_0 = 3$

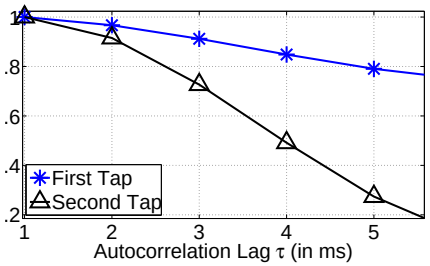


(c) $K_0 = 5$

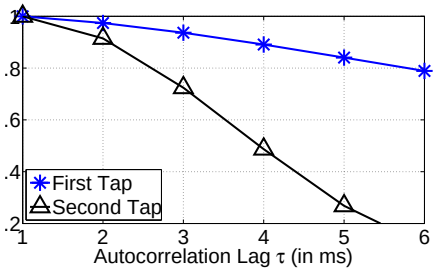


(d) $K_0 = 10$ (Note that this plot is the same as Figure 4.3(c))

Figure 4.5 Squared–envelope of the autocorrelations of the first and second tap for common parameters $\theta_0^{(0)} = \pi/5$, $v = 20$m/s, and the set of $\{K_0\}$.

component dominates, in other words when $K_0 \geq 1$, there are still cases that allow one to identify LOS even though $K_0 < 3$. This implies that LOS identification is statistically possible for even $1 \leq K_0 < 3$ in some practical scenarios, although Proposition 1 provides a universal bound for $K_0$. Furthermore, increase in $v$ causes this probability to drop even below 0.05 for time–varying specular components, namely when $\theta_0^{(0)} \neq \pi/2$. This probability increases for $K_0 < 3$ with increasing $v$ and $\theta_0^{(0)} = \pi/2$. This stems from (4.8), since $\theta_0^{(0)} = \pi/2$ makes the $\cos(\cdot)$ term depend only on $\Psi(\Delta t)$. Because $\cos(\Psi(\Delta t)) < 1$ when $\Re(\rho_{d_k}(\Delta t)) < |\rho_{d_k}(\Delta t)|$, the inequality $|\rho_{h_0}(\Delta t)| < |\rho_{h_{\bar{k}}}(\Delta t)|$ holds for some $\Delta t = \Delta t_1$. Also, $v \to \infty$ implies $\Delta t_1 \to 0$. Therefore, as $v$ increases, by the time $|\rho_{h_{\bar{k}}}(\cdot)|$ reaches its coherence time at $\Delta t_1$, $\Re(\rho_{d_k}(\Delta t))$ decreases faster and causes $\cos(\Psi(\Delta t)) < 1$ leading to lower values of $|\rho_{h_0}(\Delta t_1)|$ compared to $|\rho_{h_{\bar{k}}}(\Delta t_1)|$.

Up until this point, Case 1) is considered in simulations. However, as discussed earlier, underlying process in each channel might be different. In order to test the method proposed for Case 2)

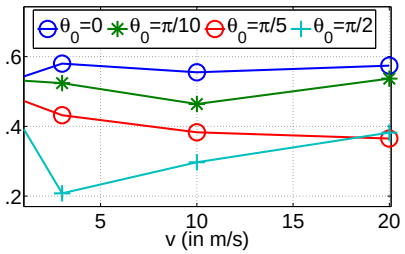


(a) $K_0 = 0.5$

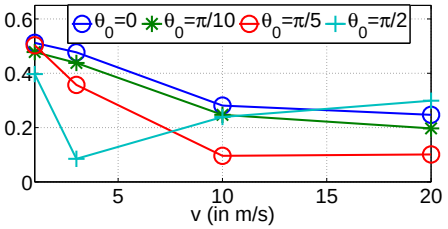


(b) $K_0 = 1$

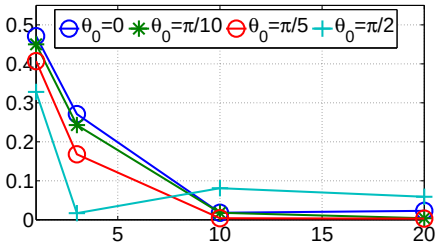


(c) $K_0 = 2$

Figure 4.6 The probability of $|\rho_{h_s}(\Delta t_1)|^2 < |\rho_{h_d}(\Delta t_1)|^2$ versus the mobile speed for different AoA.

scenarios, two diferent Doppler spectra for underlying processes are considered: Jakes' and GAUS1 type. GAUS1 type Doppler spectrum is given by [111]:

$$P(f) = G\big(A, -0.8(\omega_D/2\pi), 0.05(\omega_D/2\pi)\big) + G\big(0.1A, 0.4(\omega_D/2\pi), 0.1(\omega_D/2\pi)\big) \tag{4.24}$$

where

$$G(A, f_1, f_2) = A \exp\left(-\frac{(f - f_1)^2}{2f_2^2}\right) \tag{4.25}$$

and $A$ is the normalization constant. In Case 2) scenarios, it is assumed that the underlying process of the first tap to be of Jakes' type, whereas that of the second tap is GAUS1 based on (4.24) and (4.25).[8] Figure 4.7 shows the result for the common parameter set defined previously. As can

[8]Note that this simulation setup resembles European Co–operation in the field of Scientific and Technical research (COST) 207 Typical Urban channel model [111]. The difference is that in COST 207 Typical Urban channel model, GAUS1 is observed in the third tap, not in the second tap. Besides, the first tap consists only of the underlying process of Jakes' type without a LOS component. Since the original COST 207 Typical Urban channel model is already considered in Case 1), Case 2) simulations are established by modifying COST 207 Typical Urban channel model by providing a LOS component to the first tap and using GAUS1 type as the underlying process for the second tap.

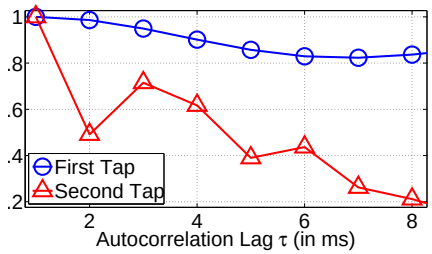


Figure 4.7 An example realization of the underlying processes which are of Jakes' and of GAUS1 type for the first and second tap, respectively.

be seen, when the second tap reaches its coherence time $\left(|\rho_{h_{\tilde{k}}}(\Delta t_1)|^2 = 0.25\right)$, there is a significant difference between $|\rho_{h_0}(\Delta t_1)|^2$ and $|\rho_{h_{\tilde{k}}}(\Delta t_1)|^2$, in accordance with Proposition 1 regardless of having different underlying processes.

As stated in Chapter 4.2.3, due to physical limitations, receivers use estimations of autocorrelation coefficients by taking limited number of slots (samples) into consideration. Therefore, the identification process is established via a non–negative threshold $z$. It must be stated that $z$ depends mainly on number of slots, $K_0$, speed $(v)$, and SNR. Therefore, it is very difficult, if not impossible, to obtain a closed–form solution to the problem of selection $z$. In this chapter, $z$ values are obtained using numerical evaluation by keeping the false alarm rate, namely $\Pr\left(LOS|\left(\mathcal{T} = NLOS\right)\right)$, at 0.05 for each specific number of slots and $v$ value along with the assumption of perfect channel estimation where $\Pr\left(\mathcal{X}|\mathcal{Y}\right)$ denotes the probability of event $\mathcal{X}$, given event $\mathcal{Y}$. As shown in Figure 4.8, desired $z$ values form a surface whose value decreases with the increase of number of slots and $v$. The threshold $z$ can be adjusted accordingly in case the receiver knows the number of observation slots and/or $v$. In the simulations of category (ii), as will be discussed subsequently, for comparison purposes, $f_s$ is 1.5KHz. The number of slots in the general parameter subset is chosen as 500 and $v$ is assumed to be unknown. Based on the results shown in Figure 4.8, the minimum of $z$ values, namely $z = 0.1$, is chosen as the threshold and performance of the method proposed is evaluated based on this value.

In category (ii), the channel estimation errors are introduced into the identification process. In order to test the performance of the method proposed, least–squares channel estimation is employed by keeping SNR=10dB along with the common parameter subset. The results are shown in Figure 4.9–4.12. It is seen from Figure 4.9 that as $N_{SLOT}$ increases, the detection rate increases, since the estimation of the autocorrelation coefficients becomes more reliable. The detection rate

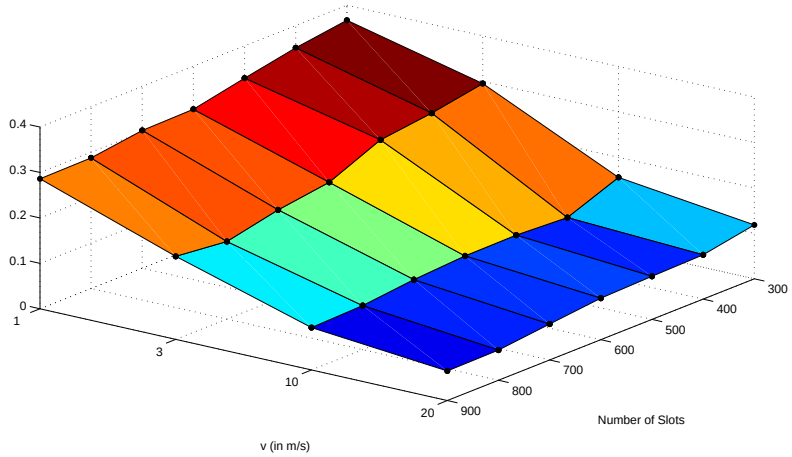


Figure 4.8 The threshold $z$ values, which keep the false alarm rate at 0.05 confidence level, for different number of slots and $v$ values.

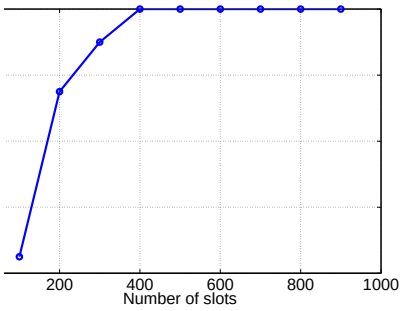


Figure 4.9 Probability of detection versus number of slots ($N_{SLOT}$) for $K_0 = 10$, $v = 20$m/s, and SNR=10dB.

becomes unity for $N_{SLOT} \geq 400$. In Figure 4.10, the impact of $K_0$ value can be observed. For the general parameter subset, even lower $K_0$ values can be detected. In order to investigate the impact of $v$, Figure 4.11 can be examined. In accordance with the discussion about the results presented in Figure 4.4, when $v \to 0$, the difference between the estimates of the autocorrelation coefficients of the taps cannot be distinguished; therefore, the detection rate is degraded. Figure 4.12 shows the impact of SNR on channel estimation and therefore identification process. For the values given in the parameter subset, it is seen that even for relatively low SNR values, the proposed method performs well.

Although the method proposed is based on the autocorrelation coefficient estimates of the channel taps, its performance in identification of LOS can be compared with those of which consider practical cases such as presented in [102]. According to [102], the method based on the comparison

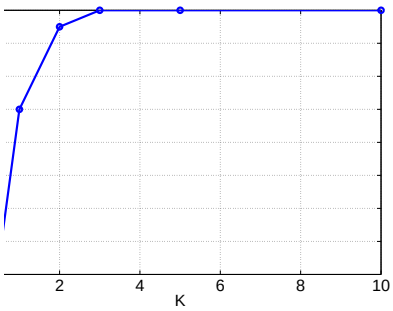


Figure 4.10 Probability of detection versus $K_0$ for $v = 20$m/s, SNR=10dB, and $N_{SLOT} = 500$.

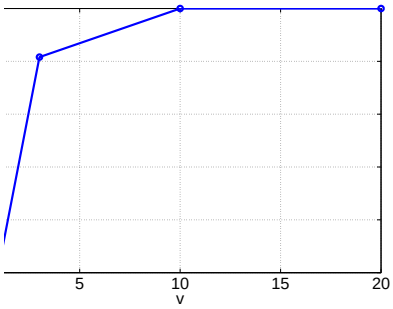


Figure 4.11 Probability of detection versus $v$ for SNR=10dB, $N_{SLOT} = 500$, and $K_0 = 10$.

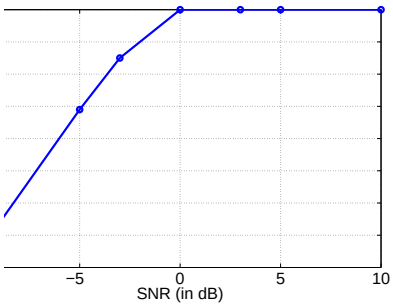


Figure 4.12 Probability of detection versus SNR for $N_{SLOT} = 500$, $K_0 = 10$, and $v = 20$m/s.

of distribution of the channel amplitudes reaches the certainty about identification of LOS after $N_{SLOT} = 880$ under a relatively fast fading channel with $v = 22.22$m/s and $K_0 \approx 35.45$ (15.5dB). With the same $v$ and $K_0 \approx 31.62$ (15dB), again in [102], the modified version of the previous algorithm reaches the certainty after $N_{SLOT} = 500$. The method proposed reaches the certainty about the identification at $N_{SLOT} = 300$ for a weaker specular component ($K_0 = 10$dB) and a lower speed value ($v = 20$m/s) via calculating the autocorrelation coefficients and a threshold value $z$, as shown in Figure 4.9. Moreover, in simulations, it is shown that for such higher $v$ values, the identification

can be established very easily for even lower $K_0$ values ($K_0 = 2 = 1.58$dB). Note that the method proposed requires neither noise level estimation nor very long observation times. Apart from that, distribution comparison based approaches collect the channel estimations and rely on the estimation of Ricean factor in addition to distribution comparison operation. However, the method proposed solely needs the channel estimation and a threshold $z$, which can be fixed or changed adaptively depending on the capability of the receiver. The method proposed does not need to estimate the Ricean factor either.

### 4.4 Concluding Remarks

LOS/NLOS is one of the very important radio propagation channel parameters. Identification of LOS helps adaptive and cognitive wireless systems to perform better from the perspective of both radio transmission and wireless applications. In this chapter, it is proven that in time–varying, frequency selective radio channels, based on the assumption that perfect channel estimation is available, autocorrelation coefficient of the first tap is always greater than those of subsequent taps ($\bar{k}$) when any one of the subsequent taps reaches its coherence time while $K_0 > 3$. Regarding this fact, a method, which is based on the comparison of the autocorrelation coefficients of the channel taps and a concept named "underlying process," is developed to identify LOS. Simulation results are presented for both theoretical and practical cases in which perfect channel estimations are not available and different Doppler spectra are considered.

Even though this chapter assumes that $M_k \geq 1$, it does not require $M_k \to \infty$. However, when UWB channels are considered, due to increased time resolution (or equivalently very large transmission bandwidth), number of resolvable paths increases, which might remove the concept of underlying process by having $M_k = 0$. In these cases, the proposed method might not be sufficient to analyze LOS with the way that is mentioned previously and illustrated in Figure 4.1. Nonetheless, it is possible to take advantage of increased time resolution by considering the frequency resolution of each path one by one [112, 113]. It is reported in [112, 113] that, with a very fine time resolution as in UWB transmission, "path history" can be extracted from the frequency dependence of each path. Since the LOS path does not have frequency dependence [113], "path history" can be used in identifying LOS in UWB cases as well.

# CHAPTER 5

# PARAMETERS AFFECTING INTERFERENCE IN NEXT GENERATION WIRELESS NETWORKS

## 5.1 Introduction

In communications system design, dealing with interference is one of the main considerations. Interference can be defined as any kind of signal received beside the desired signal and noise. Interference may occur in the following two ways depending on its origin:

1. *Self–interference*, which is caused by the own transmitted signal due to the improper system design.

   Examples include inter–symbol interference (ISI), inter–cell interference (ICI), inter–frame interference (IFI), inter–pulse interference (IPI), cross–modulation interference (CMI), and so on. Self–interference can be handled by properly designing the system and transceivers.

2. *Interference from other users*, which can be further categorized as:

   - Multi–user interference, which is the interference from users using the same system or a similar technology. co–channel interference (CCI) and adjacent channel interference (ACI) belong to this category. It can be overcome by proper multi–access design and/or employing multi–user detection techniques.
   - Interference from other types of technologies, which is a sort of interference that mostly requires interference avoidance or cancellation. It is more difficult to handle compared to multi–user interference and often it cannot be suppressed completely. narrow–band interference (NBI) is a well–known example for this type of interference.

In what follows, parameters affecting interference will be introduced and discussed.

### 5.2 Parameters Affecting Interference

Among the two types of interference listed above, the latter one (and especially co–channel interference (CCI)) draws more attention especially with the increasing demand and services in wireless communications. Emanating from the underutilization concern mentioned earlier, next generation wireless networks (NGWN) focuses on frequency reuse of one (FRO) schemes in order to avoid arduous and expensive system–wise planning step. However, FRO comes at the expense of dramatic CCI levels especially for the user equipments (UE) in the vicinity of cell borders. This fact obligates nodes in NGWNs and cognitive radios (CR) to be aware of many factors influencing interference to better perform under such conditions.

From the perspective of traditional protocol stack, there are some factors that affect CCI but cannot be populated in any of the layers, since they cannot be measured (therefore, controlled) in real–time in an adaptive manner. Weather and seasonal variations would be one of the most interesting "non–layer factors" influencing interference falling into this category. Due to the presence of high pressure air sometimes, signals can be reflected to the distances to which they are not intended [114, 115].[1] Since the signal over the same channel is able to reach the other terminal, CCI occurs.

Although cellular systems are deployed according to the theoretical models such as the use of hexagonal shape cells, in practical cases, coverage and propagation are not as regular as in the theory. Since coverage and propagation is governed by the physical environment (local topography can result in large attenuation changes over quite short distances), namely topographical and even demographical characteristics, and the traffic distribution depends also on the same factors [116, 117], "indirectly", it can be concluded that CCI is affected by physical environment as well. However, it is very difficult to model these effects, since they are mathematically intractable. Statistically speaking, one can still observe more severe in urban areas due to large number of base stations and mobiles [77, and references therein]. In indoor environments, depending on the use of devices, CCI is more likely to occur, since there are many devices (*e.g.*, microwave ovens, telephone handsets, and so on) operating on the similar bands. Especially in indoor environments, in conjunction with propagation channel properties, non–line–of–sight (NLOS) cases experience more severe interference compared to line–of–sight (LOS) cases [118]. Many possible combinations of the propagation effects

[1] For even derivations of models such as two–ray round reflection model, readers can refer [115, §3].

of several environmental characteristics with respect to interference conditions are investigated in detail in [119, and references therein].

In cellular systems, sectorization is established by replacing omni–directional antennas with narrower beam width antennas (*e.g.*, six–sector antennas of 60° or three–sector antennas of 120° openings), the capacity increases and CCI is reduced [23, 120–122].

Beamforming methods perform spatial filtering by placing comparatively sharp nulls in the direction of the interfering mobile stations, which is again related to the impact of antennas. Therefore, the interference level can be reduced significantly [123–125] If beamforming is quantified by the directivity ratio, say $d$ and $0 \leq d \leq 1$, it is reported that CCI is minimized when $d = 1$. However, the relationship between the CCI reduction and $d$ is not linear. Results are generally based on simulations [123]. Yet, it is possible to see the impact of beamforming on CCI when free–space is of interest with $P_{rx} = \frac{P_{tx}d}{4r^2}$, where $r$ denotes the distance between transmitter and receiver, $P_{tx}$ is the transmit power, and $P_{rx}$ is the received power.

Similar to antenna radiation patterns, in the literature, it is also reported that the polarization affects CCI [126]. Polarization can be used as a tool to reduce CCI relying on a method known as cross polarization discrimination (XPD). Because of XPD, when a horizontally polarized antenna receives a co–channel signal sent from a vertically polarized antenna (and the other way around), the effective signal strength is reduced by several decibels. It is also reported that the amount of XPD is reduced if the signal undergoes extensive scattering. Hence, this relationship is somehow connected to surrounding physical environment as well.

In contrast to non–layer parameters, there are many parameters that can be populated in the protocol stack. In conjunction with the discussion in Chapter 3.2.2, interference power is one of the fundamental measurement items falling into physical layer. With the emergence of CR, the term interference power gains additional concepts which have not existed before in previous communication systems such as “interference temperature” and “primary user.” Interference temperature is a sort of measure of radio frequency (RF) power that includes power of ambient noise and other interfering signals per unit bandwidth for a receiver antenna. Primary users can be defined as the users who have the higher priority or legacy rights on the usage of a specific part of the spectrum. On the other hand, secondary users are defined as those who (have lower priority) exploit this spectrum in such a way that they do not cause interference to the primary users. Therefore, secondary users need to have the capabilities of CRs, such as sensing the spectrum reliably to check whether it is being used

by a primary user and to change the radio parameters to exploit the unused part of the spectrum. Sensing the spectrum for the opportunity is therefore one of the most important attributes of CR. Although spectrum sensing is traditionally understood as measuring the spectral content or measuring the interference temperature over the spectrum, when the ultimate CR is considered, it refers to a general term that also involves obtaining the spectrum usage characteristics in multiple dimensions (including time, space, and frequency)[2] and determining what type of signal is occupying the spectrum (including the modulation, waveform, bandwidth, carrier frequency, and so forth). However, this requires more powerful signal analysis techniques with additional computational complexity. Some of the current challenges for spectrum sensing include:

- *Difficulty and complexity of wideband sensing*, which requires high sampling rate and high resolution analog to digital converter (ADC) or multiple analog front end circuitry, high speed signal processors and so on. Estimating the noise variance or interference temperature over the transmission of narrowband desired signals is not new. Such noise variance estimation techniques have been popularly used for optimal receiver designs (such as channel estimation, soft information generation, and so forth), as well as for improved hand–off, power control, and channel allocation techniques. The noise/interference estimation problem is easier for these purposes as the receiver is tuned to receive the signal that is transmitted over the desired bandwidth anyway. Also, the receiver is capable of processing the narrowband baseband signal with reasonably low complexity and low power processors. However, CRs are required to process the transmission over a much wider band for sensing any opportunity.

- *Hidden primary user problem* (such as the hidden node/terminal problem in carrier sense multiple accessing (CSMA)), which can be caused by many reasons including severe multipath fading or shadowing that the secondary user observes in scanning the primary user's transmission. The hidden terminal problem can be avoided by incorporating distributed sensing, where the information sensed between multiple terminals are shared, rather than each terminal makes the decision based on its local measurement. One of the examples of distributed sensing is known as spectrum pooling. In this technique [128], cooperative sensing decreases the probability of miss–detections and false alarms considerably. The rental users who are the users that –in case of having spectral opportunities– rent the licensed band temporarily

[2]When multi–hop systems are considered, all of these dimensions merge on transmission paths of routing which is also very important from the network layer stand point. In such scenarios, some routes might observe more interference than others [127], which carries significant importance. Note that this option is not valid in single–hop systems.

until the licensed user emerges, send their results to a base, which makes a decision and sends the final decision back to the rental users. In this type of scheme, throughout exchanging the sensing information between the base station, the mobile units may create interference to the primary users around. But, this can be overcome by a special signaling scheme which attain a reliable result very fast so that the interference to the primary users can be neglected [128]. Besides, it is again reported in [128] that, since this special signaling scheme is not involved with the medium access control (MAC) layer and directly operates on physical layer, the overhead problem on the network is minimized.

- *Primary users that use frequency hopping (FH) and spread spectrum signaling*, where the power of the primary user signal is distributed over a wider frequency even though the actual information bandwidth is much narrower. Especially, frequency hopping (FH) based signaling creates significant problems regarding spectrum sensing. If one knows the hopping pattern, and also perfect synchronization to the signal is achieved, then the problem can be avoided. But, in reality, this is not practical. Approaches based on exploiting the cyclostationarity of the signal have recently been studied to avoid these requirements. The cyclostationary based techniques exploit the features of the received signal caused by the periodicity in the signal or in its statistics (mean, autocorrelation, and so on).

- *Traffic type* is another factor that affects the interference. Statistical characteristics of the traffic type determines the evolution of interference in several dimensions such as time and frequency and helps in determining crucial quality of service (QoS) parameters such as link capacity and buffer size and in predicting bandwidth requirements. It is known that different types of traffics exhibit different statistical characteristics. Having the knowledge about the traffic type helps nodes avoid/cancel/minimize interference by different methods such as employing intelligent scheduling. However, it is worth mentioning that with the increasing services and applications, nodes in NGWNs are expected to be exposed to interference composed of several types of traffic rather than of a single type, which includes voice, multimedia, and gaming whose statistical characteristics are different from each other. Furthermore, in order to reliably characterize the network traffic, sufficient statistics need to be accumulated in real time.

- *Mobility* is crucial for wireless radio communications [129, 130]. From the perspective of interference, mobility introduces further concerns such as mobility behavior [7]. When a multi–access interference (MAI) environment is of interest, the overall interference becomes a function of mobility behavior of all of the mobile sources within the environment, which can be of individual or of group form. In case victim nodes can extract or are provided with the pattern of the mobility behavior of interfering sources, they can make use of it and improve their performances. Decentralized sensing seems to be a plausible approach for this concern which combines speed and direction information for multiple interference sources.

# CHAPTER 6

# IDENTIFICATION OF SHADOWED FAST FADING INTERFERENCE IN CELLULAR MOBILE RADIO SYSTEMS

## 6.1 Introduction

The co–channel interference (CCI) is one of the most important phenomena which needs to be taken into account in wireless network design. CCI causes very poor signal reception due to a low carrier–to–interference ratio (C/I) in the vicinity of cell borders, reduced system capacity, more frequent handoffs, and dropped calls. Therefore, identification of user equipments (UE) suffering from interference is of vital importance in order to take appropriate actions to cancel, avoid, or minimize this interference in next generation wireless networks (NGWN). One of the methods proposed for this purpose is to distinguish UEs according to their proximity to the serving base station (BS) [131, 132], which requires some sort of location sensing. received signal strength (RSS)–based techniques are proposed as well, since they are not very expensive, providing, in turn, less reliable results [133]. Due to its simplicity, energy detection (ED) approach can also be employed (after subtracting the desired part of the signal from received signal) to identify interference. However, performance of ED is drastically affected by shadow fading and noise uncertainties [134, and references therein].

In this study, an analytical method that identifies interference is proposed. Due to the fact that fast fading and shadowing processes are independent of each other and evolve on different scales, a metric based on the second–order statistics of the compound process is defined and a decision mechanism is provided. proposed method (PM) is also compared with the conventional ED approach and results are presented.

## 6.2 Statement of the Problem and Signal Model

### 6.2.1 Statement of the Problem

Consider a mobile UE (victim) over which interference is spilled on the downlink of a cellular mobile radio system with frequency division duplexing (FDD) mode of operation. In such a scenario,

the UE observes the following as complex received signal:

$$r(t) = D(t) + U(t) = D(t) + \Gamma(t) + n(t), \tag{6.1}$$

where $D(t)$ and $U(t)$ denote the desired and undesired parts, respectively; whereas $\Gamma(t)$ is the interfering signal and $n(t)$ is the ambient background noise which is assumed to be of zero–mean white Gaussian noise (WGN) form. In order to extract the desired part from the received signal, receivers generally invoke an estimation process in which training sequences, or pilot symbols, or pilot channels are used. Since the estimation might be imperfect, a widely employed error model for linear estimators in the literature is adopted for the desired part as $D(t) = \widehat{D}(t) + e(t)$, where $\widehat{D}(t)$ is the estimation itself and $e(t)$ is the estimation error modeled with an independent zero–mean complex WGN process [135, and references therein]. In this case, one can write $N(t) = n(t) + e(t)$, where $N(t)$ is assumed to be of complex additive white Gaussian noise (AWGN) form since the sum of two independent AWGNs is also of AWGN form. Thus, $r(t)$ can be represented with:

$$r(t) = \widehat{D}(t) + \underbrace{\Gamma(t) + \overbrace{n(t) + e(t)}^{N(t)}}_{\widehat{U}(t)}. \tag{6.2}$$

By subtracting $\widehat{D}(t)$ from $r(t)$ as output of the estimation, the estimated version of the undesired part is yielded via (6.2):

$$\widehat{U}(t) = r(t) - \widehat{D}(t) = \Gamma(t) + N(t). \tag{6.3}$$

Hence, the purpose is to identify the presence/absence of interference by looking at the stochastic characteristics of $\widehat{U}(t)$ which includes the interfering signal itself, ambient noise, and errors caused by imperfect estimation.[1]

### 6.2.2 Signal Model for $\Gamma(\cdot)$

When a wideband wireless signal is transmitted, it undergoes the following three effects: (E1) path loss, (E2) shadowing, and (E3) frequency–selective fading.[2] All of these effects occur on different scales of antenna displacement. Frequency–selective fading occurs more frequently compared to

[1] Notice that the purpose defined in the statement of the problem is actually the equivalent of identification of white holes by cognitive radios (CR) in the spectrum.

[2] Experiments reveal that wireless propagation causes some other phenomena to take place as well such as frequency dependent path loss. However, such effects arise in extremely large bandwidths, which is outside the scope of this study.

shadowing and to path loss. Therefore, it can be regarded as a separate stochastic process which is expressed in the baseband with $m(t) = \sum_{l=0}^{P-1} \xi_l(t) z(t - \tau_l)$ where $z(t)$ is the transmitted signal by the interferer and $\xi_l(t)$ is the $l$th complex stochastic process corresponding to $l$th delay denoted with $\tau_l$, and $P$ is the total number of paths [136]. In the literature, it is shown by adopting signal space representation that $|m(t)|$ can be represented with Nakagami–$m$ distribution which can be degenerated onto special fading distributions, such as Rayleigh or Rice distributions, with the appropriate parameter selection [136].

Path loss and shadowing can both be captured by the following single process [137, 138]:

$$s(t) = e^{(\mu(t) + \sigma g(t))}, \tag{6.4}$$

where $\mu(t)$ is path loss varying over longer periods of time; $\sigma$ is the standard deviation of log–normal shadowing, and $g(t)$ is a real–valued unit normal process $\mathcal{N}(0, 1)$ [138]. Measurements also show that $g(\cdot)$ is spatially correlated of an exponentially decaying form [139]:

$$R_g(k) = E\{g(n)g(n+k)\} = \sigma^2 \rho_g(|k\Delta t|\, v/d_\rho), \tag{6.5}$$

where $n$ denotes discrete time samples; $E\{\cdot\}$ is the statistical expectation; $\Delta t$ is the sampling period; $v$ is speed, and $d_\rho$ is the decorrelation distance at which the exponentially decaying $\rho_g(\cdot)$ drops below 0.5. Hence, interference can be represented with a compound process including path loss, shadowing, and frequency selective fading as:

$$\Gamma(t) = m(t)s(t). \tag{6.6}$$

## 6.3 Analyses

### 6.3.1 Noise–only (Interference–free) Case

As explained in Chapter 6.2, $N(t)$ containing both background noise and the estimation error is assumed to be of complex AWGN form whose real and imaginary parts are characterized by $\mathcal{N}(0, \sigma_N^2/2)$. Let $I_N(t) = |N(t)|^2$. This implies that the autocorrelation of $\ln(I_N(t))$ is found to be $R_{\ln(I_N)}(k\Delta t) = 4R_{\ln(|N|)}(k\Delta t)$ for $k \in \mathbb{Z}^+$. Note that $\ln(|N(t)|)$ is the equivalent of output of logarithm of a full–wave rectifier fed by AWGN. Therefore, in ideal cases such as having infinitely many samples at hand (*i.e.*, $|k| \to \infty$), autocorrelation coefficients (ACC) of $\ln(|N(t)|)$ are equal to

$\rho_N$ which is a constant whose value depends on $\sigma_N^2$. However, this is not achievable due to physical limitations; therefore, biased estimation of ACCs is used:

$$\rho_{\ln(I_N)}(k\Delta t) = \begin{cases} 1 & , k = 0 \quad (6.7a) \\ \rho_N\,(1 - k/L) & , |k| > 0 \quad (6.7b) \end{cases}$$

where $L$ is the total number of samples taken into account. Note that (6.7) is a straight line at non–zero lags ($|k| > 0$).

### 6.3.2 Interference–only Case

As in interference–free case, in the light of (6.6), let $I_\Gamma(t) = |\Gamma(t)|^2 = |m(t)s(t)|^2$. By plugging (6.4) into $I_\Gamma(t)$ and applying logarithm on both sides, it reads:

$$\ln\left(I_\Gamma(t + k\Delta t)\right) = 2\ln\left(|m(t + k\Delta t)|\right) + 2\left[\mu(t + k\Delta t) + \sigma g(t + k\Delta t)\right]. \quad (6.8)$$

Assuming that $k\Delta t$ is relatively short in which path loss remains constant (*i.e.*, $\mu(t) = \mu(t + k\Delta t) = \mu$), (6.8) becomes:

$$\ln\left(I_\Gamma(t + k\Delta t)\right) = \Pi + 2\left[\ln\left(|m(t + k\Delta t)|\right) + \sigma g(t + k\Delta t)\right], \quad (6.9)$$

where $\Pi = 2\mu$. Recall that $m(t)$ and $g(t)$ (therefore, their functions) are mutually independent. After some mathematical manipulations, the autocorrelation of (6.9) is found to be:

$$R_{\ln(I_\Gamma)}(k\Delta t) = \Pi^2 + 4\Pi E\left\{\ln|m(t)|\right\} + 4\left(\sigma^2 R_g(k\Delta t) + R_{\ln|m|}(k\Delta t)\right). \quad (6.10)$$

There are both deterministic (constant) and stochastic terms in (6.10). To distinguish interference–only case from noise–only case, one can focus on the stochastic part of (6.10) by assuming $\mu = 0$. In this case, the ACCs of (6.10) can be written as:

$$\rho_{\ln(I_\Gamma)}(k\Delta t) = \frac{\beta}{1+\beta}\left(\rho_g(k\Delta t) + \frac{1}{\beta}\rho_{\mathcal{M}}(k\Delta t)\right), \quad (6.11)$$

where $\beta = \sigma^2/\sigma_{\mathcal{M}}^2$, $\sigma_{\mathcal{M}}^2$ is the variance of $\ln(|m(t)|)$, and $\rho_{\mathcal{M}}(\cdot) = R_{\ln|m|}(\cdot)/\sigma_{\mathcal{M}}^2$. Notice that $\rho_{\mathcal{M}}(\cdot)$ diminishes rapidly when $1 < \beta$ (*i.e.,* when shadowing variance is large), which causes $\rho_g(\cdot)$ to

dominate (6.11). Bear also in mind that $\rho_g(\cdot)$ is the normalized version of $R_g(\cdot)$ in (6.5), which is of exponentially decaying form rather than of a straight line form.

### 6.3.3 Interference–Noise Coexistence

In such cases further analysis is not necessary, because it is clear that the ACCs of $\ln(|\widehat{U}(t)|^2)$ will not be of a straight line form due to the presence of interference. Moreover, in the presence of a strong interference, the dominant role of $\rho_g(\cdot)$ will still be observed in a similar way as denoted by (6.11). Note that the same reasoning holds as well when multiple interference sources coexist.

## 6.4 Proposed Method

In the light of the analyses in Chapter 6.3, PM evaluates the ACCs of $\ln(|\widehat{U}(t)|^2)$ at non–zero lags. Recall that (6.7) is of deterministic form (straight line), whereas (6.11) is of non–deterministic form which is driven mainly by ACCs of shadowing. Hence, if the straightness of ACCs of $\ln(|\widehat{U}(t)|^2)$ is detected, then one can conclude that interference is absent. Otherwise, one can conclude that interference is present.

Three arbitrary points on ACCs of $\ln(|\widehat{U}(t)|^2)$ are sufficient to test its straightness. For the sake of brevity, first let $\mathcal{X}(t) = \ln(|\widehat{U}(t)|^2)$ and $\rho_{\mathcal{X}}(\cdot)$ represent the ACCs of $\mathcal{X}(t)$. Let $i$th point be denoted with the pair $\mathbf{P}^{(i)}(\Delta t_i, \rho_{\mathcal{X}}(\Delta t_i))$, where $i = 1, 2, 3$, satisfying $\Delta t_1 < \Delta t_2 < \Delta t_3$. For $\mathbf{P}^{(i)}(\cdot,\cdot)$, the first term $\Delta t_i$ represents the correlation lag (abscissa), whereas the second term $\rho_{\mathcal{X}}(\Delta t_i)$ denotes the corresponding ACC (ordinate). In the PM, the first point is always fixed at first non–zero lag ($\Delta t_1 = \Delta t$) and represented with $\mathbf{P}^{(1)}(\Delta t, \rho_{\mathcal{X}}(\Delta t))$. Similarly, the third point is also fixed at the last lag ($\Delta t_3 = L\Delta t$) which is denoted with $\mathbf{P}^{(3)}(L\Delta t, 0)$. The second point, on the other hand, is obtained by waiting sufficiently long for $\rho_{\mathcal{X}}(\cdot)$ to reach a lag $\Delta t_2$ whose ordinate satisfies $\rho_{\mathcal{X}}(\Delta t_2) = \zeta\rho_{\mathcal{X}}(\Delta t)$ for any arbitrary pre–defined $\zeta \in (0, 1)$. This second point can be denoted with $\mathbf{P}^{(2)}(\Delta t_2, \zeta\rho_{\mathcal{X}}(\Delta t))$. As shown in Figure 6.1, once the ordinate $\zeta\rho_{\mathcal{X}}(\Delta t)$ is reached and corresponding abscissa of $\mathbf{P}^{(2)}$ is read, there are two possibilities in regards to the location of $\Delta t_2$ determining whether interference is absent or present. If interference is absent *i.e.*, $\mathcal{X}(t) = \ln(|N(t)|^2)$, then (6.7b) ensures that $\Delta t_2$ should coincide with $\Delta t_N = (1-\zeta)\, L\Delta t$ leading to $\mathbf{P}^{(2)} = \mathbf{P}_N^{(2)}$ as shown in Figure 6.1. Evidently, when interference exists $\Delta t_2 \neq \Delta t_N$ implying $\mathbf{P}^{(2)} = \mathbf{P}_I^{(2)} \neq \mathbf{P}_N^{(2)}$. Thus, the metric to be used in identification is given by the normalized deviation $\mathfrak{D} = |\Delta t_2 - \Delta t_N|\, L^{-1}$,

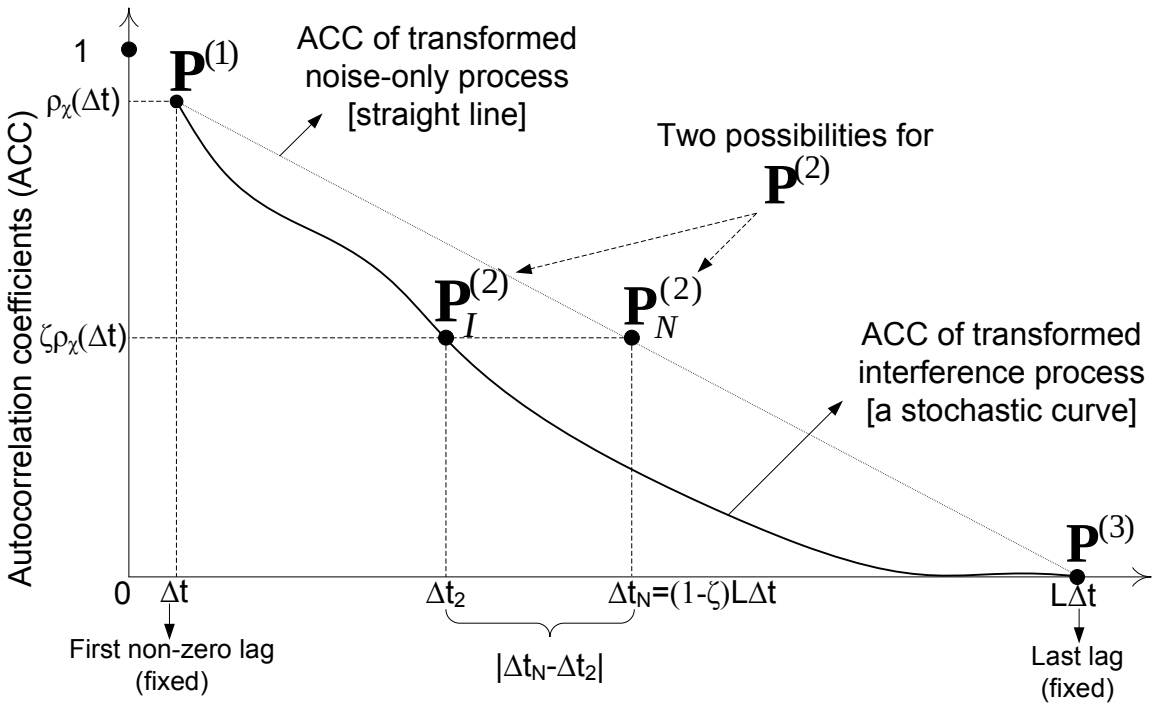


Figure 6.1 An illustration of points and notions used in the proposed method.

where $\mathfrak{D} \in [0, 1]$. Finally, the identification step can be defined by:

$$\mathfrak{M} = \begin{cases} \text{interference is present,} & \mathfrak{m} \leq \mathfrak{D} \\ \text{interference is absent,} & \text{otherwise,} \end{cases} \tag{6.12}$$

where $\mathfrak{m}$ is the normalized non–zero deviation threshold that is selected according to desired Type–I and Type–II error rates.

### 6.5 Numerical Results

In simulations, a single dominant source at 2.4GHz is assumed to interfere with a mobile UE traveling at a set of speeds $|\vec{v}| = \{3, 60, 120\}$Km/h. The sampling period $\Delta t = 1$ms and each run is 0.5s (*i.e.*, $L = 500$). Both path loss and transmit power levels of the source are assumed to be constant during a run and each run is repeated 10000 times. The most challenging scenario for the PM occurs when the UE travels with a low–speed within an environment whose $d_\rho$ is exceedingly

long such as suburbans,[3] because a sufficiently large $\mathfrak{D}$ might not be obtained in such cases. The source is assumed to transmit continuously a signal of Jakes' type Doppler with a Rayleigh faded envelope. The log–normal shadowing is imposed on the interference with $\sigma = \{4.3, 7.5\}$dB and $d_\rho = \{5.75, 350\}$m for urban and suburban environments, respectively [139]. A complex AWGN ($N(t)$) is added into the interference in order to reflect the impact of both ambient background noise and estimation error ($e(t)$) as outlined in Chapter 6.1. As described in [134, 140], $e(t)$ is assumed to introduce an uncertainty of 1dB into the background noise. Type–I and –II error rates for the identification step in (6.12) are selected to be $\mathbf{e}_{\mathrm{I}} = 0.01$ and $\mathbf{e}_{\mathrm{II}} = 0.05$, respectively. Pre–defined $\zeta$ is selected to be 0.5 to emphasize the statistical significance aspect.

In Figure 6.2, it is seen in both environments that as $\sigma_\Gamma^2/\sigma_N^2$ increases, $\mathfrak{m}$ increases too. This is because the shadowing correlation of interference becomes dominant and reveals itself in ACCs by causing $\mathfrak{D}$ to expand (*i.e.*, by deviating from the noise–like behavior). Once interference becomes the dominant part, further increase in interference power does not affect the second–order statistics much; therefore, $\mathfrak{D}$ does not expand further and $\mathfrak{m}$ converges. Also, as the speed increases, $\mathfrak{m}$ increases as well. This stems from the fact that higher $v$ values cause the ACCs of the transformed process to deviate faster from those of the straight line. Since ACCs are mainly governed by the exponential decay of $\rho_g(\cdot)$ due to shadowing as shown in (6.11), $\zeta\rho_{\mathcal{X}}(\Delta t)$ value is reached at a very early $\Delta t_2$ compared to $\Delta t_N$; therefore, a greater $\mathfrak{m}$ value is obtained.

In Figure 6.3, PM is compared with conventional ED based on probability of detection (*i.e.*, $P_D = 1 - \mathbf{e}_{\mathrm{II}}$) results when $\mathfrak{m} = 0.05$. In simulations the integration size is set to 15sample and background noise variance $\left(\sigma_n^2\right)$ is assumed to be known for the ED. It is seen that PM performs always better than ED when interference is not dominant. When interference begins to dominate (around 0dB), PM outperforms ED. Nonetheless, PM cannot reach the desired $P_D$ immediately in this region, because it still suffers from the combined impact of background noise and estimation errors which do not allow $\mathfrak{D}$ to expand. However, PM reaches the desired $P_D$ around 5dB and beyond for all speed values in both environments. When PM reaches the desired $P_D$, ED still lags behind due to intense fading (*i.e.*, large $\sigma$ and frequency–selectivity) and to mobility as investigated and presented in [134, 140, 141].

[3]Note that rural areas can also be considered as a challenging environmental class for the PM, since measurements show that their $d_\rho$ values are also on the order of a couple of hundreds of meters, implying very similar second–order shadowing correlation statistics. Therefore, for a given $\mathfrak{m}$, such an environmental difference does not cause Type–I and –II errors to deviate drastically from that for suburban environments.

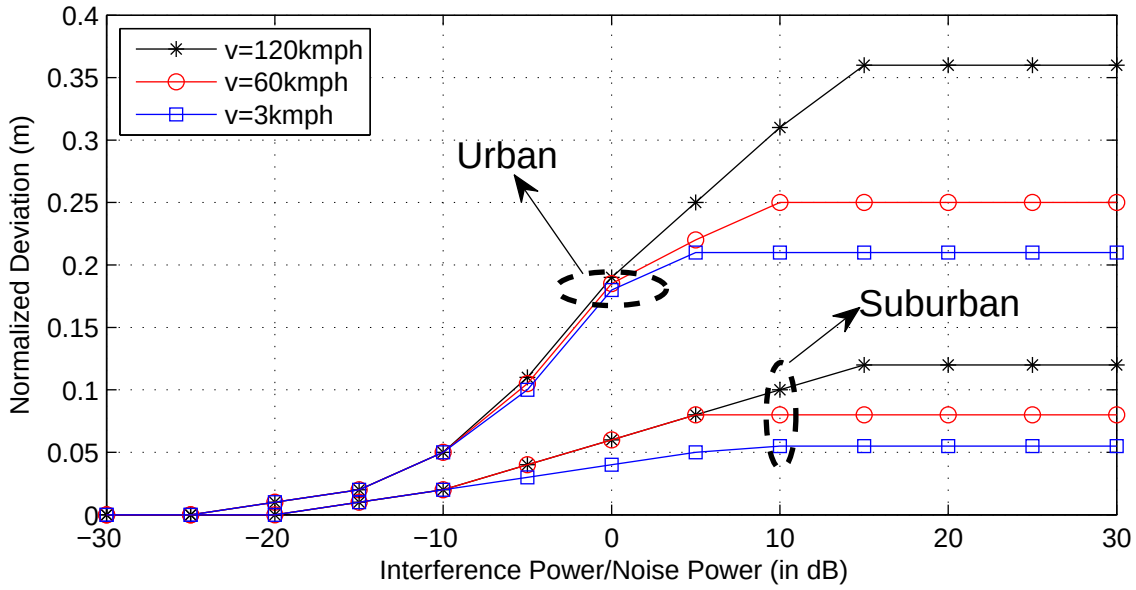


Figure 6.2 The change of $\mathfrak{m}$ with respect to $\sigma_\Gamma^2/\sigma_N^2$.

### 6.6 Concluding Remarks

UEs are required to identify interference in order to improve the overall performance in NGWNs. In this study, a second–order statistical method that identifies interference is proposed. It is shown that a generic metric can identify the interference for given reliability levels under different practical scenarios.

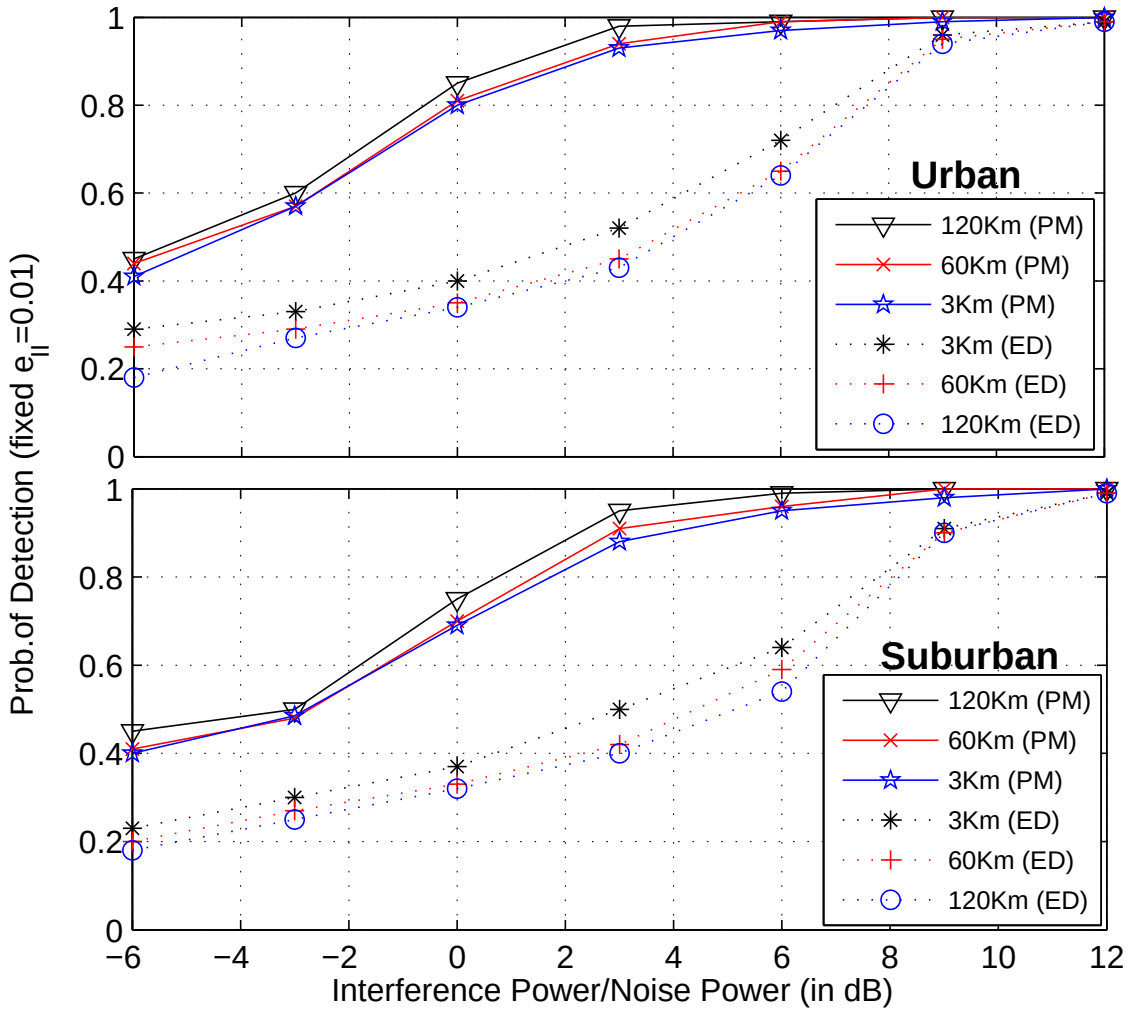


Figure 6.3 $P_D$ results with respect to $\sigma_\Gamma^2/\sigma_N^2$.

# CHAPTER 7

# PERFORMANCE BOUNDS FOR SCHEDULERS IN OFDMA–BASED SYSTEMS: VOICE TRAFFIC

## 7.1 Introduction

Due to the inherent nature of wireless communications, wireless terminals are exposed to interference. There are many types of interference such as co–channel interference (CCI), adjacent channel interference (ACI), and so on. CCI has a special place among these interference types, because it affects the overall design of a wireless system. Traditional cellular systems are designed in such a way that CCI is controlled by "reusing" frequencies in farther cells at the cost of underutilization of available resources, such as in Global System for Mobile (GSM) [23, 142]. The frequency reuse of one (FRO) is considered to be employed especially in next generation cellular mobile networks for overcoming the underutilization problem. FRO is a very promising approach, because it reduces the need for frequency planning which is a very expensive process. Nonetheless, FRO introduces significant CCI into the system especially for the user equipments (UE) residing in the vicinity of cell borders [143]. CCI can be controlled by coordinating the transmission from multiple sources [144, 145]. Interference coordination [146] and fully adaptive and dynamic resource allocation are some of the very powerful techniques to reduce CCI [144, 145, 147]. In this sense, schedulers which conduct dynamic resource allocation under FRO regime are vital units of inter–cell interference (ICI) management process in next generation wireless networks (NGWN) [148].

Traffic type plays a crucial role on behavior of interference. Therefore, ICI management is investigated in the literature by considering different types of traffic under various conditions. Combined effect of propagation and voice type traffic on CCI and performance of dynamic channel allocation for orthogonal frequency division multiple access (OFDMA)–based cellular systems are investigated in [149]. In [150], performance analysis of different scheduler schemes for ICI coordination in OFDMA–based networks is given under elastic traffic. In [151], ICI is investigated from the perspective of both streaming and elastic traffic under different frequency reuse schemes through the use

of several scheduler performance metrics such as mean number of collisions. In [152], non–real time Internet traffic is assessed for OFDMA/frequency division duplexing (FDD)–based schedulers under ICI by aiming at increasing the number of users limited to minimum rate requirements. Analytical approaches for the capacity of OFDMA–based systems in terms of resource collisions and their impacts for adaptive and elastic traffic types are provided in [153]. ICI under full–buffer type traffic is investigated in [154] from the perspective of coordination between cells. A simulation framework based on physical layer (PHY) and medium access control (MAC) layer interaction of five different traffic types with different scheduler schemes is developed for an OFDMA–based multi–cell system in [155]. Influence of different traffic types on system capacity along with scheduling operation is assessed from simulation perspective in [156]. A multi–input multi–output (MIMO)–based system under real–time traffic for OFDMA–based schedulers is investigated in [157].

Although there are many studies in the literature regarding different ICI conditions for different traffic types, to the best knowledge of authors, there is no analytical study which connects schedulers with a particular type of traffic by providing theoretical performance limits along with the factors influencing them. Performance limits and factors influencing them are key points to develop better schedulers for ICI management process in NGWNs. In this chapter, performance limits on ICI schedulers in OFDMA–based systems are derived for voice traffic based on pilot cell approach under FRO regime and factors affecting them are investigated. The contributions of this chapter is threefold. First, it is formally shown that the knowledge about the resource reservation of neighboring cell plays a crucial role on upper and lower bounds for ICI schedulers. More concretely, it is shown that theoretical upper bound corresponds to the cases that are driven by the absence of knowledge (absolute uncertainty), whereas lower bound corresponds to the cases that are driven by the presence of perfect knowledge (absolute certainty).

Second, Minimum Expected number of collision Scheduler (minimum $E\{\mathbf{K}\}$ scheduler (MES)) is developed by exploiting the results of bound analysis. It is shown that, in case one of the cells can acquire knowledge about the reserved resources of neighboring cell, MES can be implemented by organizing resources of a stack form in a random manner. With the aid of MES, bound expressions are extended by appropriately quantifying absolute uncertainty and certainty conditions in such a way that the amount of knowledge acquired is also included.

Third, considering the practical cases which impose restrictions on schedulers in terms of computational power and time along with persistent scheduling schemes proposed for voice traffic, impacts

of prolonged scheduling periods on performances of schedulers are investigated. It is shown that prolonged scheduling periods cause compression and saturation effects. Prolonged scheduling period is also included into the analysis in order to generalize bound expressions.

This chapter is organized as follows. Chapter 7.2 provides the details of the system model along with the basic assumptions necessary for the analysis. Chapter 7.3 gives the upper and lower bounds on the expected number of collisions for general cases. Based on the results in Chapter 7.3, MES is developed and knowledge acquisition is embedded into the analysis in Chapter 7.4. Chapter 7.5 discusses the effects of the prolonged scheduling period on performance. Numerical results along with relevant discussions are presented in Chapter 7.6. Finally, key findings are summarized and future directions are provided in Chapter 7.7.

## 7.2 System Model and Basic Assumptions

A typical two–cell scenario consists of two interfering cells, which may not necessarily be identical, namely $C_c$ with $c = 1, 2$, under FRO regime. Users in $c$th cell is denoted with $U_c$ which contains $\mathcal{U}_c$ UEs in it. Each cell $C_c$ performs the interior and cell edge distinction process for each, say $j$th, UE denoted with $u_{cj}$. Interior/cell edge distinction is achieved through the use of a specialized function: $\Theta(\cdot)$. For any $u_{cj}$, $\Theta(u_{cj}) = 0$ states that UE of interest is an interior user, whereas $\Theta(u_{cj}) = 1$ represents a cell edge user.[1] Such a scenario is depicted in Figure 7.1 with two example layouts. Under FRO regime with no intra–cell interference assumption, $\Theta(\cdot)$ limits interference to cell edge region in which solely ICI takes place. FRO is employed with the common subcarrier[2] set $F$ which contains $\mathcal{F}$ resource elements in it. Once $\Theta(\cdot)$ is applied, each $C_c$ determines $F_c^{(I)}$ for its cell edge users by selecting $\mathcal{F}_c$ elements among $F$. This model makes no assumption for the distribution of the users across cells. In conjunction with $\Theta(\cdot)$, more general scenarios in which all of the UEs in one of the cells are interfered by some of the UEs in a larger size cell can also be investigated with this way.

All of the UEs in cells are assumed to carry voice traffic whose samples come from a negative exponentially decaying probability density function (PDF) with a decaying rate of $\lambda_H$ which is the reciprocal of the average holding time $\mu_H$. Stemming from general characteristics of voice traffic,

[1] Here, $\Theta(\cdot)$ can be any method or a combination of several methods. reference symbol received power (RSRP) measurements with several thresholds in Third Generation Long Term Evolution (3GLTE) [133] can be considered as an instance of $\Theta(\cdot)$.

[2] From this point on, the terms resource and subcarrier are used interchangeably within the text.

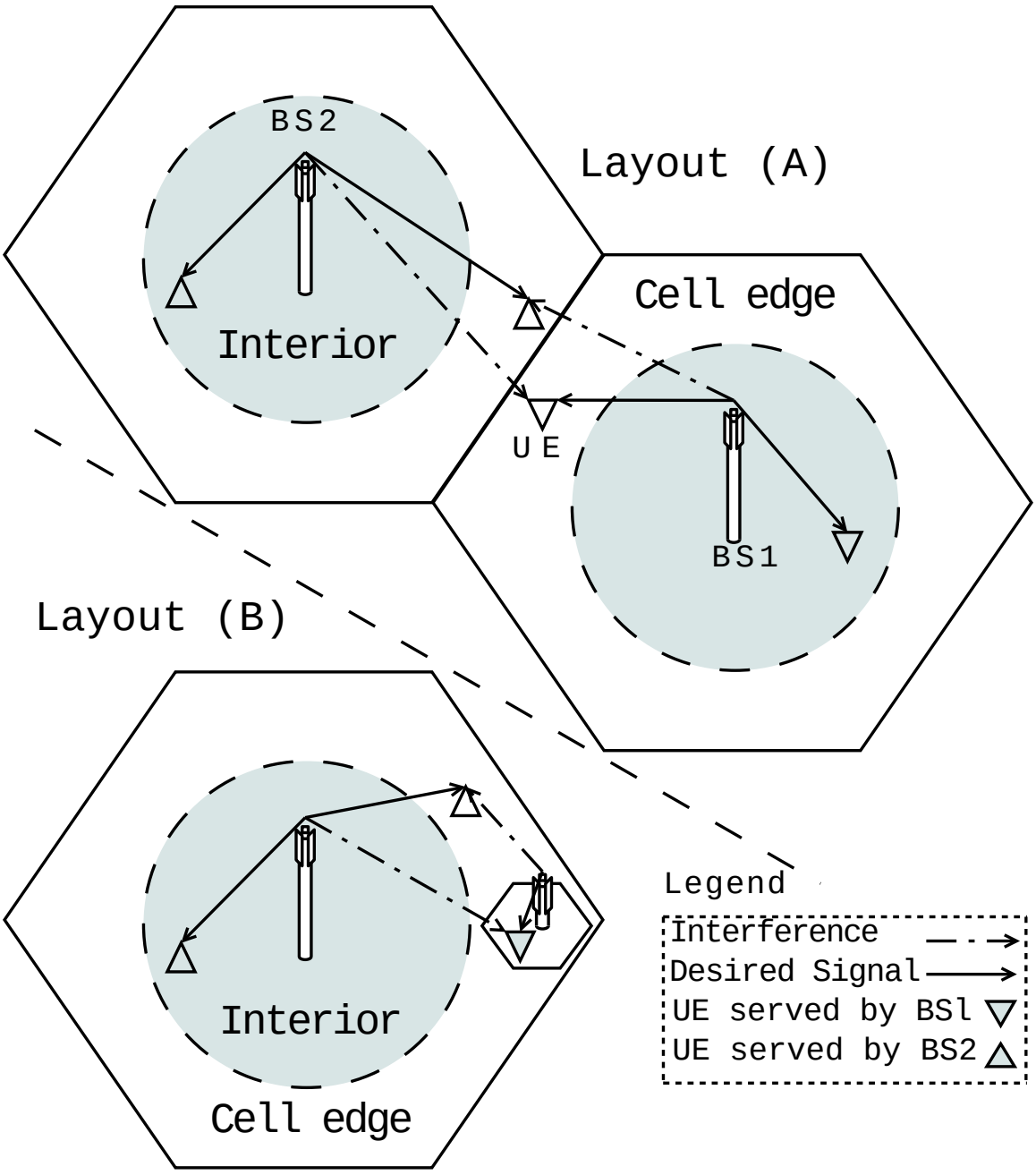


Figure 7.1 Two typical two–cell layouts in which cells are assumed to operate under FRO regime along with the "interior/cell edge" distinction.

single resource assignment per user is assumed. Assignments are performed at the beginning of each scheduling period $T_c$ for the cell $C_c$. In order to formalize and later on generalize the problem, $C_1$ is selected as pilot, whereas $C_2$ is considered to be an independent cell. Pilot cell is the one on which

parameters will be adjusted and their effects are investigated. With this simplification, the behavior of schedulers can be analyzed and easily expanded to general cases.

Throughout the analysis no handoff (handover) is assumed to take place in order to make sure of the stability of analysis. However, pure birth process for arrivals (*i.e.*, Poisson process) is considered for each $C_c$ with an average arrival rate of $\lambda_A^{(c)}$. In addition, if no resource is found for any arrival during $T_c$, then that arrival is assumed to be blocked. If any user releases any of the resources during $T_c$, it is assumed that those resources cannot be assigned until the next scheduling time.

Scheduling period $T_c$ carries a great importance for ICI management process. Therefore, further details of $T_c$ are essential for analysis. Let $T_c$ be defined in terms of $\mu_H$. This is a reasonable approach, since $\mu_H$ is the only parameter in hand providing information about the duration of resource use. Let $T_c$ be expressed in terms of number of scheduling operations as $T_c = \mu_H/\omega_c$. Note that $\omega_c$ with $\omega_c \in \mathbb{Z}^+$ provides a better perspective for the scheduling problem due to the following two reasons: First, many communication systems are based on discrete characteristics. For instance, most of the definitions in Third Generation Long Term Evolution (3GLTE), which is an OFDMA–based system, are built on a notion called transmission time interval (TTI), which is of discrete nature. Second, scheduling process itself is of discrete nature: for a given "unit period of time" either scheduling is performed or not. Thus, $\omega_c \in \mathbb{Z}^+$ provides a suitable approach for the analysis. Bounds are derived for the pilot cell under the assumption that $\mathrm{T}_1 = 1T_\Delta$, which corresponds to maximum number of scheduling operation where $T_\Delta$ denotes the minimum period of time in which only one scheduling operation can be performed. Because pure birth process is assumed, system keeps evolving throughout $T_1$ due to the arrivals. Traffic load is used for quantifying evolution of the system during any scheduling period $T$ and expressed as:

$$r_c = \frac{\lambda_A^{(c)} T}{\mathcal{F}_c}. \tag{7.1}$$

In (7.1), it is clear that $r_c \in (0, \infty)$ for $1 \leq \mathcal{F}_c$. However, cases where $1 < r_c$ can be ignored because of blocking assumption made previously; furthermore, blocked arrivals do not have any impact on performance, because no queue or any other facility is assumed in this scenario.

The building blocks of an OFDMA system are subcarriers; therefore, one of the simplest ways of quantifying ICI is to count the number of collisions occurred when scheduling is performed. This requires a formal definition of resource collisions.

**Definition 2** (Resource Collision). *If $W_t = u_{ai}(t) \cap u_{bj}(t)$ and $W_t \neq \emptyset$ for $i = 1, 2, \ldots, \mathcal{U}_a$ and $j = 1, 2, \ldots, \mathcal{U}_b$, then it is said that $\mathcal{W}_t$ "resource collision" occurs where $u_{ai}(t)$ and $u_{bj}(t)$ denote the set of resources used by $u_{ai}$ and $u_{bj}$ at instant $t$, respectively, and $\mathcal{W}_t$ is the cardinality of $W_t$.*

Even though Definition 2 postulates a way of quantifying resource collisions, it is not very suitable for characterizing an overall behavior of a dynamic system which exhibits stochastic behaviors. This arises from Definition 2 focusing on instantaneous values of collisions. Furthermore, persistent scheduling is considered for voice traffic in order to reduce over–the–air signaling in NGWNs [158]. Resources are assigned UEs and the assignment is maintained for some time in persistent scheduling schemes. From this point of view, it is more reasonable to count collisions per assignment than to count each individual collision occurred for the same assignment when each packet is transmitted, since the latter introduces redundancy. Therefore, expected number of collisions based on Definition 2 will be used in the analysis. In conjunction with the pilot cell approach, persistent scheduling is adopted with $\omega_2 = 1$.

### 7.3 Upper and Lower Bound of Expected Number of Collisions

Upper bound for expected number of collisions expresses the theoretical limit of performance of schedulers operating in a system such as described in Chapter 7.2. Different upper bounds can be defined for different strategies. However, if knowledge acquisition about resources in neighboring cell is taken into account, then it is evident that the upper bound is driven by the absence of knowledge, because schedulers exploit knowledge to reduce the number of collisions.[3]

In this sequel, it is worth mentioning how knowledge can be acquired in such a system. Knowledge is acquired by the following two methods: (E1) information exchange between schedulers and (E2) measurements such as spectrum sensing. The main distinction between these methods is that (E1) requires a backhaul to exchange information, whereas (E2) does not require any backhaul and

[3]At this point, one might raise a philosophical objection to this statement by claiming that the upper bound of number of collisions is limited to $\min(\mathcal{F}_c)$ when knowledge acquisition is possible as follows: Number of collisions is maximized when $C_1$ "imitates" $C_2$ (*i.e.*, $C_1$ attains the perfect knowledge about the reservation set of $C_2$ and follows exactly $C_2$) or vice versa; therefore, its value is $\min(\mathcal{F}_c)$. Although this claim seems to be true from the algebraic point of view, it is misleading, because every scheduler strives to minimize the expected number of collisions not to maximize it, since interference is mutually detrimental. For $1 < \mathcal{F}$, statistically, it is almost impossible that $C_1$ "imitates" $C_2$ unless $C_1$ acquires the perfect knowledge of the resource use of $C_2$. $\mathcal{F} = 1$ is the only state in which $C_1$ can exactly "know" what $C_2$ does without requirement of any knowledge acquisition. However, this state should be regarded as trivial case, since "assignment" has no meaning in this aspect.

relies on unilateral effort. It must also be stated that (E1) is more reliable[4] compared to (E2), since measurements might not be very accurate.

In the absence of knowledge, both cells are assumed to reserve their resources among $F$ randomly. Therefore, probability mass function (PMF) of number of collisions is required in order to continue the analysis.[5]

**Proposition 7.3.1** (PMF of Number of Collisions)**.** *Given that $\mathcal{F}_1$ and $\mathcal{F}_2$ resources are randomly chosen to be assigned cell edges of $C_1$ and $C_2$, respectively, among non–empty set of resources $F$ with $\mathcal{F} \ll \infty$, then the probability mass function of random variable $\mathbf{K}$ representing number of collisions is defined by a hypergeometric distribution that is expressed as:*

$$\Pr(\mathbf{K} = k) = p(k) = \frac{1}{\binom{\mathcal{F}}{\max(\mathcal{F}_1, \mathcal{F}_2)}} \binom{\mathcal{F} - \min(\mathcal{F}_1, \mathcal{F}_2)}{\max(\mathcal{F}_1, \mathcal{F}_2) - k} \binom{\min(\mathcal{F}_1, \mathcal{F}_2)}{k}, \tag{7.2}$$

*where $k$ denotes number collisions with $k \in \mathbb{Z}^+$ in $[0, \min(\mathcal{F}_1, \mathcal{F}_2)]$.*

*Proof.* See Appendix A. □

Since PMF is in hand, any statistics desired can be derived. As will be shown subsequently, (7.2) actually contains the following two important properties: (a) expected number of collisions and (b) breaking point of collisions. It is clear that (a) is related to the upper bound and calculated by the statistical expectation operator (*i.e.*, $E\{\mathbf{K}\}$). Ergo, no extra explanation is required here. As opposed to (a), (b) is related to the lower bound and needs more detailed investigation. First, (a) is analyzed with the following.

**Corollary 7.3.1** (Expected Number of Collisions of (7.2))**.** *Expected number of collisions of* (7.2) *is:*

$$\mathfrak{S} = \frac{\mathcal{F}_1 \mathcal{F}_2}{\mathcal{F}}. \tag{7.3}$$

*Proof.* See Appendix B. □

Observe that Corollary 7.3.1 provides a constant value for expected number of collisions by disregarding the evolution of the system. However, collision does not occur unless reserved resources are assigned. This requires Corollary 7.3.1 to be extended in terms of traffic loads as follows:

[4]Here, "reliability" refers to the exactitude of the knowledge. However, for the sake of completeness, it must be emphasized that reliability of (E1) actually implies very short delays in the backhaul communications. In this sense, longer delays in (E1) might lead to unreliable results as well.

[5]As expressed in Definition 2, collision is of discrete nature. This gives rise to the use of PMF rather than PDF in the analysis.

**Corollary 7.3.2** (Upper Bound). *Upper bound of expected number of collisions for minimum scheduling period is defined in terms of traffic load $r_1$ and $r_2$ by the following:*

$$\mathfrak{U} = r_1 r_2 \mathfrak{S}. \tag{7.4}$$

In contrast to upper bound, lower bound needs to be considered in the presence of knowledge due to the following reasoning: Definition 2 explicitly states that number of collisions cannot be lower than zero. Therefore, zero collision is a very important characteristic of lower bound. However, it cannot be achieved unless one of the cells is aware of the reservation of its neighbor, because cells suppose that reservation sets are chosen randomly among $F$ in the absence of knowledge, as assumed in Proposition 7.3.1. With the same token in Footnote 3, $C_1$ can achieve zero collision if and only if it attains the perfect knowledge about the reserved set of $C_2$ (or vice versa).

In this sequel, the PMF in (7.2) should be related with zero collision notion in a formal way. In order to achieve this, first the following mathematical tool is defined.

**Definition 3** (Breaking Point). *A breaking point $k_\epsilon$ of a precision $\epsilon$ is a non–zero number of collisions defined in* (7.2) *and satisfies* $\Pr(\mathbf{K} \leq k_\epsilon) \leq L < \Pr(\mathbf{K} \leq k_\epsilon + 1)$ *where $L$ is a pre–defined certainty with* $L \in [\Pr(\mathbf{K} = 0), 1)$ *and* $\epsilon = 1 - L$.[6]

Although Definition 3 outlines how the breaking point tool is constructed, its existence and uniqueness should also be verified before continuing the analysis.

**Corollary 7.3.3** (Existence and Uniqueness of Breaking Point). *There always exists a unique breaking point in* (7.2) *for a specified $L$.*

*Proof.* See Appendix C. □

Definition 3 and Corollary 7.3.3 are followed by the identification of unique regions in (7.2).

**Definition 4** (Vulnerable and Secure Zone). *Vulnerable zone is a unique region within* (7.2) *satisfying $k \leq k_\epsilon$, whereas secure zone is its complementary part satisfying $k_\epsilon < k$.*

At this point, it is worthwhile to see how PMF in (7.2) looks like for a general scenario in order both to grasp Definition 3 and Definition 4 and to have an insight into further steps of analysis, especially for investigating (b). Consider the PMF given in Figure 7.2. Visually, it is clear that within

[6]Note that $\Pr(\mathbf{K} = 0)$ corresponds to the probability of having no collisions, which is the same as $p(0)$ in (7.2).

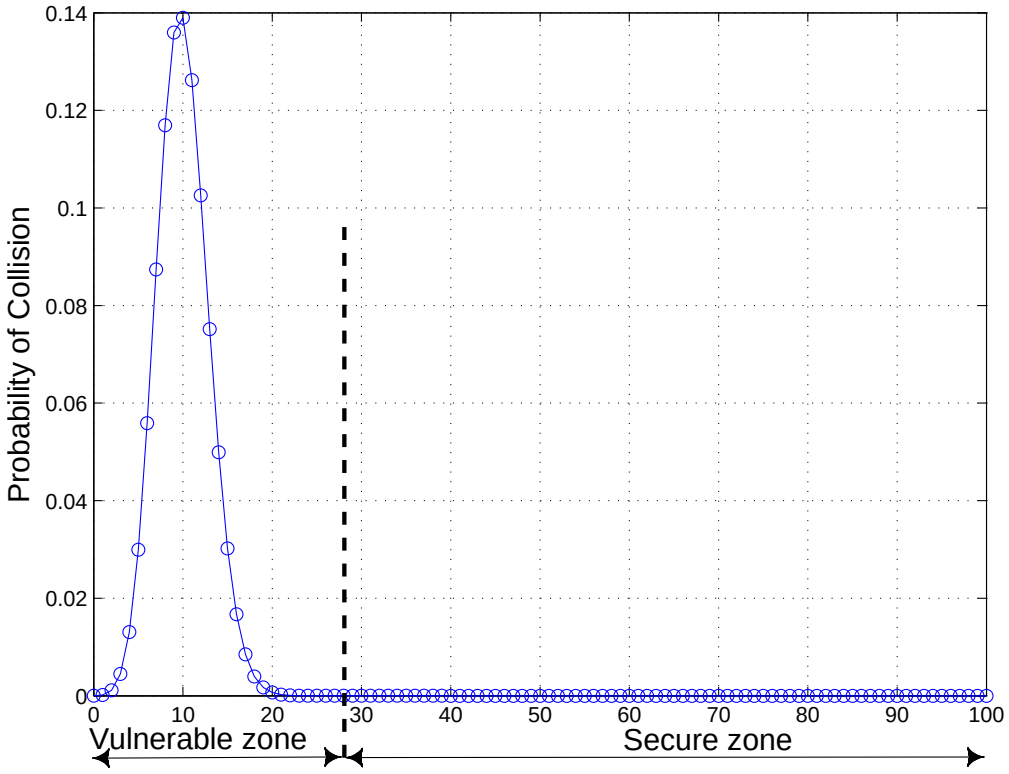


Figure 7.2 An example PMF for $\mathcal{F} = 1000$, $\mathcal{F}_1 = \mathcal{F}_2 = \mathcal{F}_z = 100$.

right hand side of the vertical dashed line (which is referred to as "secure zone" in Figure 7.2), there is no point that provides a significant probability value in contrast to those in left hand side of it. Bearing Definition 3 in mind, assume that one wants to design a system with a precision of $\epsilon = 10^{-6}$. In this case, the separator (*i.e.*, vertical dashed line) should be located on the point where $\Pr(\mathbf{K} \leq k_\epsilon) \leq 1 - \epsilon < \Pr(\mathbf{K} \leq k_\epsilon + 1)$. For the case plotted in Figure 7.2, $k_\epsilon = 26$ satisfies this condition by corresponding to a precision of $\epsilon = 8.188 \times 10^{-7}$. This implies that for the point on which the separator is located, with the given settings, it is unlikely that the number of collisions exceed 26. Conversely, with the same settings given, it is very likely to have 26 or less number of collisions.

The discussion related to Figure 7.2 points out that there is a strong connection between $L$ (or equivalently $\epsilon$) and zero collisions. In order to elucidate this connection, consider two identical systems one of whose design might regard $E\{\mathbf{K}\}$ as zero for $\epsilon_1$, whereas that of other one might treat $E\{\mathbf{K}\}$ as zero for $\epsilon_2$ where $\epsilon_1 \neq \epsilon_2$. For these two systems, $\epsilon_1$ and $\epsilon_2$ values are the design

parameters which determine zero collision limits. Consequently, breaking point cannot be used for formalizing the theoretical lower bound, since different $\epsilon$ values imply different $k_\epsilon$s. In order to find a way through this problem, limiting case of breaking points will be examined in what follows.

Consider how breaking point evolves in terms of increasing certainty level, (*i.e.*, $L \to 1$). Before proceeding further, first recall that Definition 3 stipulates $\Pr(\mathbf{K} \leq k_\epsilon) \leq L < \Pr(\mathbf{K} \leq k_\epsilon + 1)$. In the limiting case of $L$, $k_\epsilon + 1$ diminishes due to the second axiom of probability (*i.e.*, axiom of unit measure). Recall also that Corollary 7.3.3 guarantees the existence of a unique $k_\epsilon$. However, limiting case does not allow one to find $k_\epsilon + 1$ but $k_\epsilon$. Therefore, the inequality in Definition 3 is forced to degenerate into $\Pr(\mathbf{K} \leq k_\epsilon) = 1$, which also implies $k_\epsilon = \min(\mathcal{F}_1, \mathcal{F}_2)$. With the same token, limiting case leads to $p(k) = \delta(k - k_\epsilon)$ where $\delta(\cdot)$ is the Dirac delta function; therefore, $E\{\mathbf{K}\} = k_\epsilon$.[7] All of the aforementioned statements can succinctly be stated in a formal way as $\lim_{\epsilon \to 0} k_\epsilon = E\{\mathbf{K}\}$. If $E\{\mathbf{K}\}$ is denoted in terms of $\mathcal{F}_c$, it follows

$$\lim_{\epsilon \to 0} k_\epsilon = \frac{\min(\mathcal{F}_1, \mathcal{F}_2) \max(\mathcal{F}_1, \mathcal{F}_2)}{\mathcal{F}}, \tag{7.5}$$

which is the same as (B.5) in Appendix B. Thus, limiting case reveals a completely new characteristic, because it annihilates the secure zone in Definition 4 and yields the following concept.

**Corollary 7.3.4** (Bending Point)**.** *Bending point is the limiting case of any $k_\epsilon$ and it represents a constant number of resources given by:*

$$H_k = \min(\mathcal{F}_1, \mathcal{F}_2) \left(1 - \frac{\max(\mathcal{F}_1, \mathcal{F}_2)}{\mathcal{F}}\right). \tag{7.6}$$

When Definition 3 and Corollary 7.3.4 are considered together, it is not difficult to see that for the same settings there might be different $k_{\epsilon_i}$s for each $\epsilon_i$ level, whereas $H_k$ is a unique value to which each $k_{\epsilon_i}$ is asymptotic. From this point of view, bending point is the unique limit of ensemble of all possible breaking points of different certainty levels; therefore, it can safely be used for defining the lower bound.

As stated earlier, bending point actually corresponds to the state in which secure zone is annihilated. This state can best be explained in terms of evolution of system under pure birth process

[7] Existence of breaking point of a PMF under limiting conditions mandates that PMF can be of no other form but of $\delta(\cdot)$. In conformity with this limiting case, $\delta(\cdot)$ represents "absolute certainty" rather than what a usual PMF (or PDF) does. In addition, $\delta(\cdot)$ is the only PMF (or PDF) that has single non–zero probability value due to the axiom of unit measure.

assumption. The system exploits the knowledge acquired to attain zero collision; however, due to arrivals, it reaches such a particular state in which the knowledge acquired is not helpful anymore. This state is the equivalent of absence of knowledge described earlier. Hence, ideally, expected number of collisions should behave according to Corollary 7.3.2 beyond the bending point. Since ideal case refers to certainty which is of asymptotic nature (*i.e.*, a breaking point with $L \to 1$ or $\lim_{\epsilon \to 0} k_\epsilon$), $E\{\mathbf{K}\}$ is asymptotic to (7.4) as well. The lower bound of expected number of collisions is then given by the following piecewise–defined asymptote:

$$\mathfrak{L} = \begin{cases} 0, & \text{if } r_1 \leq r_1^{\mathfrak{L}} \quad (7.7a) \\ \dfrac{\mathfrak{X}}{1 - r_1^{\mathfrak{L}}} \left( r_1 - r_1^{\mathfrak{L}} \right), & \text{otherwise} \quad (7.7b) \end{cases}$$

where $r_1^{\mathfrak{L}}$ is the bending traffic load of pilot cell and expressed as:

$$r_1^{\mathfrak{L}} = \frac{H_k}{\min\left(\mathcal{F}_1, \mathcal{F}_2\right)}, \tag{7.8}$$

and $\mathfrak{X}$ denotes the constant part of $\mathfrak{U}$ when pilot cell approach is employed and given by

$$\mathfrak{X} = r_2 \mathfrak{S}.$$

## 7.4 MES and Its Performance

In this section, MES is developed based on the results presented in Chapter 7.3. With the aid of MES, it is also shown that (7.7) can be generalized by including the amount of knowledge acquired into the analysis. The principles of MES is introduced under perfect knowledge case. Generalization of (7.7) is carried out while imperfect knowledge is discussed.

### 7.4.1 MES and Its Performance in the Presence of Perfect Knowledge

Perfect knowledge refers to a state in which $C_1$ is assumed to know $F_2^{(I)}$ completely. In such a state, (7.7a) is attained if and only if the pilot scheduler does not assign the intersecting resources (*e.g.*, set $W_t$ in the sense of Definition 2). Avoiding assigning the intersecting resources is not desired, because it causes underutilization. Therefore, the best strategy for the pilot scheduler is to avoid assigning the intersecting resources unless their assignments are inevitable due to high traffic load. Such a strategy can be performed by assigning the resources of a stack form (*i.e.*, of a first–in–last–

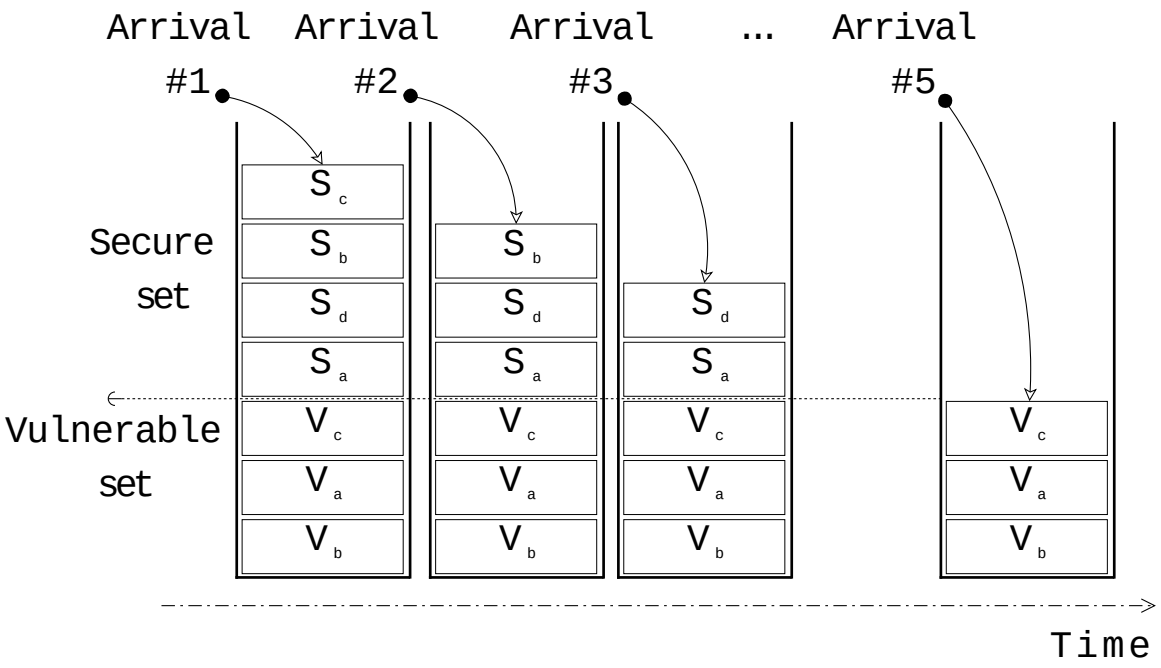


Figure 7.3 Illustration of how MES organizes its resources of a stack form and how it performs under incoming arrivals.

out (FILO) scheme). Assume that $C_1$ splits $F_1^{(I)}$ into two by identifying the "vulnerable" resources via the knowledge acquired about reservation of $C_2$ with $V = F_1^{(I)} \bigcap F_2^{(I)}$. In order for $C_1$ to form a stack of resources, $V$ is placed first into the stack (*i.e.*, planned to assign last) as illustrated in Figure 7.3. This way, $C_1$ makes sure that in order for a collision to occur, there must be $\mathcal{F}_1 - \mathcal{V}$ arrivals at least within $T_1$, where $\mathcal{V}$ is the cardinality of set $V$. Note that, in the presence of perfect knowledge about $F_2^{(I)}$, this scheme yields the minimum number of collisions, since $\mathcal{V}$ can be regarded as a breaking point. Therefore, MES deviates from zero at $r_1^{\epsilon} = 1 - \mathcal{V}/\mathcal{F}_1$. As Chapter 7.3 points out, beyond $r_1^{\epsilon}$, $E\{\mathbf{K}\}$ keeps increasing due to the FILO scheme adopted. However, once $r_1^{\mathfrak{L}}$ is exceeded, $E\{\mathbf{K}\}$ escalates asymptotic to (7.7b).

### 7.4.2 Performance of MES in the Presence of Imperfect Knowledge [Generalized Case]

Imperfect knowledge refers to the state where $C_1$ is assumed to know $V$ partially. Let partial $V$ be denoted as $V_{\mathbf{p}}$ which satisfies $V_{\mathbf{p}} \subseteq V$ with a cardinality of $\mathcal{V}_{\mathbf{p}} \leq \mathcal{V}$. Partial knowledge asserts that there are $\mathcal{G} = \mathcal{V} - \mathcal{V}_{\mathbf{p}}$ resources leaked into the secure set from vulnerable set within the stack structure. In other words, if collision occurs in such a scenario, it will definitely be caused by $\mathcal{G}$

resources in the secure set. In order to evaluate the impact of this leakage, assume that pilot cell $C_1$ performs (E2) with a success rate of $\mathfrak{s}$ where $\mathfrak{s} \in [0,1]$ yielding $\mathcal{V}_{\mathbf{p}} = \mathfrak{s}\mathcal{V}$. Thus, $\mathcal{G}$ is defined in terms of $\mathfrak{s}$ as $\mathcal{G} = (1-\mathfrak{s})\,\mathcal{V}$. As indicated in (7.7), the behavior of MES needs to be investigated based on $H_k$. In conjunction with (7.7) and (7.8), first consider the case where $H_k \neq 0$ and $r_1 \leq r_1^{\mathfrak{L}}$. Since probable collisions emanated from $\mathcal{G}$ resources leaked into the secure set, for MES, $E\{\mathbf{K}\}$ actually corresponds to $E\{\mathcal{G}\}$, which is equal to $(1-\mathfrak{s})\,E\{\mathcal{V}\}$. Observe that $E\{\mathcal{G}\}$ is a scaled version of $E\{\mathcal{V}\}$ due to the initial condition $r_1 \leq r_1^{\mathfrak{L}}$ and $E\{\mathcal{V}\}$ is the equivalent of (7.3) when all of the resources are assigned. Thus, with the aid of (7.4), it is found that $E\{\mathcal{G}\} = (1-\mathfrak{s})\,\mathfrak{X} r_1$. In Chapter 7.3, it is stated that once bending point is reached, expected number of collisions behaves as though no knowledge acquisition regime (*i.e.*, absence of knowledge) is employed. Therefore, $\mathfrak{s}$ loses its significance and $E\{\mathcal{G}\}$ will be asymptotic to (7.7b) beyond bending point. Performance of MES reveals that (7.7) can actually be generalized in such a way that $\mathfrak{L}$ includes the amount of knowledge acquired as follows:

$$\mathfrak{L} = \begin{cases} (1-\mathfrak{s})\,\mathfrak{X} r_1, & r_1 \leq r_1^{\mathfrak{L}} \quad (7.9a) \\ \dfrac{\mathfrak{X}}{1-r_1^{\mathfrak{L}}}\left(r_1 - r_1^{\mathfrak{L}}\right), & \text{otherwise} \quad (7.9b) \end{cases}$$

In (7.9), it is indicated that the behavior of $\mathfrak{L}$ might be changed by introducing knowledge acquisition into the system when $r_1 \leq r_1^{\mathfrak{L}}$, whereas it does not change when $r_1^{\mathfrak{L}} < r_1$, since (7.7b) and (7.9b) are the same. This is not surprising, because bending point is such a point beyond which the presence of knowledge does not have any effect under any circumstances, as mentioned earlier (*i.e.*, annihilation of secure zone).

## 7.5 Impacts of Scheduling Period and Generalized Bound

Practical cases involve less frequent scheduling, since scheduling is an expensive process in terms of computational power and time. Less frequent scheduling (*i.e.*, $T_\Delta < T_1$) has the following two impacts on performance: compression and saturation. These two effects are analyzed below.

### 7.5.1 Compression Effect

When scheduling period $T_1$ is prolonged while all of the other parameters are constant, the most important change occurs in evolution of the system due to pure birth process assumption. In order to identify the behavior in a normalized way, as in previous sections, pilot cell traffic approach will

be used. Assume that a new scheduling period is adopted by $C_1$ as $T_1^{\text{new}} = nT_\Delta$ with $1 < n$ and $n \in \mathbb{R}^+$. The new traffic loads in both cells for the period calculated become $r_c^{\text{new}} = \lambda_A^{(c)} nT_\Delta / \mathcal{F}_c$. If this is combined with (7.1) for $T = T_\Delta$, it yields $r_c^{\text{new}} = nr_c$. The most striking consequence of $r_c^{\text{new}}$ is that the behavior of bounds remains the same, but it is compressed into $r_1' \in \left(0, 1/n^2\right]$ where $r_1'$ represents the transformed version of $r_1$, which is again defined within the unit interval by preserving $\lambda_A^{(1)}$ (*i.e.*, $r_1' \in (0,1]$) with $r_1' = \lambda_A^{(1)} T_\Delta / \mathcal{F}_1$.[8] Note that although $T_1$ is prolonged by a factor of $n$, compression occurs within $\left(0, 1/n^2\right]$. This stems from $r_c^{\text{new}}$, because prolonged period affects both of the cells simultaneously. In order to see this, Corollary 7.3.2 can be examined. Since $r_1'$ is assumed to be the only independent variable, $\mathfrak{U}$ is rewritten in terms of $r_c^{\text{new}}$ yielding:

$$\mathfrak{U}^{\text{new}} = r_1^{\text{new}} r_2^{\text{new}} \mathfrak{S} = (nr_1')(nr_2)\,\mathfrak{S} = n^2 \mathfrak{X} r_1'. \tag{7.10}$$

Observe that $\mathfrak{U}$ for $r_1 \in (0,1]$ is the same as $\mathfrak{U}^{\text{new}}$ for $r_1' \in \left(0, 1/n^2\right]$, which is the evidence of compression effect at a rate of $n$.

### 7.5.2 Saturation Effect

Despite (7.10) provides the precise behavior of $\mathfrak{U}^{\text{new}}$, one might wonder if (7.3) is violated by a particular $n$ value. For instance, some $n$ satisfying $\frac{1}{r_2} < n$ actually seems to cause (7.10) to exceed $\mathfrak{S}$ for $\frac{1}{n} < r'$. This concern is already cleared by the domain of $k$ in Proposition 7.3.1. Nonetheless, (7.10) should be rewritten in the following form in order to avoid any confusions:

$$\mathfrak{U}^{\text{new}} = (nr_1') \min(nr_2, 1) \mathfrak{S} = n \mathfrak{S}_{\min} r_1', \tag{7.11}$$

where $\mathfrak{S}_{\min} = \min(n\mathfrak{X}, \mathfrak{S})$. To proceed further, let the remaining $r_1' \in \left(1/n^2, 1\right]$ interval be decomposed into the following two subintervals: $r_1' \in \left(1/n^2, 1/n\right]$ and $r_1' \in (1/n, 1]$. Because $C_1$ can still accept new arrivals within $\left(1/n^2, 1/n\right]$ and $r_2$ is assumed to be constant, $E\{\mathbf{K}\}$ increases with the same rate, that is $n \min(nr_2\mathfrak{S}, \mathfrak{S})$, due to the same reasons provided for (7.11). When the last subinterval $(1/n, 1]$ is considered, $\frac{1}{n} < r_1'$ implies that $C_1$ runs out of resources and further arrivals do not affect the number of collisions due to blocking assumption; therefore, $E\{\mathbf{K}\}$ remains constant at $\mathfrak{U}^{\text{new}} = \mathfrak{S}_{\min}$. Note that $\mathfrak{U}^{\text{new}}$ equals $n\mathfrak{X}$ for $r_2 \leq 1/n$, whereas it equals $\mathfrak{S}$ for $1/n < r_2 \leq 1$,

[8] Such a transformation is necessary from the perspective of analysis, because arrival rate is an independent process whose parameter $\lambda_A^{(c)}$ cannot be changed by the system. Therefore, when $T_1^{\text{new}}$ is adopted for the pilot cell approach, $r_1' \in (0,1]$ is required in order to evaluate the behavior of the system in a comparative way.

which verifies that any $T_\Delta < T_1$ gives rise to saturation, if all of the other parameters are assumed to remain the same in the system.

Compression and saturation effects can be combined to generalize the bound expressions. From (7.4) and (7.9a), it is clear that the only difference between upper and lower bound is the knowledge acquisition where upper bound represents the absence of knowledge. As will be shown subsequently, knowledge acquisition allows one to unify the lower and upper bounds, whereas prolonged scheduling period allows (7.9) to be generalized. Since (7.8) is already defined in terms of traffic load, $\mathfrak{L}$ can be expressed in terms of $\mathfrak{s}$ and $n$ with the aid of (7.9) as follows:

$$\mathfrak{L}' = \begin{cases} n\mathfrak{S}_{\min}\left(1-\mathfrak{s}\right) r_1', & 0 < r_1' \leq \frac{r_1^{\mathfrak{L}}}{n} \quad (7.12a) \\ \dfrac{n\mathfrak{S}_{\min}}{1-r_1^{\mathfrak{L}}}\left(r_1' - \dfrac{r_1^{\mathfrak{L}}}{n}\right), & \frac{r_1^{\mathfrak{L}}}{n} < r_1' < \frac{1}{n} \quad (7.12b) \\ \mathfrak{S}_{\min}, & \frac{1}{n} < r_1' \leq 1 \quad (7.12c) \end{cases}$$

There are two important facts regarding (7.12). First, compression and saturation effects form a pattern in both upper and lower bounds. It can be seen in (7.11) for upper bound and (7.12) for lower bound that they include $n\mathfrak{S}_{\min}$ and $\mathfrak{S}_{\min}$ for compression and saturation effects, respectively. Second, for $\mathfrak{s} < 1$ and $1 < n$, (7.12a) provides larger asymptotic values compared to (7.12b) when $r_1'$ is in the vicinity of $r_1^{\mathfrak{L}}/n$. This can be verified by applying $r_1' = r_1^{\mathfrak{L}}/n$ and $r_1' = r_1^{\mathfrak{L}}/n + \xi$ in (7.12a) and (7.12b), respectively, where $\xi$ is infinitesimal. Since both (7.12a) and (7.12b) are slants with particular slopes, intersection point of these two slants can be used for purifying the intervals of (7.12) even though they actually do not intersect due to intervals in which they are defined. This way, $\mathfrak{L}'$ can be redefined in a more concise way as follows:

$$\mathfrak{L}' = \begin{cases} n\left(1-\mathfrak{s}\right)\mathfrak{S}_{\min} r_1', & 0 < r_1' \leq r' \quad (7.13a) \\ \dfrac{n\mathfrak{S}_{\min}}{1-r_1^{\mathfrak{L}}}\left(r_1' - \dfrac{r_1^{\mathfrak{L}}}{n}\right), & r' < r_1' \leq \frac{1}{n} \quad (7.13b) \\ \mathfrak{S}_{\min}, & \frac{1}{n} < r_1' \leq 1 \quad (7.13c) \end{cases}$$

where $r'$ is the intersection point of the slants in (7.12a) and (7.12b), and it is found to be:

$$r' = \frac{r_1^{\mathfrak{L}}}{n\left(\mathfrak{s} + r_1^{\mathfrak{L}} - \mathfrak{s} r_1^{\mathfrak{L}}\right)}. \quad (7.14)$$

Observe that $r'$ is the translated (or generalized) version of $r_1^{\mathfrak{C}}$ in the presence of both $\mathfrak{s}$ and $n$. It is also easy to verify that (7.13) along with (7.14) encompasses (7.4), (7.7), and (7.9) with appropriate $\mathfrak{s}$ and $n$ values.

### 7.6 Numerical Results

In the simulations, FRO regime is employed with $\mathcal{F} = 1000$ resources and $\mathcal{F}_1 = \mathcal{F}_2 = \mathcal{F}_z = 100$. Each simulation setup is run 10000 times in order to obtain reliable statistics. Theoretical bounds are obtained for $T_1 = T_\Delta$ and all of the time related parameters such as $\mu_H$ are defined in terms of $T_\Delta$ as well. A typical voice encoder period of 20ms is chosen for $T_\Delta$ and $T_2 = \mu_H = 120T_\Delta$, which corresponds approximately to half of the mean talk spurt duration of 5s (*i.e.*, time period of staying in active state in two–state voice activity model) [159]. Each arrival is considered to be assigned single resource. Resource collision is calculated based on Definition 2 for each scheduling period at each step, then $E\{\mathbf{K}\}$ is calculated.

To begin with, upper and lower bounds are plotted in Figure 7.4 for $r_2 = 0.5$. As can be seen, upper bound is a slant whose slope is $r_2\mathcal{F}_z^2/\mathcal{F}$, whereas lower bound obeys (7.13) for $\mathfrak{s} = n = 1$ with $r_1^{\mathfrak{C}} = 0.9$.

In order to see how MES behaves under different scenarios, knowledge acquisition regime is employed in simulations while the previous settings are maintained. The performance of MES for $\mathfrak{s} = 1$ is given in Figure 7.5. As described earlier, $\mathfrak{s} = 1$ allows MES to avoid collision by forming its assignment set as a stack. The impact of $\epsilon$ and corresponding $k_\epsilon$ is seen when $0.8 \leq r_1 < r_1^{\mathfrak{C}}$. In Chapter 7.3, recall that for the same settings $k_\epsilon$ is found to be 26 of a $\epsilon = 10^{-6}$ precision implying $\mathcal{V} = 26$ or $r_1^\epsilon = 0.74$. This discrepancy stems from the fact that simulation could not reach the desired accuracy, because it ran only $10^4$ times. In order to confirm this, the PMF is reexamined for $\epsilon = 10^{-4}$ and $\mathcal{V}$ is found to be 20, which corresponds to $r_1^\epsilon = 0.8$ and confirms the results in Figure 7.5.[9] This example sheds light on the reason why the use of bending point is essential for the analysis.

The impact of knowledge acquisition on the performance of MES is given in Figure 7.6 for several scenarios with $\mathfrak{s} \in [0, 1]$. The results are in conformity with (7.13). For instance, the scheduler with

[9]The relationship between $\epsilon$ and simulated value of breaking point can also be verified from (7.2) with the same argument presented in Chapter 7.3. In (7.2), $p(k)$ is always greater than zero for all finite values of $\mathcal{F}$. This implies that if one were to run the same simulation for infinite amount of time, there would definitely be a collision even for the case $\mathcal{V} = \min(\mathcal{F}_1, \mathcal{F}_2)$, which corresponds to $r_1^\epsilon = 0$.

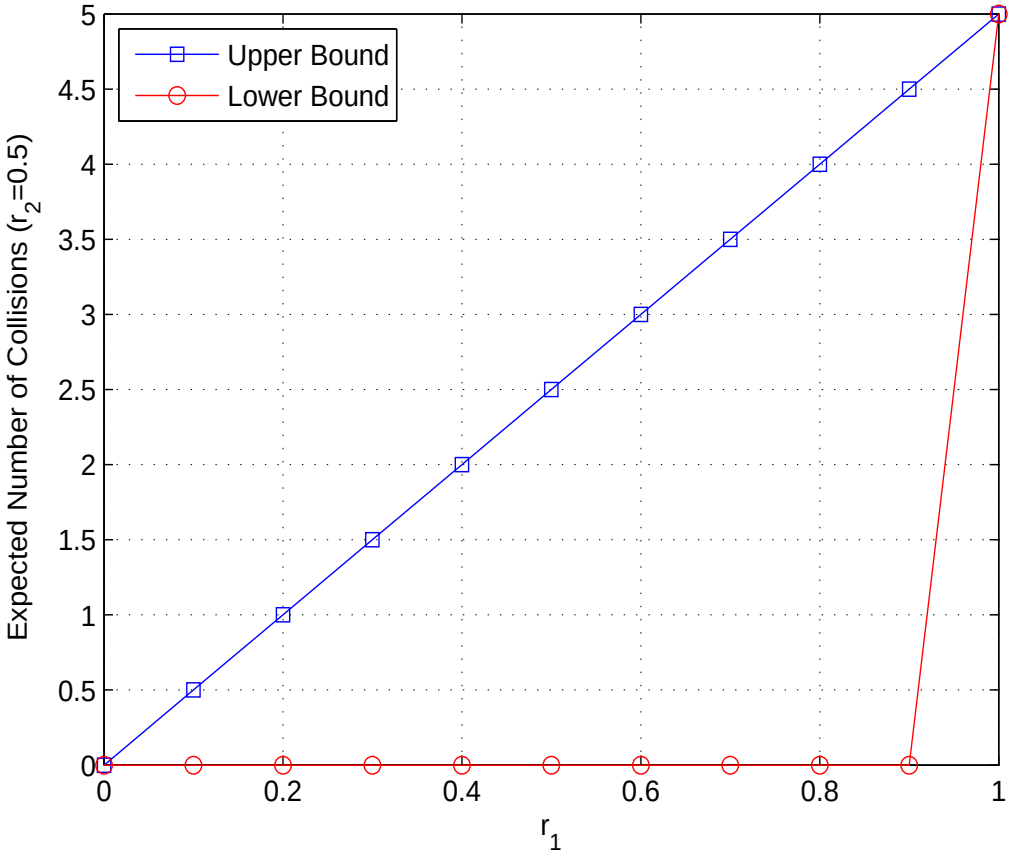


Figure 7.4 An example plot of both upper and lower bounds for $\mathcal{F} = 1000$, $\mathcal{F}_1 = \mathcal{F}_2 = 100$, and a fixed traffic load in $C_2$ with $r_2 = 0.5$.

$\mathfrak{s} = 0.5$ and $n = 1$ follows (7.13a) with a slant whose slope is $\approx 2.78$. Again, as in other $\mathfrak{s}$ values, $\mathfrak{s} = 0.5$ is asymptotic to (7.13b) beyond $r'$, as predicted. Note also that upper bound is attained when $\mathfrak{s} = 0$.

Up until now, $T_1 = T_\Delta$ is considered. In order to see the impact of $T_{\text{new}}$, the performance of MES is plotted in Figure 7.7 for $n = 2, 4, 8$ with $r_2 = 0.2$ and $\mathfrak{s} = 0.4$. In Figure 7.7, both the compression and saturation effects are clearly seen while $r_1' \to 0$. In order to exemplify how bounds delineate MES, $n = 4$ is chosen. As stated in (7.13a), lower bound follows a slant whose slope is $n\,(1 - \mathfrak{s})\,\mathfrak{S}_{\min} = 19.2$ for $0 < r_1' \leq r'$. The performance is upper bounded by a slant whose slope is $n\mathfrak{S}_{\min} = 32$, as given in (7.11). Note that upper bound can also be obtained by applying $\mathfrak{s} = 0$ in (7.13a) and (7.14), respectively. Saturation effect is seen in each realization of $n$, for $\frac{1}{n} < r'$. Note also that how clipping (*i.e.*, $\mathfrak{S}_{\min}$) takes place for $n = 8$ in $\frac{1}{n} < r'$, because $\frac{1}{r_2} < n$ is satisfied.

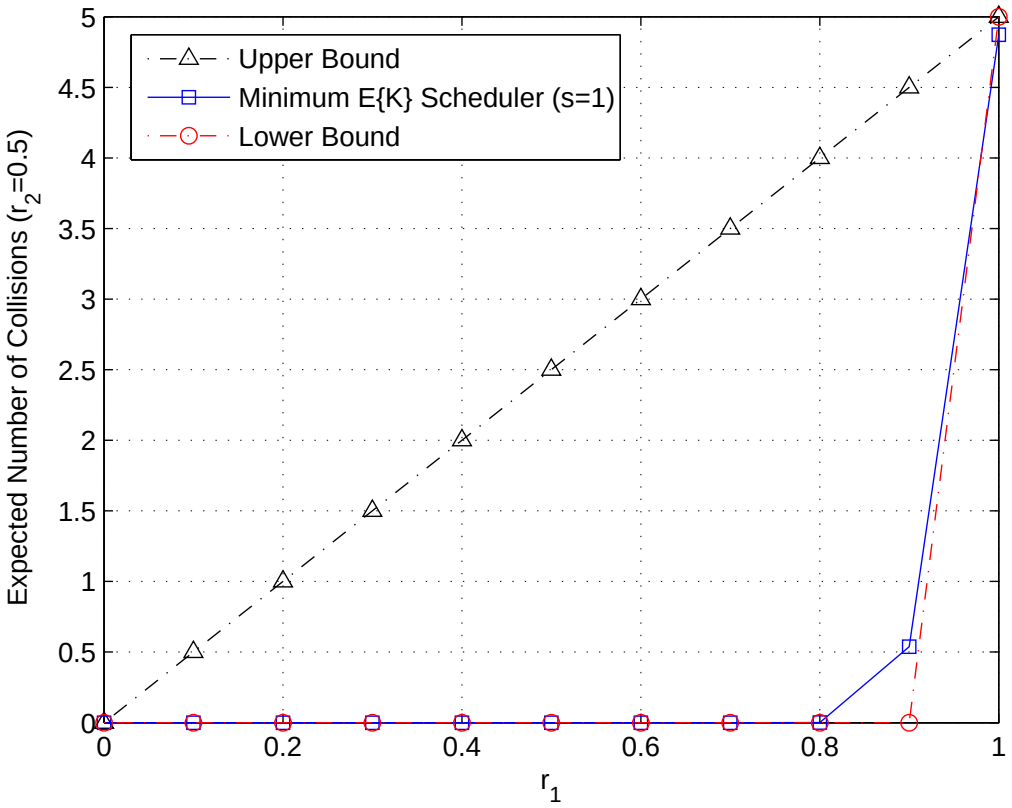


Figure 7.5 Performance of MES for $\mathfrak{s} = 1$ delineated by the corresponding upper and lower bounds.

### 7.7 Concluding Remarks

In this chapter, upper and lower bound of scheduler performances for resource collisions in broadband OFDMA–based systems are derived for voice traffic. Under FRO regime, it is shown that upper bound is the expected value of a hypergeometric PMF, whereas lower bound is a piecewise–defined asymptote, which bends at a particular point. It is found that prolonged scheduling periods lead to compression and saturation effects on the performance of schedulers. Hence, analysis is extended in such a way as to generalize the bound expressions in terms of both the knowledge acquired and scheduling period.

Although voice is still considered to be the most dominant traffic type, Internet draws significant attention as well. Exhibiting very different traffic characteristics renders Internet a challenging issue for ICI management. Investigating the performance bounds of schedulers for Internet traffic is of

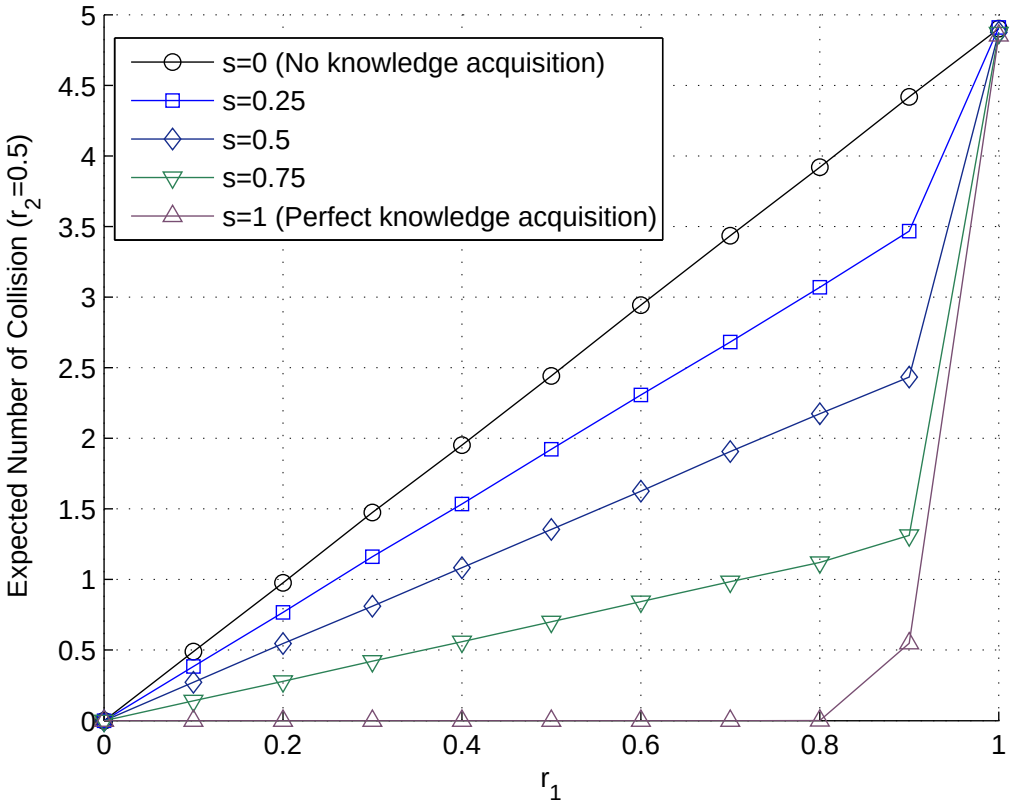


Figure 7.6 Performance of MES under different knowledge acquisition scenarios for $\mathfrak{s} \in [0, 1]$, $\mathcal{F} = 1000$, $\mathcal{F}_1 = \mathcal{F}_2 = 100$, and a fixed traffic load in $C_2$ with $r_2 = 0.5$.

extreme importance for NGWNs. Therefore, derivation of these bounds will help researchers develop better schedulers for different types of traffic.

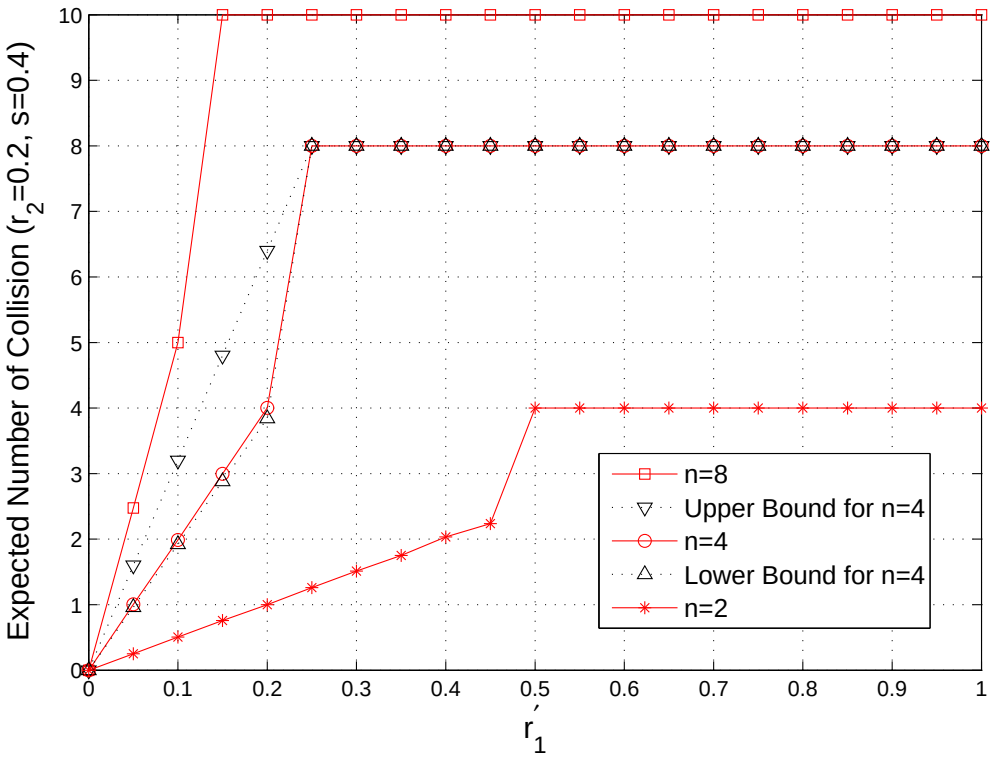


Figure 7.7 Performance of MES under three different scheduling periods which are obtained by $n = 2, 4, 8$ for $\mathfrak{s} = 0.4$, $\mathcal{F} = 1000$, $\mathcal{F}_1 = \mathcal{F}_2 = 100$, and a fixed traffic load $r_2 = 0.2$.

Table 7.1 Symbol list

| Symbol | Explanation |
|---|---|
| $C_c$ | $c$th cell |
| $U_c$ | Set of all of the users in $C_c$ |
| $\mathcal{U}_c$ | Number of users in $C_c$ |
| $u_{cj}$ | $j$th user in $C_c$ |
| $\Theta(\cdot)$ | Interior/cell edge distinction operator |
| $F$ | Set of all of the resources |
| $\mathcal{F}$ | Number of resources in $F$ |
| $F_c^{(I)}$ | Set of reserved resources for cell edge in $C_c$ |
| $\mathcal{F}_c$ | Number of resources in $F_c^{(I)}$ |
| $\lambda_H$ | Decaying rate of negative exponential PDF for a voice calls |
| $\mu_H$ | Average resource holding time for a voice call |
| $T_c$ | Scheduling period for $C_c$ |
| $\lambda_A^{(c)}$ | Arrival rate of Poisson process for $C_c$ |
| $T_\Delta$ | Minimum scheduling period |
| $r_c$ | Traffic load of $C_c$ |
| $\mathbf{K}$ | Random variable that represents number of collisions |
| $\Pr\{\mathcal{E}\}$ | Probability of event $\mathcal{E}$ |
| $p(k)$ | Probability of $\mathbf{K}$ taking the value $k$ |
| $E\{\mathbf{K}\}$ | Statistical expectation for random variable $\mathbf{K}$ |
| $\mathfrak{U}$ | Upper bound of expected number of collisions |
| $L$ | Certainty level for breaking point |
| $\epsilon$ | Precision for breaking point $(1-L)$ |
| $k_\epsilon$ | Breaking point of precision $\epsilon$ |
| $H_k$ | Bending point |
| $\mathfrak{L}$ | Lower bound of expected number of collisions |
| $r_1^{\mathfrak{L}}$ | Bending point of traffic load for pilot cell |
| $\mathfrak{X}$ | Constant part of $\mathfrak{U}$ under pilot cell approach |
| $\mathfrak{s}$ | The percentage of the knowledge acquired by the pilot cell |
| $n$ | Prolongation factor of new scheduling period for the pilot cell |
| $\mathfrak{S}_{\min}$ | Clipped expected number of collisions value obtained when $1 < n$ |
| $r_1'$ | Generalized pilot cell traffic load for different $\mathfrak{s}$ and $n$ values |

# CHAPTER 8

# INTERFERENCE AWARE VERTICAL HANDOFF FOR NGWNS

## 8.1 Introduction

As wireless communication evolves, many different signaling schemes and methods emerge and are standardized. Despite the obvious dominance of some specific types of networks in daily life such as cellular mobile networks, emergence of new standards forces different types of networks to coexist. Therefore, the concept "next generation wireless network (NGWN)" needs to allow for heterogeneous structure and to aim at collaboration of these various wireless technologies in order to provide quality of service (QoS) supported and cost efficient connections at anywhere and anytime.

Even though heterogeneous network structure is a very big concern by itself, terminals within the networks bring about some other issues for the next generation wireless net-works. In this regard, it can be said that the next generation wireless networks need to include terminals that are able to: (I) be aware of the existence of heterogeneous net-works around and (II) manage seamless transitions between existing networks when necessary. Considering (I) and (II) together, one can deduce that recently emerging technology called cognitive radio (CR) can be a remedy for both, since CRs are able to be aware of, learn about, and adapt to the changing conditions in radio environment [1]. Here, note that the term "radio environment" has many aspects such as physical propagation environment, radio frequency spectrum, available networks and terminals around, and so on. Because these aspects are highly dynamic, capabilities of CRs become crucial from the perspective of both individual terminals and networks including them. Along with CR, cooperative networks concept should also be considered in the context of next generation wireless systems. The cooperative networks concept assumes that all of the wireless technologies such as cellular networks, wireless local/metropolitan area net-works, wireless personal area networks, short range communications, and digital video/audio broadcasting can coexist in a heterogeneous wireless-

access infrastructure and cooperate in an optimal way in order to provide high speed and reliable connectivity anywhere and anytime [2].

In addition to the considerations related to the capabilities of both terminals and net-works, next generation wireless networks should also provide high data rate transmission despite their heterogeneous topology and complex structure. Moreover, they are desired to perform as close to wired networks as possible over wireless medium in terms of cost efficiency and of supporting highly sophisticated services that imply seamless transmission of different traffic types such as voice, data, and video.

Handoff is described as a process of transferring an ongoing call or data session from one access point to another in wireless networks. When all of the aforementioned aspects are contemplated, it is not difficult to conclude that handoff will be one of the vital mechanisms for next generation wireless networks. Traditional handoff process, which is called horizontal handoff, takes place to provide an uninterrupted service when a user moves between two adjacent cells. Generally, horizontal handoff process is initialized when the link quality condition parameters such as received signal strength indicator (RSSI), signal–to–noise ratio (SNR), and so on drop below a specified handoff threshold. Because the next generation wireless systems involve a heterogeneous topology, traditional handoff mechanisms will not be sufficient. Therefore, a new type of handoff, which is known as "vertical handoff," is introduced. Vertical handoff is defined as a process which transfers a user connection from one technology to another such as a transfer from Global System for Mobile (GSM) to wireless local area network (WLAN) or to Worldwide Interoperability for Microwave Access (WiMAX). Vertical handoff requires more intelligent algorithms which evaluate more parameters such as interference power, monetary cost, QoS, remaining energy, and so on in addition to already existing link quality condition quantifiers. Among all of the parameters, interference must be treated in a separate place, since every wireless system is interference limited. In traditional cellular-based systems, harmful impact of interference is tried to avoid/minimize by reusing the available frequencies in distant cells, which is called "frequency reuse." In the literature, frequency reuse is quantified by a factor called "frequency reuse factor" which represents the distinct number of frequency sets (or equivalently, number of cells) in a cluster. In this regard, minimum frequency reuse factor can be one and it is called "frequency reuse of one (FRO)" or universal frequency reuse. FRO implies that each cell is allowed to use the entire spectrum available. Although frequency reuse is a very effective method in combating interference, it comes at the expense of inefficient spectrum usage and

of expensive design processes. In contrast to traditional systems, FRO seems to be the strongest candidate in order to avoid expensive planning process and to overcome the problem of underutilized resource use in next generation wireless networks. It must be noted that FRO causes significant interference levels especially in the vicinity of cell borders in return. This renders interference one of the most critical parameters in handoff process for next generation wireless networks.

In the light of discussions given above, it is clear that interference, data rate, and mobility constitute the three prominent aspects of the next generation wireless networks. In this study, a new smart mobile terminal (SMT) is proposed. The proposed SMT is assumed to have cognitive capabilities such as sensing the environment periodically for available radio access technologys (RAT), evaluating their working conditions using its fuzzy logic based algorithm, triggering handoff process if necessary, and deciding the best access point (AP) to camp on. The decision is based on interference rate, data rate, and RSSI due to the following reasons: Interference rate quantifies how severe the ambient co–channel interference (CCI) power level, data rate takes into account the available transmission rate for applications carried out, whereas RSSI roughly helps to evaluate the mobility. The proposed SMT is modeled and simulated using OPNET Modeler Software for performance evaluation. Besides, the fuzzy logic based handoff algorithm incorporated in SMT is implemented in MATLAB Software. The contributions of this chapter can be summarized as follows:

- Considering the fact that most of the wireless communication systems are interference limited, in contrast to the most of the fuzzy-based algorithms, the decision mechanism in the method proposed takes into account interference rates from different base stations as input to its fuzzy logic system in order to make a more reliable handoff.

- A new adaptive multi–criteria handoff decision system, which has the ability to adapt its structure according to the application requirements and network conditions, is proposed.

- A new cognitive smart terminal, which senses the environment for available AP and changes its working parameters such as frequency band, bandwidth, modulation scheme, medium access control (MAC) protocol and so on in order to camp on an appropriate AP, is developed.

The remainder of the paper is organized as follows: Chapter 8.2 presents related works to the vertical handoff in the literature. Chapter 8.3 provides the proposed models for SMT, handoff, and base station (BS). Chapter 8.4 includes example heterogeneous network scenarios which have over-

lapping RATs with different working parameters as well as proposed SMT, followed by performance evaluation. The chapter is concluded with Chapter 8.5 providing final remarks and a discussion.

## 8.2 Related Works

Although the vertical handoff concept is relatively new, several studies can still be found in the literature. In [3], the authors discuss different factors and metrics which are considered when triggering handoff. Besides, they describe a vertical handoff decision function (VHDF) which enables devices to assign weights to different network factors such as monetary cost, QoS, power requirements, personal preference, and so on.

A novel fuzzy logic–based handoff decision algorithm for the mobile subsystem of tactical communications systems is introduced in [4]. Handoff decision metrics used in [4] are: RSSI, the ratio of the used capacity to the total capacity for the access points, and relative directions and speeds of the mobiles to APs. The authors compare their algorithm with the RSSI–based handoff decision algorithm as well. Note that in [4, Eq.(3)], ambient interference power is embedded into the parameter of capacity, rather than being used as a direct input to the decision process.

In [5], the author presents a review on the proposed vertical handoff management, and focuses on the decision making algorithms in vertical handoff. The article [6] presents a tutorial on the design and performance issues for vertical handoff in an envisioned multi–network fourth–generation environment. In [7], the authors give a fuzzy logic based vertical handoff scheme involving some key parameters and the solution of the wireless network selection problem using a fuzzy multiple attribute decision making (FMADM) algorithm.

It is considered that adaptation is crucial for next generation wireless networks from every aspect, such as handoff management and scheduling, since FRO seems to be one of the strongest deployment candidates [8-10]. Because interference is a very dynamic phenomenon, success of the adaptation of next generation wireless networks depends on being aware of the factors affecting it [11, 12]. Therefore, the traditional fuzzy-based algorithms might not be able to meet the requirements of NGWN unless they take into account interference in their decision procedures. To the best knowledge of authors, none of the fuzzy–based handoff algorithms considers ambient interference power level as a direct input to their decision mechanisms.

## 8.3 The Proposed Models and Algorithms for Vertical Handoff

Vertical handoff is a process issue compared to horizontal handoff as explained earlier. The cognitive smart terminal proposed in this study is in complete charge of managing the handoff process as well as its other functions. It scans the environment periodically for available APs, obtains the operating parameters, combines and processes all necessary parameters using its fuzzy logic–based classifier, initializes handoff process, and chooses the best candidate AP. The following subsections include the proposed models and algorithms implemented using OPNET Modeler simulation tool and MATLAB software.

### 8.3.1 Smart Terminal Process Model

The proposed smart terminal process model has a cross-layer design and is developed using OPNET Modeler software. It includes physical, medium access control (MAC), and some upper layer functions. It has a carrier sense multiple accessing/collision avoidance (CSMA/CA) MAC module for the wireless fidelity (WiFi) capability and a GSM module to handle GSM operations. Besides, it has a fuzzy logic–based smart handoff decision unit which is in charge of managing all of the handoff operations.

Figure 8.1 outlines the state transition diagram of the SMT process model. The process starts with the Init state. This state performs a delay until the other processes in the simulation are initialized and loads the control variables. Then the process enters the Spectrum Scan and Handoff Decision states which are responsible for scanning the environment for available APs and managing the entire handoff process exploiting the proposed fuzzy logic–based handoff algorithms. The WiFi Mode and GSM Mode states stand for WiFi and GSM functionalities, respectively.

During the spectrum sensing phase, SMT listens to wireless medium for any handoff broadcast packet which might be sent by potential APs for a specified time span. All of the GSM APs have a broadcast control channel (BCCH) which is the first channel of allocated spectrum and is used for broadcasting network information periodically for possible handoff process in addition to its other functions. The detailed information about GSM technology can be found in [13]. The WiFi APs broadcast a handoff information packet periodically for this purpose as well. During the listening period, the SMT changes its working parameters such as frequency, modulation, data rate, and bandwidth in order to adapt to any possible AP and to receive handoff broadcast packet.

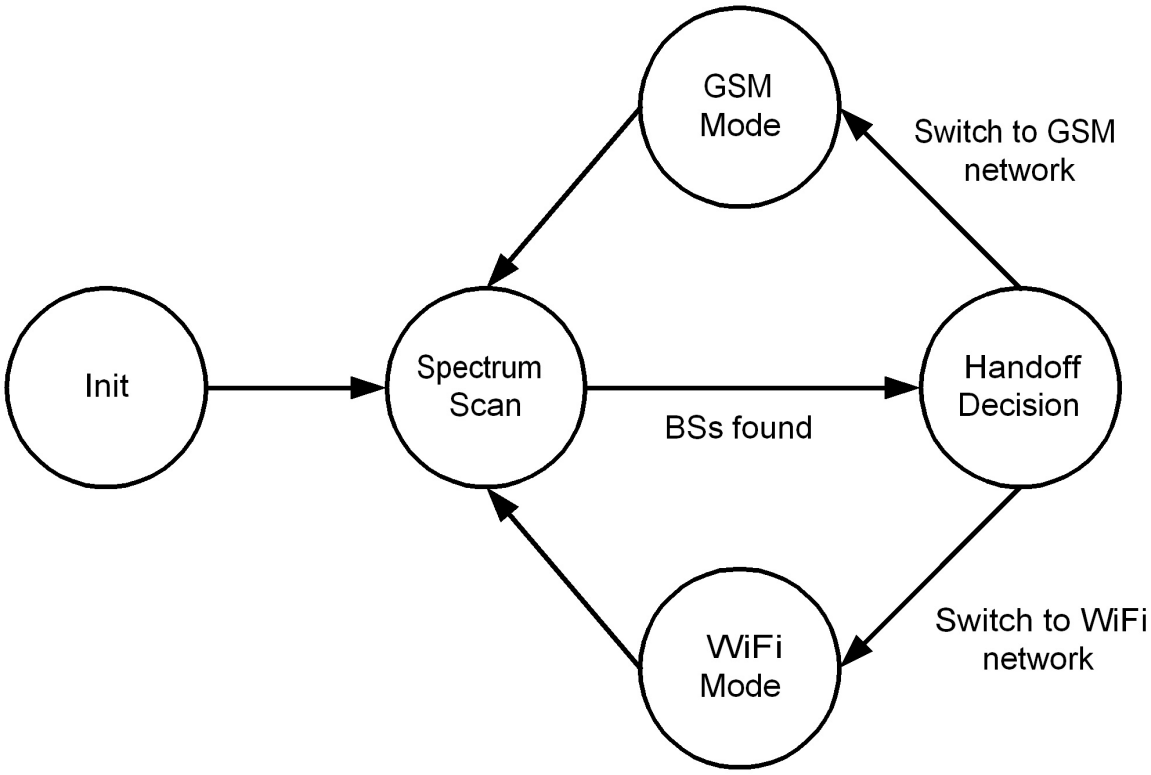


Figure 8.1 The SMT cross–layer process model.

When any AP is available, SMT receives the handoff broadcast packet and extracts the network working parameters. It then invokes fuzzy–based handoff decision algorithm which takes these parameters as inputs; processes them; and produces an output called access point candidacy value (APCV). APCV is generally defined by a real number in order to quantify the strength of the candidacy level of the AP found. For instance, APCV can be designed to vary between one and ten where one denotes the weakest, whereas ten represents the strongest candidacy level of quantification. Subsequently, all the aforementioned network parameters along with APCV are stored in the handoff decision table (HDT) for further use.

All of these steps are repeated until the scan process is terminated. In each turn, SMT listens to the environment for potential APs, receives the handoff broadcast packet of the AP found, calculates the APCV using its adaptive fuzzy inference system, and stores all the pieces of information required in the HDT.

The sequence diagram of the proposed handoff decision algorithm is outlined in Figure 8.2. This schema is repeated in every 10s throughout the simulation run time.

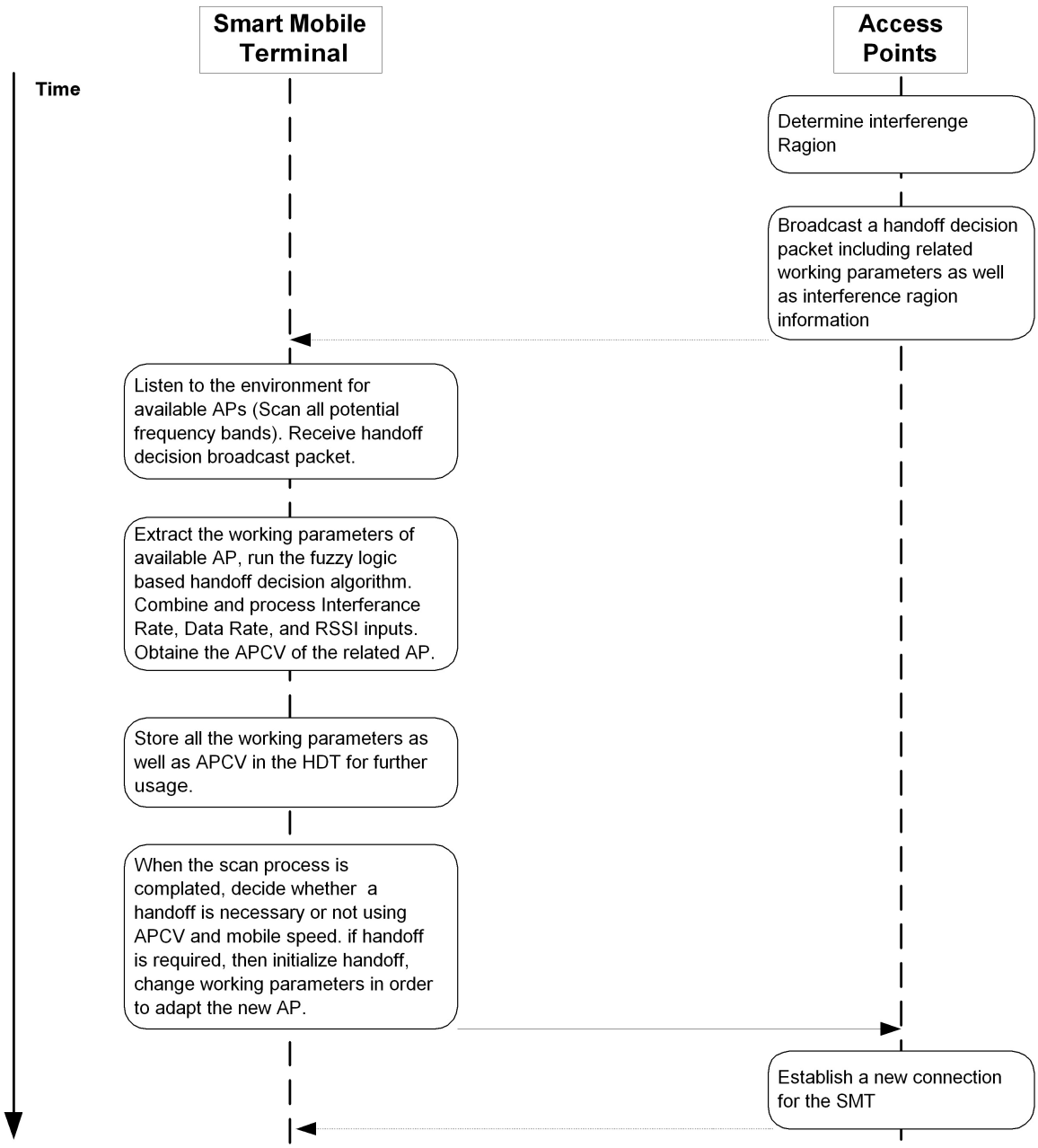


Figure 8.2 Sequence diagram of the proposed handoff decision algorithm.

As soon as the scan process is completed, APCV of each available AP is compared with that of current APs. If the difference between the compared values is equal to or greater than the handoff resolution (HR), that is a value determined by user, then the second condition, *i.e.*, mobile speed, is evaluated. The mobile speed 10km/h is selected as a threshold value. Any speed value below this threshold is regarded as walking speed and in this case, either any GSM or WiFi AP can be

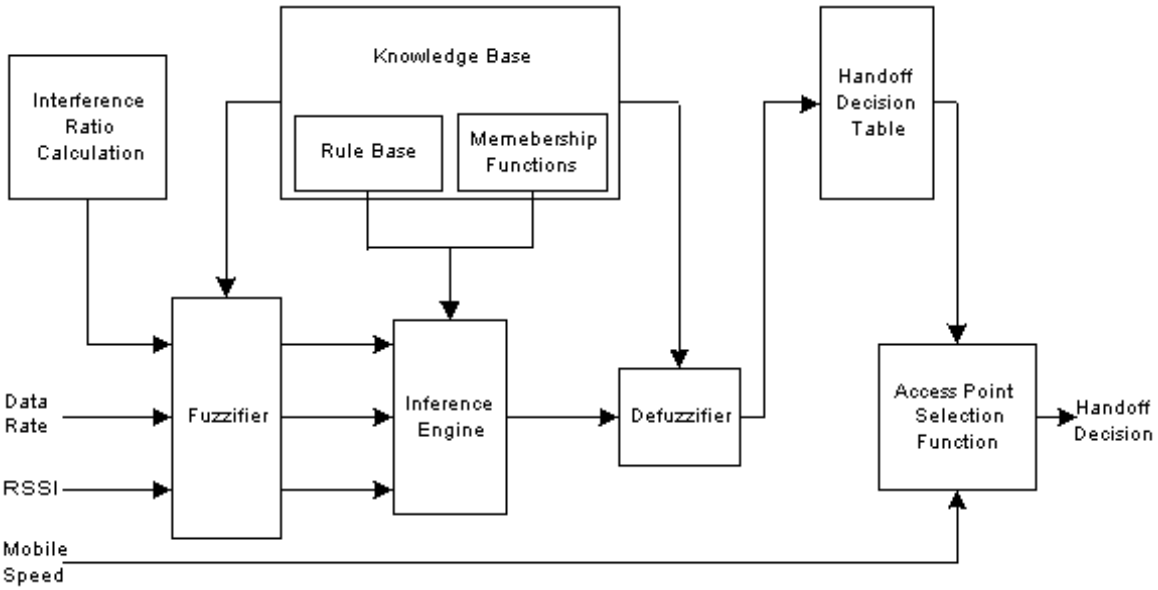


Figure 8.3 Block diagram of the proposed fuzzy logic-based handoff system.

chosen as a serving node. Otherwise, only GSM network can be preferred, since the WiFi AP might serve SMT only for a very short duration. When these conditions are satisfied, handoff process is initialized.

### 8.3.2 Proposed Handoff Decision Algorithm

Sophisticated handoff decision algorithms should consider more than one criteria and a methodology to combine and process them. Different decision algorithms have been proposed in the literature for vertical handoff as mentioned earlier. Artificial intelligence-based systems such as fuzzy logic and artificial neural networks are good candidates for pattern classifiers due to their non-linearity and generalization capability [4, 14]. Therefore, in the proposed handoff decision system a fuzzy logic based approach has been adopted.

Vertical handoff decision algorithm should initialize handoff process considering avail-able network interfaces (link capacity, power consumption, link cost, and so on), system information (remaining battery), and user/application requirements (cost, QoS parameters, and so on). The block diagram of the proposed handoff decision system is given in Figure 8.3.

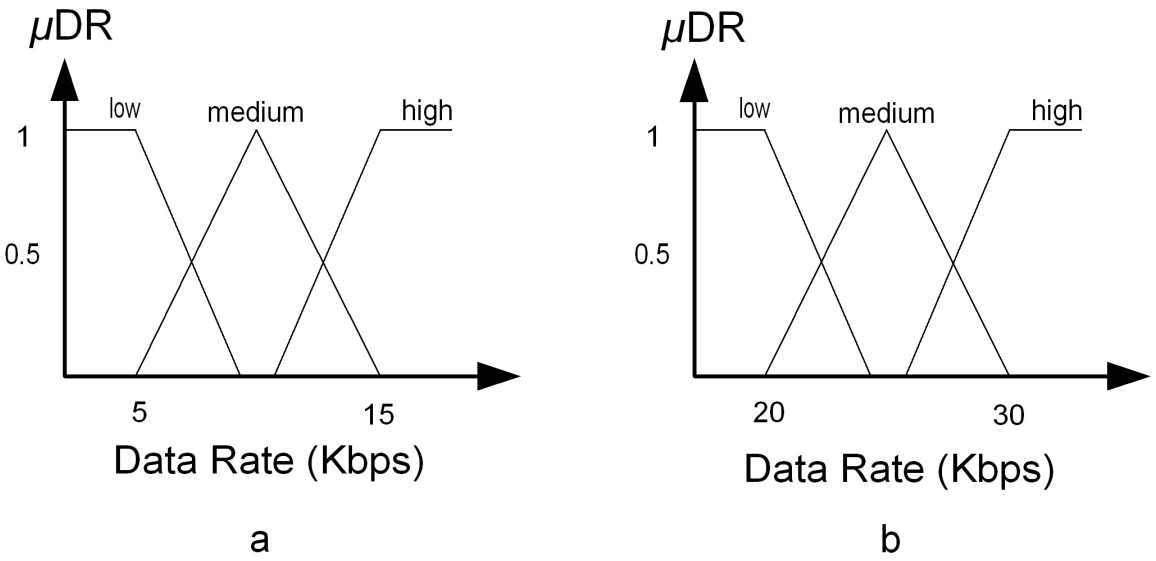


Figure 8.4 Fuzzy membership function for two different data rates (DR).

The algorithm combines the user/application requirements and network capabilities, and produces an output which is utilized to make handoff decision and to choose the best candidate AP.[1] In the proposed handoff system, there are three inputs (data rate, interference rate, and RSSI) for fuzzy inference system. Membership functions of these inputs are given in Figure 8.4, Figure 8.5, and Figure 8.6, respectively. In the figures, the horizontal axis indicates the crisp values of the aforementioned handoff parameters, whereas the vertical axis (*i.e.*, $\mu$ values) stands for the membership value of related parameter. The crisp inputs are converted into the fuzzy variable by means of these membership functions. Trim and trapezoid shapes are chosen as fuzzy membership functions due to their capability of achieving better performance especially in real time applications.

The data rate (DR) input has the ability to change its structure according to the application requirements as well. For instance, if the DR requirement of an application is 9.6Kbps (GSM data transfer), then the membership function is similar to the one given in Figure 8.4. On the other hand, when the application needs more bandwidth, *e.g.*, 25Kbps (GPRS Class 6 traffic), then it dynamically changes its structure to adapt the new working condition as seen from Figure 8.4.

The interference rate parameter is also obtained by each AP and sent to the SMT in order to be considered in handoff decision process. In the proposed algorithm, interference rate refers to a special fuzzy logic variable whose value is determined by the ambient CCI power level. In GSM,

[1]It is worth mentioning here that data rate and interference ratio calculations in Figure 8.3 can be considered as parameters related to the user/application requirements, since there are certain values for these parameters mandated by the application (*e.g.*, data transmission or voice services).

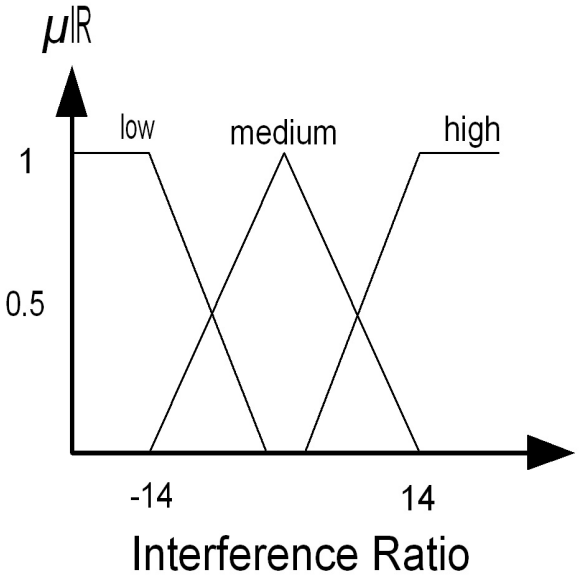


Figure 8.5 Fuzzy membership function for two different interference rates (IR).

The specification regarding the CCI level (GSM 05.05) recommends that the carrier-to interference ratio (C/I) is at least 9dB in order to meet the bit-error rate (BER) requirement. This indicates that for a reference signal level of -101dBm, which is the standard value for a GSM mobile station, CCI power level should be less than -110dBm. However, in a typical GSM deployment, it is reported that C/I is around 14dB-15dB [15]. In this sense, interference rate parameter is designed in such a way that the power level difference between the desired signal and interference is lower than -14dB is assigned to be a low fuzzy logic value, whereas a difference that is greater than 14dB is selected to be a high fuzzy logic variable. The corresponding membership function for the interference rate parameter can be seen in Figure 8.5.

The RSSI input of the fuzzy system has also the ability to change its structure according to the network requirements. The RSSI membership function for GSM and WiFi networks are different as shown in Figure 8.6.

As stated earlier, according to the inputs of available APs the fuzzy inference system produces an output value between one and ten which describes the candidacy level of related AP. Any handoff initialization process is decided upon this value. One of the most crucial parts of this study is the new adaptive fuzzy inference system which is developed in order to make handoff decision. A fuzzy logic system consists of three main parts: Fuzzifier, Inference Engine, and Defuzzifier. Fuzzifier converts a crisp input into a fuzzy variable where physical quantities are represented by linguistic variables with

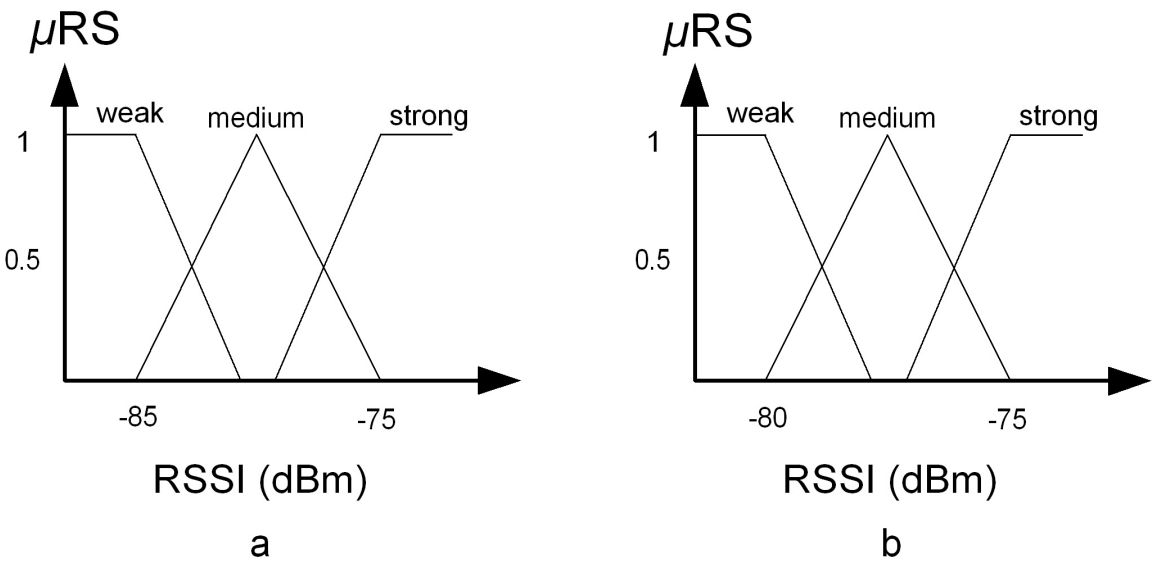


Figure 8.6 Fuzzy membership functions for two different RSSIs (RS).

| Rule | IF | THEN |
|---|---|---|
| 1 | (DataRate is low) and (InterferenceRate is low) and (RSSI is weak) | (APCV is 1) |
| 2 | (DataRate is low) and (InterferenceRate is low) and (RSSI is medium) | (APCV is 2) |
| 3 | (DataRate is low) and (InterferenceRate is low) and (RSSI is strong) | (APCV is 1) |
| … | … | … |
| 21 | (DataRate is high) and (InterferenceRate is low) and (RSSI is strong) | (APCV is 10) |

Figure 8.7 Example fuzzy rules.

appropriate membership functions. These linguistic variables are then used in rule base of Fuzzy Inference Engine. Since there are three input variables each has three levels (*i.e.*, low, medium, and high), there are 27 rules used for producing a new set of fuzzy linguistic variables. Some of the fuzzy rules in the rule base are tabulated in Figure 8.7. For instance, Rule 1 corresponds to the following IF-THEN structure: if the potential AP supports low data rate, it is in a bad interference condition, and its RSSI is weak, then the APCV of the AP is 1, which means it is not a strong candidate. On the other hand, Rule 21 outputs a greater APCV value, *i.e.*, 10, which implies the APs candidacy level is quite high.

Defuzzifier is responsible for converting this fuzzy engine output into a number called APCV. The output of the fuzzy system, APCV, is then combined with the mobile speed parameter to make handoff decision.

The analytic model of the fuzzy inference system is as follows [4, 16]. Three dimensional pattern vector (input of the fuzzifier) for candidate access points is:

$$\mathrm{PV}_c = [\mathrm{DR}_c; \mathrm{IR}_c; \mathrm{RS}_c] \tag{8.1}$$

where DR is data rate, IR is interference rate, and RS is RSSI value of available AP. Three dimensional fuzzy pattern vector (output of fuzzifier and input of inference engine) for candidate access points:

$$\mathrm{PV}_F = [\mathrm{DR}_1; \mathrm{IR}_2; \mathrm{RS}_3] \tag{8.2}$$

Since product inference rule is utilized in the fuzzy inference engine then, for a new pattern vector, contribution of each rule in the fuzzy rule base is:

$$C_r = \prod_{i=1}^{3} \mu_{F_i}(P_i), \tag{8.3}$$

where $\mu_{F_i}(P_i)$ is the membership value of the $P_i$ for fuzzy set $F_i$, and obtained from the aforementioned membership functions. There are 27 rules in the proposed system and a center average defuzzifier is used. Hence, the output of the defuzzifier (i.e., APCV) becomes:

$$M_a = \frac{\sum_{l=1}^{27} y^l C_r}{\sum_{l=1}^{27} C_r}, \tag{8.4}$$

where $y^l$ is the output of the rule $l$.

### 8.3.3 GSM Base Station

In GSM, each BS periodically broadcasts handoff decision packet using its BCCH in order to convey network information to any terminal in the vicinity for a possible handoff. In addition to this, in the proposed method, BS is in charge of both determining its interference rate and conveying this information to the SMT with the aid of its handoff broadcast packet. Figure 8.8 shows the proposed GSM process model realized using OPNET Modeler.

As in the former process model, the process starts with the init state as well, then enters the idle state, and waits there until a specific interrupt arrives. The fromRx state machine delivers

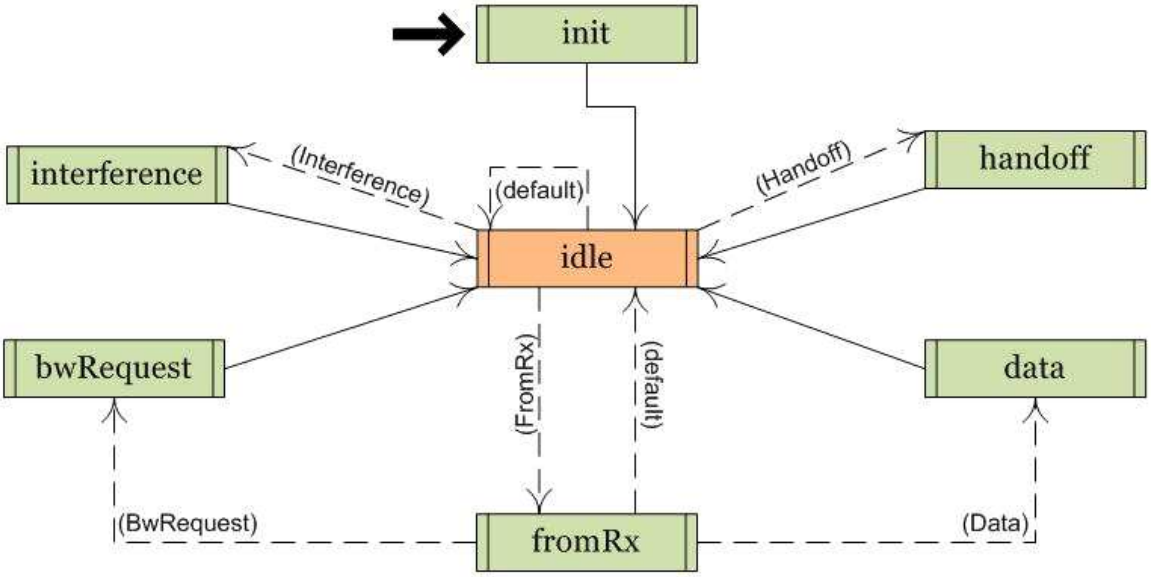


Figure 8.8 Proposed process model for APs.

arriving packets to the next state machine, which can be either bwRequest or data state machine depending on the packet formats. If the bwRequest state machine is selected, then connection establishment/termination requests are handled. In case the data state machine is selected, then the received data is delivered to its destination. The interference state machine determines the interference rate of the BS and inserts this information into the related field of handoff broadcast packet. Finally, the handoff broadcast packet is created, provided with all of the required information, and then broadcasted to the environment in the handoff state machine.

## 8.4 Numerical Results and Discussions

### 8.4.1 Assumptions

In this study, two different simulation scenarios are evaluated in order to investigate performance of the developed models and algorithms. The first one, which is illustrated in Figure 8.9 and referred as "Scenario 1" in the remainder of the paper, has a higher interference rate, whereas the second one, which is given in Figure 8.10 and referred as "Scenario 2" in the remainder of the paper, has a lower interference rate. Having these two scenarios in hand, the impact of interference can be extracted and interpreted from the simulation results. Three wireless networks are considered in the simulation scenarios. One of them is a WiFi network and the rest are GSM networks each of

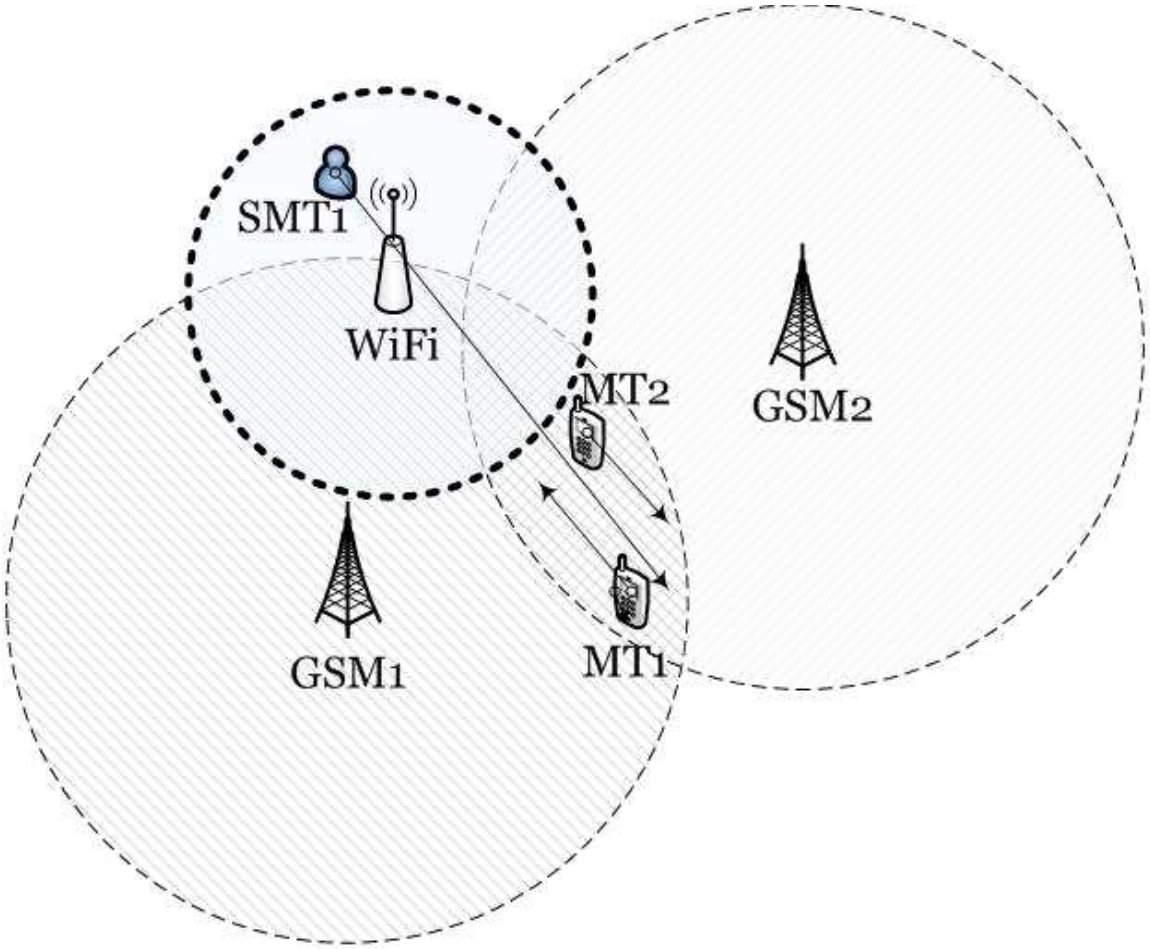


Figure 8.9 Vertical handoff example with higher interference rate (referred as Scenario 1).

which has specific working parameters. GSM-WiFi pair is selected due to the following reasons: Both GSM and WiFi are very well-established and vastly deployed standards that are currently being used; therefore, they constitute an appropriate case study for vertical handoff performance evaluations. In addition, GSM is a cellular standard in which handoff is one of the default network facilities, whereas WiFi does not have the concept handoff in the first place. From this perspective, handoff becomes a more challenging problem com-pared to other possible network pairs, such as GSM-CDMA pair, since CDMA contains the handoff concept as well. Also, in spite of the fact that many GSM deployments are not of FRO mode, GSM specification allows FRO mode of operation. Therefore, in order to evaluate the impact of FRO on the method proposed, a GSM deployment of FRO is considered. This way, it is possible to get a clue about the performance of the method proposed in next generation wireless networks which are expected to deploy FRO.

Beside the networks, there are two mobile terminals which are served by GSM networks individually along with a smart terminal (SMT1) which has the capability of generating time sensitive voice traffic (13Kb/s), GSM data traffic (9.6Kb/s), and Class 6 GPRS data traffic (25Kb/s). In both scenarios, MTi denotes the ith mobile terminal served by base station labeled with BSi. These mobile nodes are of crucial importance for the method proposed, because they generate wireless traffic which causes interference to SMT1 and affects the decision regarding the handoff. It is worth mentioning that since interference spilled over SMT1 is a function of time and space, directions of motion of mobile terminals are important in terms of performance evaluation of the method proposed. Note that SMT1 moves along the trajectory shown in Figure 8.9 and Figure 8.10 of a specified speed during the simulation run time, senses the environment continuously for candidate APs, and has the aforementioned adaptive fuzzy logic-based handoff decision system as well as the capability of performing both WiFi and GSM functionalities.

In this sequel, one might wonder about the impact of traffic loads of APs present in the environment on the performance of the method proposed. In both of the scenarios considered in this study, it is assumed that one of the GSM base stations can provide less data rate compared to the other. This assumption is actually the common consequence of the following two items: Either (I) applications of the user of interest require different bandwidths, such as 9.6Kbps for voice application and 25Kbps for data transmission, or (II) regardless of the application requirements of the user of interest, GSM base stations can offer different data rates for a newcomer due to their different traffic loads. In other words, one of the GSM base stations can offer less data rate, because it cannot offer higher data rate due to its high traffic load present. From this point of view, results for the scenarios considered in this study already include the impact of traffic loads of APs present in the environment.

Diameter of the cluster which constructs the overall network topology is chosen to be four kilometers. The simulation was run for 3600 seconds and other relevant parameters are given in [13].

In addition to the scenario assumptions given above, due to its importance, interference assumptions need to be explained further for the sake of completeness. Considering the fact that dynamic condition of the mobile radio propagation environment changes very rapidly, the received signal at a receiver can be defined for mobile radios by the following two processes:

$$r(t) = m(t)s(t) \tag{8.5}$$

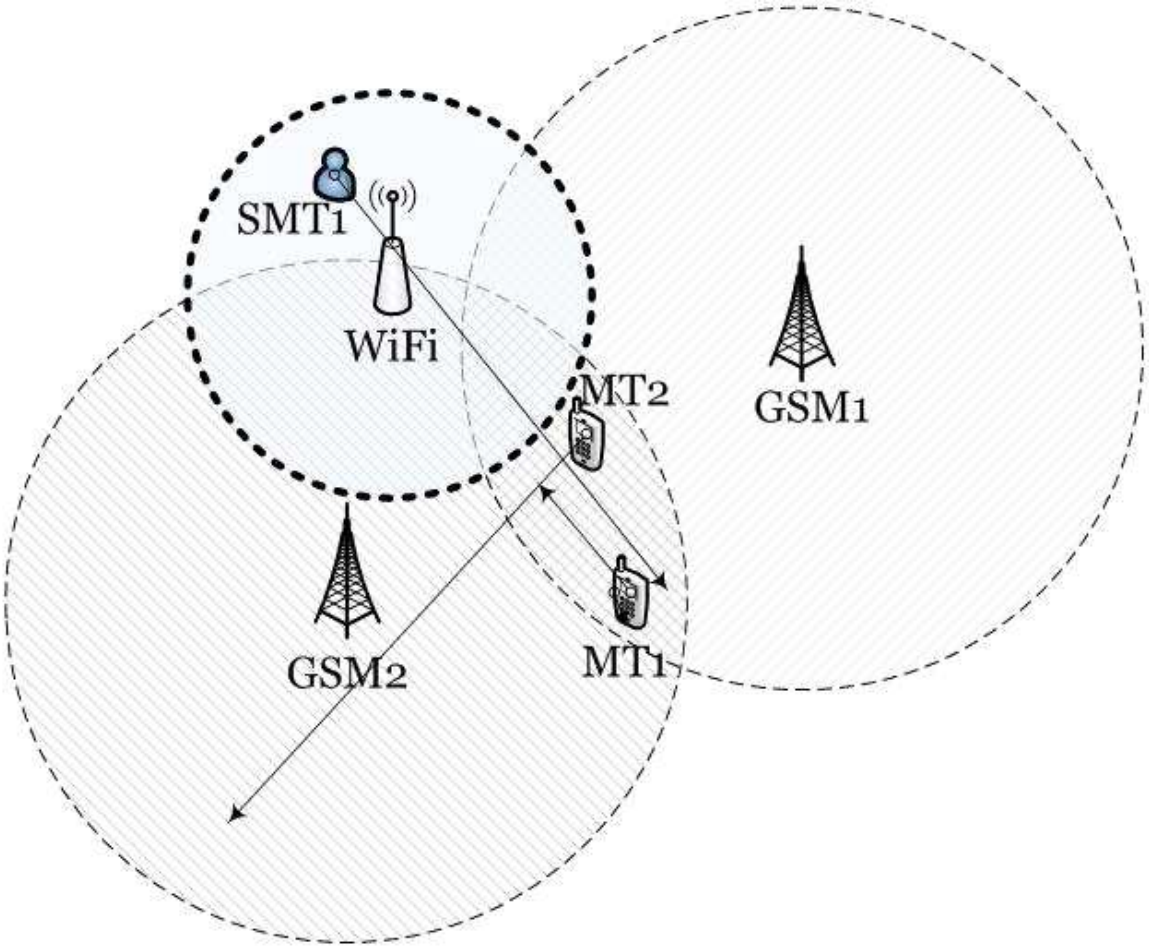


Figure 8.10 Vertical handoff example with lower interference rate (referred as Scenario 2).

where $m(t)$ is the fast fading (*i.e.*, short–term multipath fading) component and $s(t)$ is the local mean (*i.e.*, long-term shadow fading) of the received signal [17, 18]. Generally, $m(t)$ and $s(t)$ are identified in terms of probability distributions, since both are random processes. In the literature, Rayleigh and Rice distributions are frequently assigned the envelope of for non-line-of-sight (NLOS) and line-of-sight (LOS) cases, respectively. Field measurements reveal that shadowing process follows a log-normal distribution with a standard deviation $\sigma$ which is defined, again, in linear scale [18]. Hence, the following formal model is adopted for representing $s(t)$:

$$s(t) = e^{(\sigma g(t))} \tag{8.6}$$

where $\sigma$ is the standard deviation of the shadowing and $g(t)$ is a normal process with $\mathcal{N}(0,1)$. It is also important to note that $m(t)$ and $s(t)$ are statistically independent processes [18, 19].

In regard to shadowing process $s(t)$, empirical studies show that there is a correlation in shadowing with respect to distance between two points in the space. Spatial correlation of shadowing is reported to be of an exponentially decaying form [20]. Considering practical purposes, there are several models proposed in the literature. For instance, [21] defines the normalized relationship between shadowing and its spatial correlation as:

$$\rho(\Delta d) = e^{\left(-\frac{\Delta d}{d_\rho}\ln 2\right)} \tag{8.7}$$

where $d_\rho$=5m for indoor and $d_\rho$=20m for outdoor environments exemplifying practical scenarios.

### 8.4.2 Simulations and Performance Analysis

Before proceeding to the performance results and related discussions, it is appropriate to evaluate how well the Gauss-Markov assumption can capture the shadowing process introduced in Chapter 8.4.1. In order to verify the validity of Gauss–Markov assumption, the settings given for a suburban area in [23] are adopted with the following variables: $b = 0.82$ , $v = 3$m/s, $\Delta t = 1$s, and $d_\rho = 100$m.[2] Within the decorrelation distance, each value of the shadowing process is obtained with the aid of (7) for the aforementioned parameter set. The process is initiated by an initial value which comes from the normal process with similar to that in (5).

The first performance simulation set focuses on the case in which SMT1 moves along with the trajectory as illustrated in Figure 8.9 and Figure 8.10 of a specified speed. The simulation of the example scenarios has been run for different applications and working conditions, *i.e.*, voice transfer and data transfer (9.6Kb/s and 25Kb/s), in order to evaluate the performance of the proposed approach comparatively. The performance metrics examined are; APCV of each available AP, number of handoff(s), and average end-to-end (EED) delay between SMT1 and APs.

Figure 8.11 illustrates the outputs of adaptive fuzzy logic–based handoff decision algorithm for a voice transfer application in Scenario 1. APCV of each available AP is computed once in every 10s during the spectrum sensing process by the proposed fuzzy logic based algorithm employed in

[2]It is known that WLAN is designed for very low mobility scenarios which can be considered of pedestrian speed classes in ITU-R Standard Channel Models. Therefore, considering a mobile which is faster than an average pedestrian speed is not reasonable, since a high-speed user handed over a WLAN base station cannot maintain the connection. Note also that since a high-speed user cannot be accommodated by WLAN, it cannot be handed over any GSM base station stemming from the fact that handoff mandates an existing connection by its very definition.

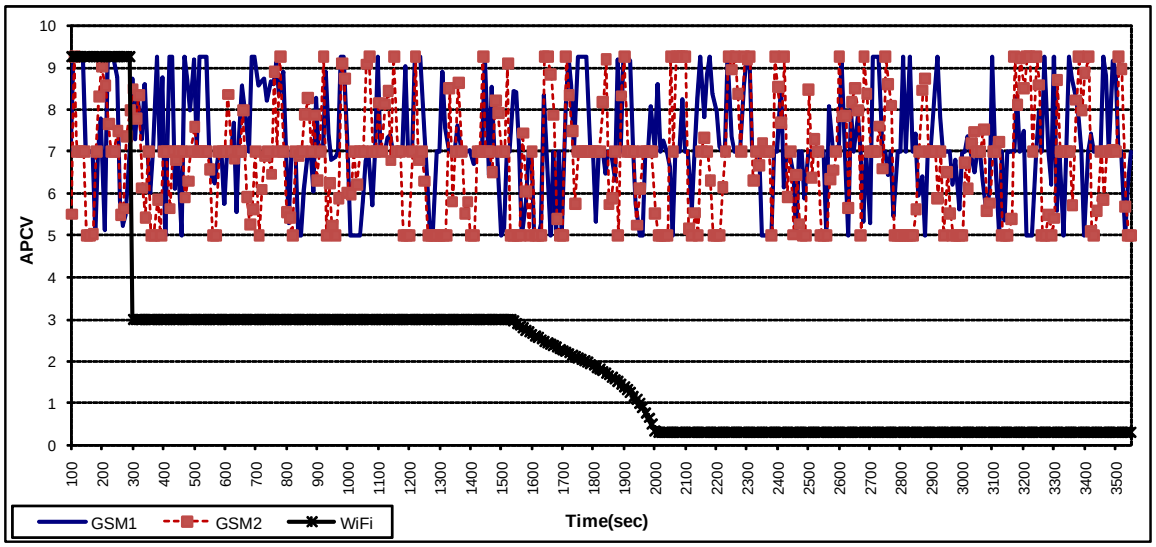


Figure 8.11 APCV output of the proposed handoff decision algorithm for voice transfer application in Scenario 1.

SMT1. As can be seen from the figure, the APCV of the WiFi hot spot is greater than those of the others when the simulation starts. At 300ms, WiFi is not able to provide higher data rates anymore causing a decrease in the output of the proposed fuzzy system. Furthermore, because SMT1 moves out of the coverage area of WiFi, a rapid attenuation in RSS is experienced. Hence, the APCV is reduced once more between simulation times 1550 and 2000 seconds. When producing APCV, in case two candidate GSM BSs are of interest, the interference rate becomes the determinant input stemming from the fact that GSM BSs have approximately similar RSSI and DR values. The APCV of the candidate GSM BSs varies between 5 and 9.25 as can be seen from Figure 8.11. Note that, for the GSM BSs, behavior of the interference rate looks similar to each other due to the motion of both mobile terminals in the vicinity of cell borders. These random movements cause random fluctuations in the interference rates observed as well. As a consequence, determining the candidate BS depends on the instantaneous interference rate values.

Figure 8.12 presents the number of handoffs as a function of HR value for Scenario 1. As expected, the number of handoffs increases when SMT has a lower HR value. Hence, the lower the HR, the higher the number of handoffs. In order to determine an optimum HR value, user preferences, application requirements, and/or network conditions need to be taken into account.

Figure 8.13 illustrates the outputs of adaptive fuzzy logic–based handoff decision algorithm for Scenario 2 along with the same procedure carried out in Scenario 1. Note that in Scenario 2, the


Figure 8.12 Number of handoffs versus HR for Scenario 1.

behavior of APCV for WiFi behaves exactly the same as in Scenario 1. When producing APCV, in case two candidate GSM BSs are considered, the interference rate is still the determinant input because GSM BSs have approximately similar RSSI and DR values. In general, APCV of GSM1 is greater than that of GSM2 most of the times during the simulation. Especially after 1000s of the simulation run time, the dominance of the APCV value of GSM1 is obvious. This stems from the motion of MT2 towards GSM2 implying a diminishing interference power observed by GSM1. Therefore, the probability of selecting GSM1 as serving BS increases in time.

Figure 8.14 presents the number of handoffs as a function of HR value for Scenario 2. The number of handoff increases when SMT has a lower HR value, as in Scenario 1. As compared to the one given in Figure 8.12, the number of handoff is quite less in Figure 8.14 as expected, since GSM1 has lower interference rates most of the times during the simulation.

In order to evaluate the performance of our proposed algorithms comparatively, Figure 8.15 can be examined. Figure 8.15 illustrates the measured GSM and WiFi RSSI results as a function

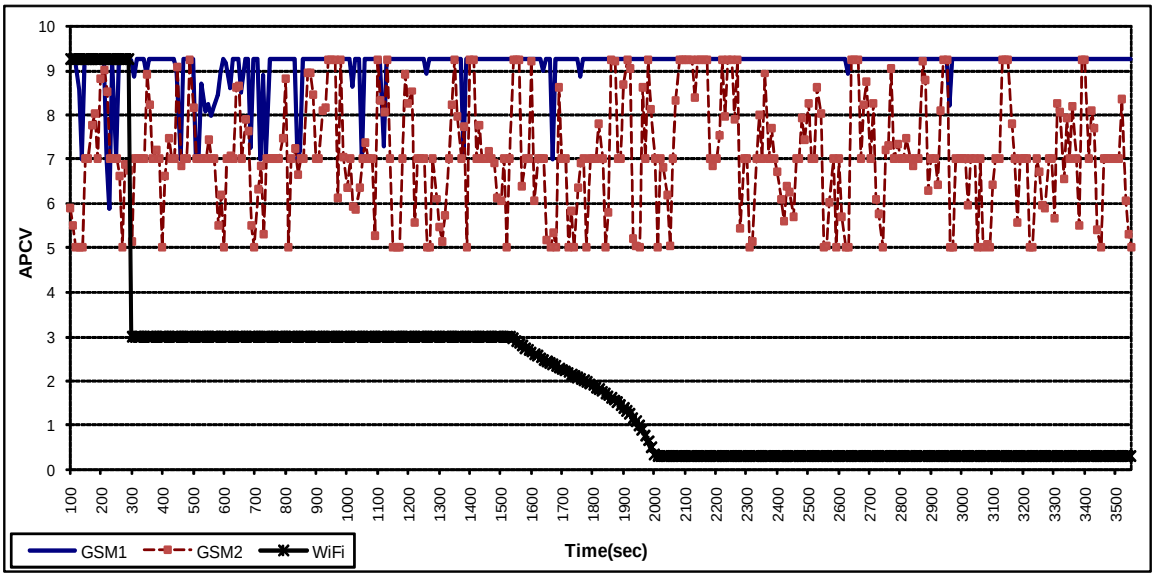


Figure 8.13 APCV output of the proposed handoff decision algorithm for voice transfer application in Scenario 2.

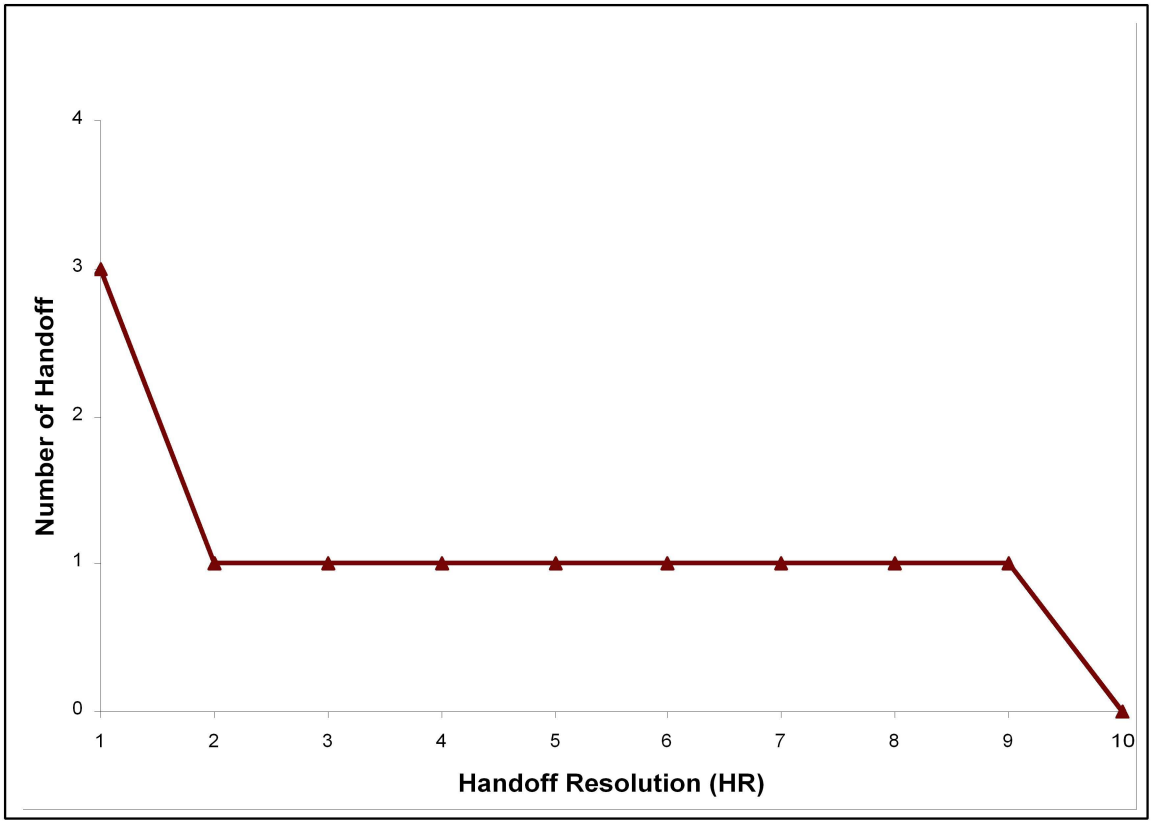


Figure 8.14 Number of handoffs versus HR for Scenario 2.

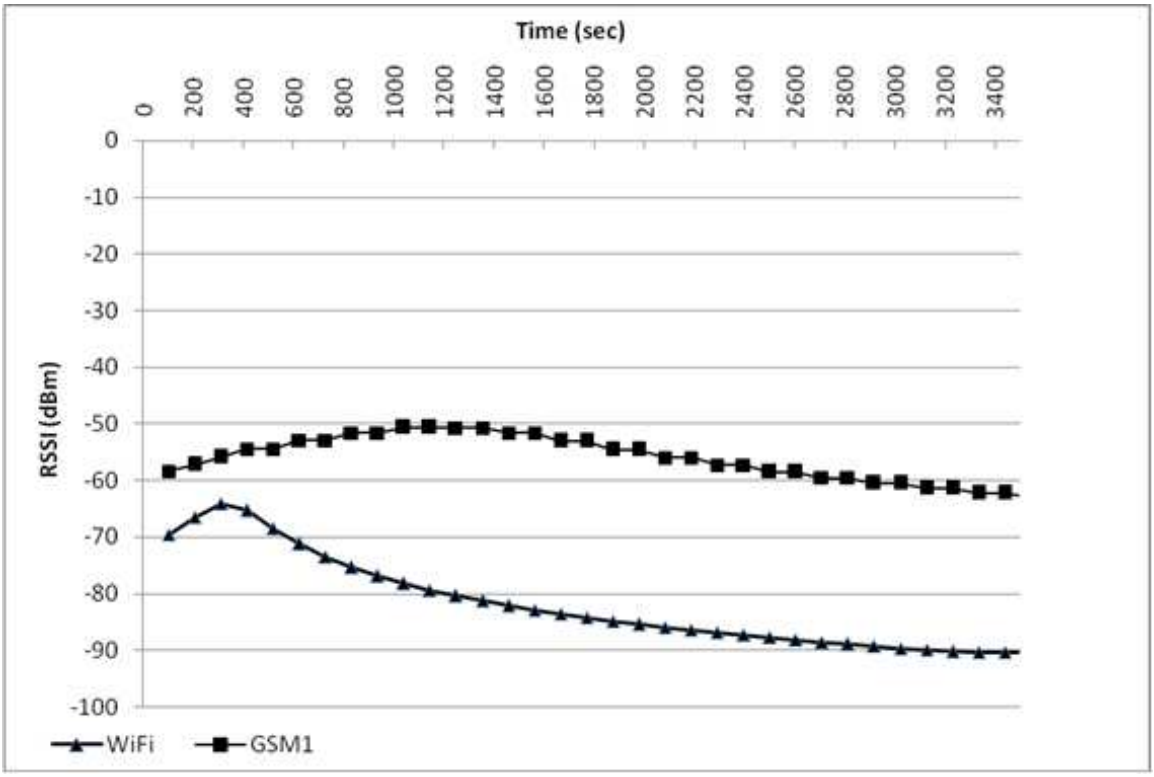


Figure 8.15 RSSI–based performance evaluation chart.

of the simulation run time. If any RSSI based horizontal handoff algorithm considered, which is alternative to the proposed multi–criteria approach, the following two conclusions can be drawn from the performance figure: (I) Since the RSSI values of the GSM are greater than those of WiFi along with the simulation run time; the SMT always prefers the GSM base station to camp on. However, this truth is not indicated in our study, it means additional monetary cost, since the WiFi is less expensive than GSM network. (II) According to our scenario (*i.e.*, Scenario 2), the supported bandwidth by the WiFi is greater than GSM from simulation starting time to the 300 sec. During this time proposed scheme chooses the WiFi AP, whereas the RSSI based traditional algorithms chooses the GSM BS due to its greater RSSI values, which can be raised unexpected results in terms of QoS parameters.

In Figure 8.16, average EED results (between SMT1 and APs) of different application traffics are presented as a function of the simulation run time. The EED results are obtained for Scenario 2 which represents the better interference rate conditions. Note that although all of the settings used for Scenario 2 are the same as those for Scenario 1, the mobility behavior of MTs in Scenario

2 is different than that in Scenario 1. A different mobility behavior with the same settings, as will be discussed here, will affect the results due to changing interference conditions; therefore, it will form a different simulation environment from the perspective of decision process proposed. In the light of this, SMT1 firstly camps on WiFi hot spot since it has a sufficient data and lower interference rate along with a high RSSI. After 300s, the data rate supported by the WiFi AP dramatically decreases. Even though both RSSI and interference rate are appropriate, fuzzy-based handoff decision scheme decides to change the AP considering inadequacy in the DR offered. As can be seen from the Figure 8.10, there are two alternative APs. For data transfer application with 9.6Kb/s and voice transfer application GSM1 is selected as the new AP since both the DR and RSSI value meet the QoS requirements along with a relatively lower interference rate. The latency results of voice transfer are lower than those of data transfer with 9.6Kb/s. This is not surprising, because one slot is guaranteed for voice transfer application, whereas even reserving one slot might not be possible for data transfer due to dynamic network load conditions.

When the data transfer application with 25Kb/s is running on SMT1, a conflict between data and interference rate arises. On the one hand, GSM1 observes a lower interference rate compared to GSM2. On the other hand, GSM2 can provide a higher DR compared to GSM1. Results show that GSM2 AP is selected after the decrease in DR offered by WiFi at 300s of the simulation run time. This stems from the fact that fuzzy logic system weights the data and interference rate inputs differently because of QoS requirements of the application running on SMT1. As can be seen from Figure 8.16, the average delay for this application is lower than those for the other applications, since GPRS Class 6 traffic type can be assigned up to four slots.

## 8.5 Conclusions

Vertical handoff is defined as a process which transfers a user connection from one technology to another. It is expected that the next generation wireless systems will include several different network technologies cooperating with each other; therefore, vertical handoff mechanisms should be investigated in detail. In general, handoff mechanisms allow for many parameters including user profiles, application requirements, and network conditions. In this chapter, an adaptive fuzzy-based handoff decision system which combines data and interference rate, RSSI, and speed parameters is proposed in order to satisfy both user and network requirements for next generation wireless heterogeneous networks.

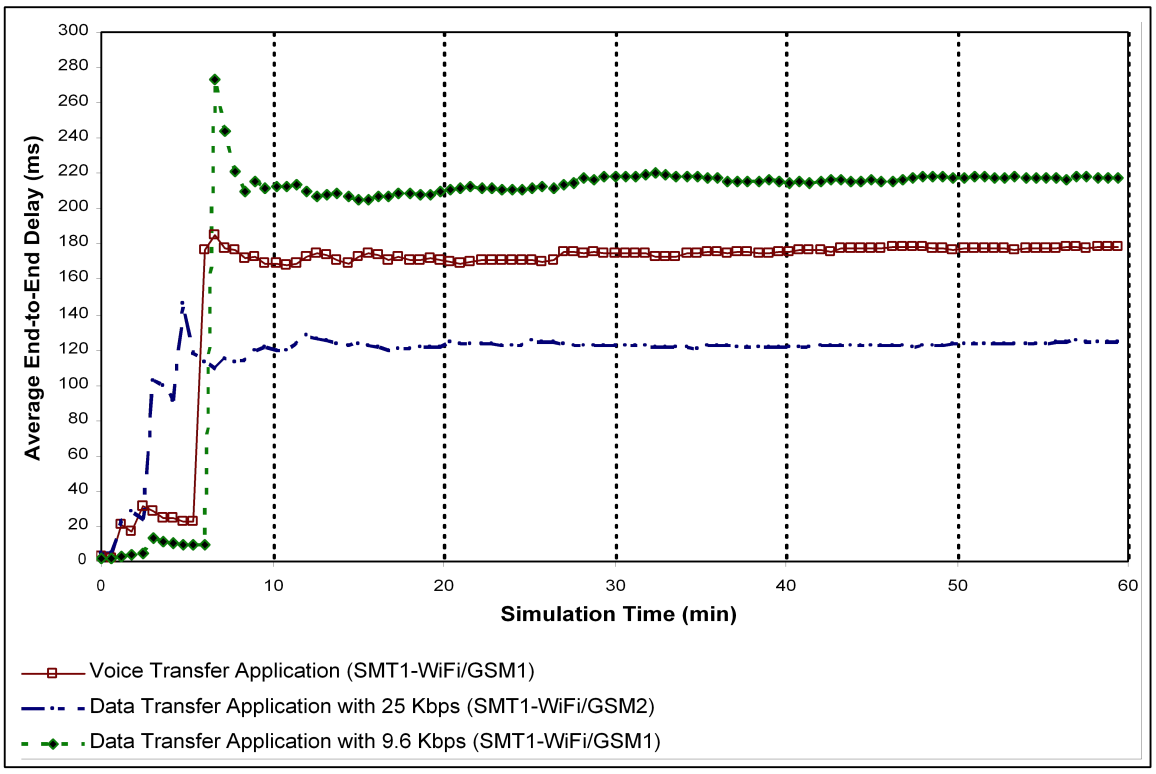


Figure 8.16 EED results (SMT1-APs) for different application traffics.

Simulation results show that the proposed fuzzy logic-based vertical handoff decision algorithm is able to determine the most appropriate access network under different dynamic working conditions. Moreover, this study reveals that interference plays a crucial role in making vertical handoff for NGWN.

# CHAPTER 9

# CONCLUSION AND FUTURE WORK

In this dissertation, a detailed investigation on environment, channel, and interference awareness for next generation wireless networks (NGWN) is established; critical issues and challenges are identified and addressed. Considering the technological convergence in the evolution of wireless systems, awareness is considered from the perspective of cognitive radio (CR) as well.

In this framework, a list of specific contributions in different chapters of this dissertation is given below. In what follows, possible extensions of this study along with future directions will be discussed too.

## 9.1 List of Specific Contributions

Similar to the elements given in Chapter 1.1, the list of specific contributions of this dissertation can be divided into the following parts:

- Environment awareness for NGWNs
  - Physical propagation environments are classified from the perspective of important wireless channel characteristics.
  - A conceptual model for NGWNs and CR networks is developed based on the traditional protocol layers defined by open systems interconnection reference (OSI).
  - An environmental awareness algorithm is provided for NGWNs and CR.
- Channel awareness for NGWNs
  - A comprehensive list of wireless channel parameters along with possible ways of measuring them is presented.
  - A new method that identifies one of the most critical wireless channel parameters, namely line–of–sight (LOS), is given.

- Interference awareness for NGWNs
  - A detailed list of interference related parameters are provided.
  - A novel method that identifies interference in NGWNs in the presence of noise is developed.
  - Performance of inter–cell interference schedulers is investigated for orthogonal frequency division multiple access (OFDMA)–based NGWNs carrying voice traffic.
  - A novel interference aware vertical handoff decision algorithm for NGWNs is proposed.

## 9.2 Concluding Remarks and Future Directions

In the light of the studies presented in this dissertation, the following items can be considered as possible research topics.

- Combined Impact of angle–of–arrival (AoA) and speed on wireless channel. As discussed in Chapter 4, channel statistics is affected drastically by AoA and speed. In order to better identify and estimate the channel parameters such as line–of–sight (LOS), the combined impact of AoA and speed can be investigated. Furthermore, a new way of looking at the mobility concept in wireless community, which is called motion intensity, can be incorporated into the analyzes of identifying and estimating several other wireless channel parameters.

- Traffic type awareness. Especially in multi–access wireless communications systems, traffic type awareness becomes more critical. Being aware of traffic type helps schedulers better adapt themselves to changing interference conditions. Considering the vast variety of traffic types to be carried by NGWNs such as data, multimedia, gaming, and voice, understanding the statistics of each type of traffic constitutes one of the most challenging research items in this manner. Furthermore, investigation of the statistics of mixture of all these traffic types is a follow–up research item in the frame of interference awareness.

- Cross–layer adaptation and optimization. In spite of the drastic developments in technology, peculiar to communication systems, it can be observed that the fundamental design architecture, which is known as "layered architecture," still remains the same. Layered architecture still accomplishes many of the important tasks; however, it leads to inefficiency and underutilization most of the times. The fundamental design architecture inherently hinders applicability

of some of the new developments such as cross–layer adaptation and optimization considered for NGWNs and CRs [82]. From this perspective, gathering all possible parameters defined in each layer and in sensor and optimizing them can be considered as the two future research topics.

## REFERENCES


[1] S. Yarkan and H. Arslan, "Exploiting Location Awareness toward Improved Wireless System Design in Cognitive Radio," *IEEE Communications Magazine*, vol. 46, no. 1, pp. 128–136, Jan. 2008.

[2] H. Arslan and S. Yarkan, *Cognitive Radio, Software Defined Radio, and Adaptive Wireless Systems (Signals and Communication Technology)*. Springer, 2007, ch. Enabling Cognitive Radio Through Sensing, Awareness, and Quantification.

[3] S. Yarkan and H. Arslan, "Exploiting location awareness towards improved wireless system design in cognitive radio," Patent Filed, 2006, uSF Ref. No. 07A006PR.

[4] H. Arslan and S. Yarkan, "Real Time Measurements for Adaptive and Cognitive Radio Systems," *EURASIP Journal on Wireless Communications and Networking*, vol. 2009, pp. 1–15, 2009, doi:10.1155/2009/202909.

[5] S. Yarkan and H. Arslan, "Identification of LOS and NLOS for wireless transmission," in *Proceedings of IEEE Cognitive Radio Oriented Wireless Networks and Communications, CROWNCOM 2006*, vol. 1, no. 1, Mykonos Island, Greece, June 07–11, 2006, pp. 1–6.

[6] ——, "Identification of LOS in time–varying, frequency selective radio channels," *EURASIP Journal on Wireless Communications and Networking*, no. 4, pp. 1–14, 2008.

[7] S. Yarkan, A. Maaref, K. H. Teo, and H. Arslan, "Impact of Mobility on the Behavior of Interference in Cellular Wireless Networks," in *Proc. IEEE Global Communications Conference (GLOBECOM 2008)*, New Orleans, Los Angeles, U. S. A., Nov. 30 Dec. 4, 2008.

[8] K. H. Teo, S. Yarkan, H. Arslan, and A. Maaref, "Method for managing interference in a mobile network," Patent Filed, 2009, MERL–2029.

[9] S. Yarkan, H. Arslan, and K. H. Teo, "Identification of Shadowed Fast Fading Interference in Cellular Mobile Radio Systems," *IEEE Communications Letters*, 2009, under review.

[10] K. H. Teo, S. Yarkan, and H. Arslan, "Method for deciding whether a mobile terminal reside in interference zone for frequency division duplex wireless communication systems," Patent Filed, 2009, MERL–2048.

[11] S. Yarkan, K. H. Teo, H. Arslan, and J. Zhang, "Upper and Lower Bounds on Subcarrier Collision for Inter–cell Interference Scheduler in OFDMA–Based Systems: Voice Traffic," *Physical Communication*, 2009, under review.

[12] K. H. Teo, S. Yarkan, and H. Arslan, "Method for scheduling resource to reduce inter-cell interference for voice communication in ofdma networks," Patent Filed, 2009, MERL–2137.

[13] C. Çeken, S. Yarkan, and H. Arslan, "Interference Aware Vertical Handoff Decision Algorithm for Quality of Service Support in Wireless Heterogeneous Networks," *Computer Networks*, no. 10.1016/j.comnet.2009.09.018, 2009, to appear.

[14] S. Yarkan and H. Arslan, "Statistical Wireless Channel Propagation Characteristics in Underground Mines at 900MHz," in *Proceedings of IEEE Military Communications Conference, MILCOM 2007*, Orlando, Florida, U.S.A., Oct. 29–31, 2007.

[15] S. Yarkan, S. Güzelgöz, H. Arslan, and R. R. Murphy, "Underground Mine Communications: A Survey," *IEEE Communications Surveys & Tutorials*, vol. 11, no. 3, pp. 125–142, 3rd Quarter 2009.

[16] S. Yarkan, S. Güzelgöz, and H. Arslan, "Wireless Channel Propagation Characteristics in Underground Mines: A Statistical Analysis and A Radio Controlled Robot Experiment," in *Proc. The second IEEE International Conference on Wireless Communications in Underground and Confined Areas (ICWCUCA)*, Val–d'Or, Canada, Aug. 25–27, 2008, accepted for publication.

[17] ——, "Statistical Wireless Channel Propagation Characteristics in Underground Mines at 900MHz: A Comparative Analysis With Indoor Channels," *IEEE Transactions on instrument and Measurement*, 2009, under review.

[18] S. Güzelgöz, S. Yarkan, and H. Arslan, "Investigation of Time Selectivity of Wireless Channels through the Use of RVC," *Physical Communication*, 2009, under revision.

[19] S. Yarkan and H. Arslan, "Binary Time Series Approach to Spectrum Prediction for Cognitive Radio," in *Proc. 66th IEEE Vehicular Technology Conference, [VTC 2007–Fall]*, Baltimore, Maryland, U. S. A., Sep. 30– Oct. 3, 2007, pp. 1563–1567.

[20] S. Yarkan, H. Arslan, and K. H. Teo, "On Shadowed Frequency-Selective Interference and Reporting Period for Broadband Wireless Communication Networks," *IEEE Transactions on Wireless Communications*, 2009, under review.

[21] J. Mitola III, "Cognitive radio an integrated agent architecture for software defined radio," Ph.D. dissertation, KTH Royal Institute of Technology, Stockholm, Sweden, May 8, 2000. [Online]. Available: http://www.it.kth.se/~jmitola/Mitola_Dissertation8_Integrated.pdf

[22] H. Arslan, *Signal Processing for Mobile Communications Handbook, M. Ibnkahla, Ed. Boca Raton, FL: CRC.* CRC Press, 2004, ch. 28, Adaptation Techniques and the Enabling Parameter Estimation Algorithms for Wireless Communication Systems, pp. **28**–1 – **28**–26.

[23] T. S. Rappaport, *Wireless Communications: Principles and Practice*, 2nd ed., ser. Prentice Hall Communications Engineering and emerging Technologies Series. New Jersey, U.S.A.: Prentice–Hall, Inc., 2002.

[24] A. Committee, "231: Digital mobile radio towards future generation systems – final report," European Communities, Tech. Rep., 1999.

[25] ITU–R, "Guidelines for evaluation of radio transmission technologies for IMT–2000," ITU–R, Tech. Rep. Recommendation ITU–R M.1225, 1997.

[26] C. E. Shannon, "The Mathematical Theory of Communication," *The Bell System Technical Journal*, vol. 27, pp. 379–423; 623–656, July, October, 1948.

[27] K. L. Blackard, T. S. Rappaport, and C. W. Bostian, "Measurements and models of radio frequency impulsive noise for indoor wireless communications," *IEEE Journal on Selected Areas in Communications*, vol. 11, no. 7, pp. 991–1001, Sep. 1993.

[28] R. S. Blum, R. J. Kozick, and B. M. Sadler, "An Adaptive Spatial Diversity Receiver for Non–Gaussian Interference and Noise," *IEEE Transactions on Signal Processing*, vol. 47, no. 8, pp. 2100–2111, Aug. 1999.

[29] T. K. Sarkar, Z. Ji, K. Kim, A. Medouri, and M. Salazar-Palma, "A survey of various propagation models for mobile communication," *IEEE Antennas and Propagation Magazine*, vol. 45, no. 3, pp. 51–82, Jun. 2003.

[30] W. R. Braun and U. Dersch, "A physical mobile radio channel model," *IEEE Transactions on Vehicular Technology*, vol. 40, no. 2, pp. 472–482, May 1991.

[31] H. Arslan, L. Krasny, D. Koilpillai, and S. Channakeshu, "Doppler spread estimation for wireless mobile radio systems," in *Proc. IEEE WCNC Conf.*, vol. 3, Chicago, IL, Sep. 2000, pp. 1075–1079.

[32] M. Sakamoto, J. Huoponen, and I. Niva, "Adaptive channel estimation with velocity estimator for W-CDMA receiver," in *Proc. IEEE Veh. Technol. Conf.*, vol. 3, Tokyo, Japan, May 2000, pp. 2024–2028.

[33] C. Tepedelenlioğlu and G. B. Giannakis, "On velocity estimation and correlation properties of narrow–band mobile communication channels," *IEEE Transactions on Vehicular Technology*, vol. 50, no. 4, pp. 1039–1052, Jul. 2001.

[34] D. Mottier and D. Castelain, "A doppler estimation for UMTS-FDD based on channel power statistics," in *Proc. IEEE Veh. Technol. Conf.*, vol. 5, Amsterdam, Netherland, Sep. 1999, pp. 3052–3056.

[35] L. Wang, M. Silventoinen, and Z. Honkasalo, "A new algorithm for estimating mobile speed at the TDMA-based cellular system," in *Proc. IEEE Veh. Technol. Conf.*, vol. 2, Atlanta, GA, May 1996, pp. 1145–1149.

[36] C. Xiao, K. Mann, and J. Olivier, "Mobile speed estimation for TDMA-based hierarchical cellular systems," in *Proc. IEEE Veh. Technol. Conf.*, vol. 2, Amsterdam, The Netherlands, Sep. 1999, pp. 2456–2460.

[37] W. C. Y. Lee, *Mobile Communications Engineering*. New York: McGraw-Hill Int., 1982.

[38] M. Austin and G. Stüber, "Eigen-based doppler estimation for differentially coherent CPM," *IEEE Trans. Veh. Technol.*, vol. 43, pp. 781–785, Mar. 1994.

[39] G. Pollini, "Trends in handover design," *IEEE Commun. Mag.*, vol. 34, no. 3, pp. 82–90, Mar. 1996.

[40] J. H. A. Sampath, "Estimation of maximum doppler frequency for handoff decisions," in *Proc. IEEE Veh. Technol. Conf.*, Secaucus, NJ, May 1993, pp. 859–862.

[41] L. Lindbom, "Adaptive equalization for fading mobile radio channels," Licentiate thesis, Technology Department, Uppasala University, Uppasala, Sweden, 1992.

[42] M. Morelli, U. Mengali, and G. Vitetta, "Further results in carrier frequency estimation for transmissions over flat fading channels," *IEEE Commun. Lett.*, vol. 2, pp. 327–330, Dec. 1998.

[43] L. Krasny, H. Arslan, D. Koilpillai, and S. Channakeshu, "Doppler spread estimation in mobile radio systems," in *Proc. IEEE WCNC Conf.*, vol. 5, no. 5, May 2001, pp. 197–199.

[44] K. Kawabata, T. Nakamura, and E. Fukuda, "Estimating velocity using diversity reception," in *Proc. IEEE Veh. Technol. Conf.*, vol. 1, Stockholm, Sweden, Jun. 1994, pp. 371–374.

[45] H. Arslan and T. Yücek, "Delay spread estimation for wireless communication systems," in *Proc. The Eighth IEEE symposium on computers and communications (ISCC'2003)*, Antalya, Türkiye, Jul. 2003, pp. 282–287.

[46] J.-T. Chen, J. Liang, H.-S. Tsai, and Y.-K. Chen, "Joint MLSE receiver with dynamic channel description," *IEEE J. Sel. Areas Commun.*, vol. 16, pp. 1604–1615, Dec. 1998.

[47] L. Husson, and J-C. Dany, "A new method for reducing the power consumption of portable handsets in TDMA mobile systems: Conditional equalization," *IEEE Trans. Veh. Technol.*, vol. 48, no. 6, pp. 1936–1945, Nov. 1999.

[48] H. Schober and F. Jondral, "Delay spread estimation for OFDM based mobile communication systems," in *Proc. European Wireless Conf.*, Florence, Italy, Feb. 2002, pp. 625–628.

[49] F. Sanzi and J. Speidel, "An adaptive two-dimensional channel estimator for wireless OFDM with application to mobile DVB-T," *IEEE Trans. Broadcast.*, vol. 46, no. 2, pp. 128–133, Jun. 2000.

[50] K. Witrisal, Y.-H. Kim, and R. Prasad, "A new method to measure parameters of frequency selective radio channel using power measurements," *IEEE Trans. Commun.*, vol. 49, pp. 1788–1800, Oct. 2001.

[51] ——, "RMS delay spread estimation technique using non-coherent channel measurements," *IEE Electron. Lett.*, vol. 34, no. 20, pp. 1918–1919, Oct. 1998.

[52] K. Witrisal and A. Bohdanowicz, "Influence of noise on a novel RMS delay spread estimation method," in *Proc. IEEE PIMRC Conf.*, vol. 1, London, U.K., Sep. 2000, pp. 560–566.

[53] H. Arslan and T. Yücek, "Estimation of frequency selectivity for OFDM based new generation wireless communication systems," in *Proc. 2003 World Wireless Congress*, San Francisco, CA, May 2003.

[54] A. Paulraj and B. Ng, "Space-time modems for wireless personal communications," *IEEE Personal Commun. Mag.*, vol. 5, no. 1, pp. 36–48, Feb. 1998.

[55] M. K. Özdemir, H. Arslan, and E. Arvas, "Mutual coupling effect in multi-antenna wireless communication systems," in *Proc. IEEE GlobeCom Conf.*, San Francisco, CA, Dec. 2003.

[56] ——, "A mutual coupling model for MIMO systems," in *Proc. IEEE TCWCT Conf.*, Honolulu, HI, Oct. 2003.

[57] D. S. Shiu, G. J. Foschini, M. J. Gans, and J. M. Kahn, "Fading correlation and its effects on the capacity of multielement antenna systems," *IEEE Trans. Commun.*, vol. 48, no. 3, pp. 502–513, Mar. 2000.

[58] M. T. Ivrlac, W. Utschick, and J. A. Nossek, "Fading correlations in wireless MIMO communication systems," *IEEE J. Sel. Areas Commun.*, vol. 21, no. 5, pp. 819–828, Jun. 2003.

[59] S. Catreux, V. Erceg, D. Gesbert, and J. Robert W. Heath, "Adaptive modulation and mimo coding for broadband wireless data networks," *IEEE Communications Magazine*, vol. 40, no. 6, pp. 108–115, Jun. 2002.

[60] E. Telatar, "Capacity of multiantenna Gaussian channels," AT&T Bell Laboratories, Tech. Rep., Jun. 1995.

[61] G. J. Foschini and M. J. Gans, "On limits of wireless communications in a fading environment when using multiple antennas," *Wireless Personal Commun.*, vol. 6, no. 3, pp. 311–335, Mar. 1998.

[62] S. Sampei, *Applications of Digital Wireless Technologies to Global Wireless Communications*. New Jersey, USA: Prentice Hall, 1997.

[63] S. Nanda, K. Balachandran, and S. Kumar, "Adaptation techniques in wireless packet data services," *IEEE Trans. Commun.*, vol. 38, no. 1, pp. 54–64, Jan. 2000.

[64] ANSI, "TIA/EIA 136-131-B," *TDMA Third generation wireless: Digital Traffic Channel Layer 1*, Mar. 2000.

[65] T. Ikeda, S. Sampei, and N. Morinaga, "TDMA-based adaptive modulation with dynamic channel assignment for high-capacity communication systems," *IEEE Trans. Commun.*, vol. 49, no. 2, pp. 404–412, Mar. 2000.

[66] R.V. Nobelen, N. Seshadri, J. Whitehead and S. Timiri, "An adaptive radio link protocol with enhanced data rates for GSM evolution," *IEEE Commun. Mag.*, pp. 54–63, Feb. 1999.

[67] A. Furuskar, S. Mazur, F. Muller, and H. Olofsson, "EDGE: enhanced data rates for GSM and TDMA/136 evolution," *IEEE Personal Commun. Mag.*, vol. 6, no. 3, pp. 56–66, Jun. 1999.

[68] K. Balachandran, S. Kabada, and S. Nanda, "Rate adaptation over mobile radio channels using channel quality information," in *Proc. IEEE Globecom'98 Commun. Theory Mini Conf. Record*, 1998, pp. 46–52.

[69] M. Türkboylari, and G.L. Stüber, "An efficient algorithm for estimating the signal-to-interference ratio in TDMA cellular systems," *IEEE Trans. Commun.*, vol. 46, no. 6, pp. 728–731, Jun. 1998.

[70] H. Arslan and G. E. Bottomley, "Channel estimation in narrowband wireless communication systems," *Wireless Commun. and Mobile Comput.*, vol. 1, no. 2, pp. 201–219, Apr. 2001.

[71] H. Arslan and G. Bottomley, "Channel estimation in narrowband wireless communication systems," *Wireless Communications and Mobile Computing (WCMC) Journal*, vol. 1, no. 2, pp. 201–219, Apr./Jun. 2001.

[72] K. Homayounfar, "Rate adaptive speech coding for universal multimedia access," *IEEE Signal Process. Mag.*, vol. 20, no. 2, pp. 30–39, Mar. 2003.

[73] S. Wolf, C. A. Dvorak, R. F. Kubichek, C. R. South, R. A. Schaphorst, and S. D. Voran, "How will we rate telecommunications system performance?" *IEEE Communications Magazine*, vol. 29, no. 10, pp. 23–29, Oct. 1991.

[74] S. Voran, "Objective estimation of perceived speech quality–part i: Development of the measuring normalizing block technique," *IEEE Transactions on Speech and Audio Processing*, vol. 7, no. 4, pp. 371–382, Jul. 1999.

[75] J. Mitola and G. M. Jr., "Cognitive radio: making software radios more personal," *IEEE Personal Communications*, vol. 6, no. 4, pp. 13–18, Aug. 1999.

[76] G. Edwards and R. Sankar, "Microcellular handoff using fuzzy techniques," *Wireless Networks*, vol. 4, pp. 401–409, Aug. 23, 1998.

[77] S. Farahvash and M. Kavehrad, "Co-channel Interference Assessment for Line–of–Sight and Nearly Line–of–Sight Millimeter–Waves Cellular LMDS Architecture," *International Journal of Wireless Information Networks*, vol. 7, no. 4, pp. 197–210, 2000.

[78] A. F. Almutairi, A. K. Ali, and M. H. Karaata, "Adaptive distribution–based handover scheme for cellular communication networks," *Wireless Communications and Mobile Computing*, vol. 5, pp. 209–217, Aug. 23, 2005.

[79] S. Al–Jazzar and J. Caffery Jr., "New algorithms for NLOS identification," in *Proc. The 14th IST Mobile and Wireless Communications Summit*, Dresden, Germany, Jun. 19–23, 2005.

[80] S. Venkatraman and J. C. Jr., "Statistical approach to non–line–of–sight BS identification," in *Proc. The 5th International Symposium on Wireless Personal Multimedia Communications*, vol. 1, Honolulu, Hawaii, U.S.A., Oct. 27–30, 2002, pp. 296–300.

[81] S. Sesia, I. Toufik, and M. Baker, *LTE, The UMTS Long Term Evolution: From Theory to Practice*. Wiley-Blackwell, 2009.

[82] H. Arslan and S. Yarkan, *Cognitive Radio, Software Defined Radio, and Adaptive Wireless Systems (Signals and Communication Technology)*. Springer, 2007, ch. Cross–Layer Adaptation and Optimization for Cognitive Radio.

[83] Y. Selen, H. Tullberg, and J. Kronander, "Sensor selection for cooperative spectrum sensing," in *in Proc. 3rd IEEE Symposium on New Frontiers in Dynamic Spectrum Access Networks (DySPAN) 2008*, Chicago, Illinois, U.S.A., Oct. 14–17, 2008, pp. 1–11.

[84] Y. Chen, K. H. Teo, S. Kishore, and J. Zhang, "A Game-Theoretic Framework for Interference Management through Cognitive Sensing," in *Proc. IEEE International Conference on Communications (ICC '08)*, Beijing, China, May 19–23, 2008, pp. 3573–3577.

[85] ——, "Inter–Cell Interference Management in WiMAX Downlinks by A Stackelberg Game between BSs," in *Proc. IEEE International Conference on Communications (ICC '08)*, Beijing, China, May 19–23, 2008, pp. 3442–3446.

[86] S. M. Mishra, A. Sahai, and R. W. Brodersen, "Cooperative sensing among cognitive radios," in *In Proc. of the IEEE International Conference on Communications (ICC)*, Istanbul, Türkiye, Jun. 11–15, 2006, pp. 1658–1663.

[87] H. Arslan and T. Yücek, *Cognitive Radio, Software Defined Radio, and Adaptive Wireless Systems (Signals and Communication Technology)*. Springer, 2007, ch. Spectrum Sensing for Cognitive Radio Applications.

[88] Federal Communications Commission, "Millimeter Wave Propagation: Spectrum Management Implications," Federal Communications Commission, Office of Engineering and Technology, New Technology Development Division, Washington, District of Columbia, U. S. A., Bulletin 70, Jul. 1997.

[89] A. Molisch, "Ultrawideband propagation channels–theory, measurement, and modeling," *IEEE Transactions on Vehicular Technology*, vol. 54, no. 5, pp. 1528–1545, Sep. 2005.

[90] J. Kunisch and J. Pamp, "Measurement results and modeling aspects for the UWB radio channel," in *Proc. IEEE Conference on Ultra Wideband Systems and Technologies Digest of Technical Papers*, 2002, pp. 19–23.

[91] A. Durantini, W. Ciccognani, and D. Cassioli, "UWB Propagation Measurements by PN–Sequence Channel Sounding," in *Proc. IEEE Conference on Communications*, vol. 6, Paris, France, Jun. 20–24, 2004, pp. 3414–3418.

[92] FCC. (1996, Jul. 26,) Revision of the commissions rules to ensure compatibility with enhanced 911 emergency calling systems, RM-8143, CC Docket 94–102. FCC. Washington, DC. [Online]. Available: http://hraunfoss.fcc.gov/edocs_public/attachmatch/DA-03-1902A1.pdf

[93] C. Botteron, A. Høst-Madsen, and M. Fattouche, "Effects of system and environment parameters on the performance of network–based mobile station position estimators," *IEEE Transactions on Vehicular Technology*, vol. 53, no. 1, pp. 163–180, Jan. 2004.

[94] M. P. Wylie and J. Holtzman, "The non–line of sight problem in mobile location estimation," in *Proc. 5th IEEE International Conference on Universal Personal Communications*, vol. 2, Cambridge, Massachusetts, U. S. A., Sep. 1996, pp. 827–831.

[95] S. Gezici, H. Kobayashi, and H. V. Poor, "Nonparametric nonline–of–sight identification," in *Proc. IEEE 58th Vehicular Technology Conference, VTC 2003–Fall*, vol. 4, Orlando, Florida, U.S.A., Oct. 6–9, 2003, pp. 2544–2548.

[96] Y.-C. Tseng, S.-L. Wu, W.-H. Liao, and C.-M. Chao, "Location awareness in ad–hoc wireless mobile networks," *Computer*, vol. 34, no. 6, pp. 46–52, Jun. 2001.

[97] J. M. III, "Cognitive INFOSEC," *IEEE MTT–S International Microwave Symposium Digest*, vol. 2, pp. 1051–1054, Jun. 8–13, 2003.

[98] H. Çelebi and H. Arslan, "Cognitive Positioning Systems," *IEEE Transactions on Wireless Communications*, vol. 6, no. 12, pp. 4475–4483, Dec. 2007.

[99] J. Vidal and R. E. Jativa, "First arriving path detection for subscriber location in mobile communication systems," in *Proceedings of IEEE International Conference on Acoustics, Speech, and Signal Processing ICASSP'02*, vol. 3, Orlando, Florida, U.S.A., May 13–17, 2002, pp. III–2733 – III–2736.

[100] J. Borras, P. Hatrack, and N. B. Mandayam, "Decision theoretic framework for NLOS identification," in *Proc. IEEE 48th Vehicular Technology Conference, VTC 1998*, vol. 2, Ottawa, Canada, May 18–21, 1998, pp. 1583–1587.

[101] M. Feder and N. Merhav, "Universal composite hypothesis testing: A competitive minimax approach," *IEEE Transactions on Information Theory*, vol. 48, no. 6, pp. 1504–1517, Jun. 2002.

[102] A. Lakhzouri, E. Simona, L. Ridha, and H. M. Renforse, "Extended Kalman filter channel estimation for line–of–sight detection in WCDMA mobile positioning," *EURASIP Journal on Applied Signal Processing*, no. 13, pp. 1268–1278, Dec. 2003.

[103] R. A. Iltis, "Joint estimation of PN code delay and multipath using the extended Kalman filter," *IEEE Transactions on Communications*, vol. 38, no. 10, pp. 1677–1685, Oct. 1990.

[104] R. A. Iltis and L. Mailaender, "An adaptive multiuser detector with joint amplitude and delay estimation," *IEEE Journal on Selected Areas in Communications*, vol. 12, pp. 774–785, Jun. 1994.

[105] K. J. Kim and R. A. Iltis, "Joint Detection and Channel Estimation Algorithms for QS–CDMA Signals Over Time–Varying Channels," *IEEE Journal on Selected Areas in Communications*, vol. 50, no. 5, pp. 845–855, May 2002.

[106] A. Lakhzouri, E. S. Lohan, R. Hamila, and M. Renfors, "Solving closely–spaced multipaths via extended Kalman filter in WCDMA downlink receivers," in *Proc. 5th European Personal Mobile Communications Conference*, Glasgow, United Kingdom, Apr. 22–25, 2003, pp. 271–275.

[107] A. Lakhzouri and E. S. L. M. Renfors, "Estimation of closely–spaced paths via particle filters for WCDMA positioning," in *Proc. First International Symposium on Control, Communications and Signal Processing*, Hammamet, Tunisia, Mar. 21–24, 2004, pp. 791–794.

[108] G. L. Turin, F. D. Clapp, T. L. Johnston, S. B. Fine, and D. Lavry, "A statistical model of urban multipath propagation," *IEEE Transactions on Vehicular Technology*, vol. VT–21, no. 1, pp. 1–9, Feb. 1972.

[109] H. Suzuki, "A statistical model for urban radio propagation," *IEEE Transactions on Communications*, vol. COM–25, no. 7, pp. 673–680, Jul. 1977.

[110] X. Zhao, J. Kivinen, P. Vainikainen, and K. Skog, "Characterization of Doppler Spectra for Mobile Communications at 5.3 GHz," *IEEE Transactions on Vehicular Technology*, vol. 52, no. 1, pp. 14–23, Jan. 2003.

[111] COST 207 Management Committee, "COST 207: Digital Land Mobile Radio Communications," Commission of the European Communities, Final Report, 1989.

[112] R. C. Qiu and I.-T. Lu, "Wideband wireless multipath channel modeling with path frequency dependence," in *in Proc. IEEE International Conference on Communications, Converging Technologies for Tomorrow's Applications, ICC '96*, vol. 1, IEEE. Dallas, Texas, U.S.A.: IEEE, Jun. 23–27, 1996, pp. 277–281.

[113] ——, "Multipath resolving with frequency dependence broadband wireless channel modeling," *IEEE Transactions on Vehicular Technology*, vol. 48, no. 1, pp. 273–285, Jan. 1995.

[114] C. W. Rhodes, "Reduction of NTSC co–channel interference by referencing carrier frequencies to the LORAN–C signal," *IEEE Transactions on Broadcasting*, vol. 41, no. 2, pp. 37–43, Jun. 1995.

[115] B. L. Cragin, "Prediction of Seasonal Trends in Cellular Dropped Call Probability," in *Proc. IEEE International Conference on Electro/Information Technology*, East Lansing, Michigan, U. S. A., May 7–10, 2006, pp. 613–618.

[116] A. R. S. Bahai and H. Aghvami, "Network planning and optimization in the third generation wireless networks," in *Proc. First International Conference on 3G Mobile Communication Technologies*, London, United Kingdom, Mar. 27–29, 2000, pp. 441–445.

[117] V. M. Jovanovic and J. Gazzola, "Capacity of present narrowband cellular systems: interference–limited or blocking–limited?" *IEEE Personal Communications [see also IEEE Wireless Communications]*, vol. 4, no. 6, pp. 42–51, Dec. 1997.

[118] M. Yang, D. Kaffes, D. Mavrakis, and S. Stavrou, "The Impact of Environment Variation on Co–channel Interference in WLAN," in *Proc. Twelfth International Conference on Antennas and Propagation (ICAP 2003)*, vol. 1. University of Exeter, United Kingdom: IEE, Mar. 31–Apr. 3, 2003, pp. 71–75.

[119] G. L. Stüber, *Principles of Mobile Communications.* Kluwer Academic Publishers, 1996, fourth Printing, ISBN: 0–7923–9732–0.

[120] G. K. Chan, "Effects of Sectorization on the Spectrum Efficiency of Cellular Radio Systems," *IEEE Transactions on Vehicular Technology*, vol. 41, no. 3, pp. 217–225, Aug. 1992.

[121] P. S. Rha, "Frequency reuse scheme with reduced co–channel interference for fixed cellular systems," *Electronics Letters*, vol. 34, no. 3, pp. 237–238, Feb. 5, 1998.

[122] T. Mayer, C. Robertson, and T. T. Ha, "Co–channel interference reduction on the forward channel of a wideband CDMA cellular system," in *Proc. IEEE Military Communications Conference (MILCOM '99)*, vol. 2, Atlantic City, New Jersey, U. S. A., Sep. 31– Oct. 3, 1999, pp. 785–790.

[123] T. Ohgane, "Spectral efficiency improvement by base station antenna pattern control for land mobile cellular systems," in *Proc. IEEE Global Telecommunications Conference including a Communications Theory Mini–Conference (GLOBECOM '93)*, vol. 2. Houston, Texas, U. S. A.: IEEE, Nov. 29– Dec. 2, 1993, pp. 913–917.

[124] M. C. Wells, "Super–Resolution Broad Null Beamforming for Co–channel Interference Cancellation in Mobile Radio Networks," *IEE Proceedings–Communications*, vol. 143, no. 5, pp. 304–310, Oct. 1996.

[125] P. D. Karaminas and A. Manikas, "Super–Resolution Broad Null Beamforming for Co–channel Interference Cancellation in Mobile Radio Networks," *IEEE Transactions on Vehicular Technology*, vol. 49, no. 3, pp. 689–697, May 2000.

[126] L. Matabishi, "Theoretical Implementation of Antenna Polarization to Improve the Reduction of Co–channel Interference in Mobile Cellular Systems," in *Proc. IEEE International Symposium on Microwave, Antenna, Propagation and EMC Technologies for Wireless Communications (MAPE 2005)*, vol. 1, Beijing, China, Aug. 8–12, 2005, pp. 431–433.

[127] R. Menon, A. B. MacKenzie, R. M. Buehrer, and J. H. Reed, "A Game–Theoretic Framework for Interference Avoidance in Ad hoc Networks," in *Proc. IEEE Global Telecommunications Conference (GLOBECOM '06)*, vol. 1, San Francisco, California, U. S. A., Nov. 27– Dec. 1, 2006, pp. 1–6.

[128] T. Weiss and F. K. Jondral, "Spectrum pooling: an innovative strategy for the enhancement of spectrum efficiency," *IEEE Communications Magazine*, vol. 42, no. 3, pp. S8–14, Mar. 2004.

[129] Y.-D. Yao and A. U. H. Sheikh, "Investigations into Co–channel Interference in Microcellular Mobile Radio Systems," *IEEE Transactions on Vehicular Technology*, vol. 41, no. 2, pp. 114–123, May 1992.

[130] B. C. Jones and D. J. Skellern, "An Integrated Propagation–Mobility Interference Model for Microcell Network Coverage Prediction," *Wireless Personal Communications*, vol. 5, pp. 223–258, 1997.

[131] Huaewi, "Further Analysis of Soft Frequency Reuse Scheme," 3GPP TSG RAN, London, U.K., Agenda Item 10.2.1 R1–050841, Aug. 29– Sep. 2, 2005, WG1#42, Discussion & Decision.

[132] Ericsson, "Additional RSRP reporting trigger for ICIC," 3GPP TSG RAN, Shenzhen, China., Agenda Item 6.3.3 R1–0801536, Mar. 31–Apr. 04, 2008, WG1#52bis, Discussion and decision.

[133] Ericsson, "Physical Layer Measurement Period of UE Measurements," 3GPP TSG RAN, Sophia Antipolis, France, Agenda Item 4.6 R4–070407, Apr. 2–4, 2007, WG4#42bis, Discussion.

[134] A. Ghasemi and E. S. Sousa, "Opportunistic spectrum access in fading channels through collaborative sensing," *Journal of Communications*, vol. 2, no. 2, p. 71, Mar. 2007.

[135] Y. Ma and J. Jin, "Effect of Channel Estimation Errors on M–QAM With MRC and EGC in Nakagami Fading Channels," *IEEE Transactions on Vehicular Technology*, vol. 56, no. 3, pp. 1239–1250, May 2007.

[136] S. A. Abbas and A. U. Sheikh, "A Geometric Theory of Nakagami Fading Multipath Mobile Radio Channel with Physical Interpretations," in *Proc. IEEE 46th Vehicular Technology Conference*, vol. 2, Atlanta, Georgia, U. S. A., Apr. 28– May 1, 1996, pp. 637–641.

[137] M. Pätzold, U. Killat, and F. Laue, "A Deterministic Digital Simulation Model for Suzuki Processes with Application to a Shadowed Rayleigh Land Mobile Radio Channel," *IEEE Transactions on Vehicular Technology*, vol. 45, no. 2, pp. 318–331, May 1996.

[138] X. Cai and G. B. Giannakis, "A Two–Dimensional Channel Simulation Model for Shadowing Processes," *IEEE Transactions on Vehicular Technology*, vol. 52, no. 6, pp. 1558–1567, Nov. 2003.

[139] M. Gudmundson, "Correlation Model for Shadow Fading in Mobile Radio Systems," *Electronics Letters*, vol. 27, no. 23, pp. 2145–2146, Nov. 7th, 1991.

[140] J.-W. Lee, J.-H. Kim, H.-J. Oh, and S.-H. Hwang, "Energy detector using adaptive–fixed thresholds in Cognitive Radio systems," in *Proc. 14th Asia–Pacific Conf. on Comm.*, Tokyo, Japan, Oct. 14–16, 2008, pp. 1–4.

[141] S. P. Herath, N. Rajatheva, and C. Tellambura, "Unified Approach for Energy Detection of Unknown Deterministic Signal in Cognitive Radio Over Fading Channels," in *Proc. IEEE Int. Conf. on Comm. Workshops*, Jun. 2009, pp. 1–5.

[142] I. Katzela and M. Naghshineh, "Channel assignment schemes for cellular mobile telecommunication systems: a comprehensive survey," *IEEE Personal Communications [see also IEEE Wireless Communications]*, vol. 3, no. 3, pp. 10–31, Jun. 1996.

[143] M. Sternad, T. Svenssony, T. Ottossony, A. Ahlen, A. Svenssony, and A. Brunstrom, "Towards Systems Beyond 3G Based on Adaptive OFDMA Transmission," in *Proc. of IEEE Special Issue on Adaptive Transmission*, vol. 95, no. 10, Oct. 2007, pp. 3472–3477, Invited Paper.

[144] G. Li and H. Liu, "Downlink dynamic resource allocation for multi–cell OFDMA system," in *Proceedings of 58th IEEE Vehicular Technology Conference, VTC 2003–Fall*, vol. 3, Oct. 6–9, 2003, pp. 1698–1702.

[145] P. Magnusson, J. Lundsjö, J. Sachs, and P. Wallentin, "Radio Resource Management Distribution in a Beyond 3G Multi–Radio Access Architecture," in *Proceedings of IEEE Global Telecommunications Conference, GLOBECOM '04*, vol. 6, Dallas, Texas, U.S.A., Nov. 29–Dec. 3, 2004, pp. 3472–3477.

[146] R. Bachl, P. Gunreben, S. Das, and S. Tatesh, "The Long Term Evolution Towards a New 3GPP Air Interface Standard," *Bell Labs Technical Journal*, vol. 11, no. 4, pp. 25–51, 2007.

[147] K. Hooli, J. Lara, S. Pfletschinger, M. Sternad, and S. Thilakawardana, "Radio Resource Management Architecture for Spectrum Sharing in B3G Systems," in *Proceedings of Wireless World Research Forum Meeting 15*, vol. 3, Paris, France, Dec. 8–9, 2005, pp. 1–6.

[148] M. C. Necker, "Towards frequency reuse 1 cellular FDM/TDM systems," in *Proceedings of the 9th ACM international symposium on Modeling analysis and simulation of wireless and mobile systems (MSWiM '06)*. Terromolinos, Spain: ACM Press, 2006, pp. 338–346.

[149] E. Oh, M. gyun Cho, S. Han, C. Woo, and D. Hong, "Performance Analysis of Dynamic Channel Allocation Based on Reuse Partitioning in Multi–Cell OFDMA Uplink Systems," *IEICE Trans Fundamentals*, vol. E89–A, no. 6, pp. 1566–1570, Jun. 2006.

[150] G. Fodor, M. Telek, and C. Koutsimanis, "Performance analysis of scheduling and interference coordination policies for OFDMA networks," *Computer Networks*, vol. 52, pp. 1252–1271, 2008.

[151] C. T. T. Chahed, "Modeling of streaming and elastic flow integration in OFDMA–based IEEE802.16 WiMAX," *Computer Networks*, vol. 30, pp. 3644–3651, 2007.

[152] D.-H. Kim, B.-H. Ryu, and C.-G. Kang, "Packet Scheduling Algorithm Considering a Minimum Bit Rate for Non-realtime Traffic in an OFDMA/FDD–Based Mobile Internet Access System," *ETRI journal*, vol. 26, no. 1, pp. 48–52, Feb. 2004.

[153] S.-E. Elayoubi, B. Fourestie, and X. Auffret, "On the capacity of OFDMA 802.16 systems," in *Proc. IEEE International Conference on Communications (ICC'06)*, vol. 4, Istanbul, Turkey, Jun. 11–15, 2006, pp. 1760–1765.

[154] X. Kai, T. Xiaofeng, W. Ying, and Z. Ping, "Inter–cell packet scheduling in ofdma wireless network," in *Proc. IEEE 65th Vehicular Technology Conference (VTC2007–Spring)*, Dublin, Ireland, Apr. 22–25, 2007, pp. 3115–3119.

[155] T. Kwon, H. Lee, S. Choi, J. Kim, D.-H. Cho, S. Cho, S. Yun, W.-H. Park, and K. Kim, "Design and implementation of a simulator based on a cross-layer protocol between MAC and PHY layers in a WiBro Compatible IEEE 802.16e OFDMA system," *IEEE Communications Magazine*, vol. 43, no. 12, pp. 136–146, Dec. 2005.

[156] A. Fernekeb, A. Klein, B. Wegmann, and K. Dietrich, "Influence of Traffic Models and Scheduling on the System Capacity of Packet–Switched Mobile Radio Networks," in *Proc. 15th IST Mobile and Communications Summit*, Mykonos, Greece, Jun. 2006, pp. 1–5.

[157] H. Lei, X. Zhang, and Y. Wang, "Real–Time Traffic Scheduling Algorithm for MIMO–OFDMA Systems," in *Proc. IEEE International Conference on Communications (ICC'08)*, Beijing, China, May 19–23, 2008, pp. 4511–4515.

[158] D. Jiang, H. Wang, E. Malkamaki, and E. Tuomaala, "Principle and Performance of Semi–Persistent Scheduling for VoIP in LTE System," in *Proc. Intl. Conf. on Wireless Comm., Networking & Mobile Comp.*, Shangai, China, Sep. 21–25, 2007, pp. 2861–2864.

[159] 3GPP, "LTE physical layer framework for performance verification," 3rd Generation Partnership Project (3GPP), St. Louis, Michigan, U. S. A., TSG RAN WG1 Meeting #48 R1–070674, Feb. 12–16, 2007, Decision.

# APPENDICES

## Appendix A

*Proof.* In the light of Definition 2, it is clear that maximum number of collisions can be $\min(\mathcal{F}_1, \mathcal{F}_2)$. The number of all possible resource assignment pairs is then equal to the number of elements in the Cartesian product of the sets of all available selections in each cell and given by:

$$K_S = \binom{\mathcal{F}}{\min(\mathcal{F}_1, \mathcal{F}_2)} \binom{\mathcal{F}}{\max(\mathcal{F}_1, \mathcal{F}_2)}.$$

Consider the cell whose $\mathcal{F}_c$ is the minimum. In this cell $C_c$, the number of all possible selections that yields exactly $k$ number of collisions is found as follows: The number of all possible selections within that cell for $\min(\mathcal{F}_1, \mathcal{F}_2)$ is:

$$K_1 = \binom{\mathcal{F}}{\min(\mathcal{F}_1, \mathcal{F}_2)}. \tag{A.1}$$

Among $K_1$ selections, the number of selections that yields exactly $k$ collisions is given by:

$$K_2 = \binom{\mathcal{F} - \min(\mathcal{F}_1, \mathcal{F}_2)}{\max(\mathcal{F}_1, \mathcal{F}_2) - k}. \tag{A.2}$$

This stems from the fact that, if $\min(\mathcal{F}_1, \mathcal{F}_2)$ of the resources are reserved among $\mathcal{F}$, then remaining number of resources in the neighboring cell that might cause collision is simply $\mathcal{F} - \min(\mathcal{F}_1, \mathcal{F}_2)$. Among $\mathcal{F} - \min(\mathcal{F}_1, \mathcal{F}_2)$ resources, if exactly $k$ resources are colliding, then $k$ resources can be considered as reserved (since they are colliding, they will be in the selections anyway). This implies that, remaining selections (number of resources) are reduced to $\max(\mathcal{F}_1, \mathcal{F}_2) - k$. Hence, the total number of selections among this set is expressed by $K_2$. The number of all possible different orderings for $k$ resources causing collisions among $\min(\mathcal{F}_1, \mathcal{F}_2)$ is

$$K_3 = \binom{\min(\mathcal{F}_1, \mathcal{F}_2)}{k}.$$

Since the probability space, namely $K_S$, is known and the number of all possible selections are defined, the desired probability mass function (PMF) can be obtained by:

$$p(k) = \frac{K_1 K_2 K_3}{K_S} \tag{A.3}$$

which is the equivalent of (7.2) and this completes the proof. □

## Appendix B

*Proof.* For the sake of brevity in notation, let $\min(\mathcal{F}_1, \mathcal{F}_2) = M_{\min}$ and $\max(\mathcal{F}_1, \mathcal{F}_2) = M_{\max}$. Stemming from the fact that $k$ can take values in the range of $[0, \min(\mathcal{F}_1, \mathcal{F}_2)]$ and probability mass function (PMF) in (7.2) is of discrete nature, statistical expectation is given by $E\{\mathbf{K}\} = \sum_{k=0}^{M_{\min}} k\, p(k)$. If $p(k)$ is replaced with its equivalent in (7.2) bearing $r\binom{n}{r} = n\binom{n-1}{r}$ in mind, then:

$$E\{\mathbf{K}\} = \frac{M_{\min}}{\binom{\mathcal{F}}{M_{\max}}} \sum_{k=1}^{M_{\min}} \binom{\mathcal{F} - M_{\min}}{M_{\max} - k} \binom{M_{\min} - 1}{k - 1}. \tag{B.1}$$

If all of the common terms in the summation are regrouped, then it reads:

$$\begin{aligned} E\{\mathbf{K}\} = & \frac{M_{\min}\,(\mathcal{F} - M_{\min})!}{\binom{\mathcal{F}}{M_{\max}}\,(M_{\max} - M_{\min})!\,(\mathcal{F} - M_{\max} - M_{\min} + 1)!} \times \\ & \cdot \sum_{k=1}^{M_{\min}} \frac{\binom{M_{\min}-1}{k-1}}{\prod_{j=k}^{M_{\min}-1} (M_{\max} - j) \prod_{q=2}^{k} (\mathcal{F} - M_{\max} - M_{\min} + q)} \end{aligned} \tag{B.2}$$

When the denominators in the summation are equalized with appropriate coefficients, (B.2) becomes:

$$\begin{aligned} E\{\mathbf{K}\} = & \frac{M_{\min}\,(\mathcal{F} - M_{\min})!}{\binom{\mathcal{F}}{M_{\max}}\,(M_{\max} - M_{\min})!\,(\mathcal{F} - M_{\max} - M_{\min} + 1)!} \times \\ & \cdot \frac{1}{\prod_{j=1}^{M_{\min}-1} (M_{\max} - j)\,(\mathcal{F} - M_{\max} - j + 1)} \sum_{k=1}^{M_{\min}} \binom{M_{\min} - 1}{k - 1} \times \\ & \cdot \underbrace{\prod_{j=2}^{k} (M_{\max} - j + 1)}_{\mathfrak{A}_1} \underbrace{\prod_{q=k}^{M_{\min}-1} (\mathcal{F} - M_{\max} - M_{\min} + q + 1)}_{\mathfrak{A}_2}. \end{aligned} \tag{B.3}$$

In (B.3), for a given $k$, consider sum of first and last terms of products $\mathfrak{A}_1$ and $\mathfrak{A}_2$, respectively (*i.e.,* $j = 2$ and $q = M_{\min} - 1$). If a change of variable is applied for this case with sum of these two terms

as $u = \mathcal{F} - 1$, after some mathematical manipulations (B.3) simplifies to:

$$E\{\mathbf{K}\} = \frac{M_{\min}\,(\mathcal{F} - M_{\min})!}{\binom{\mathcal{F}}{M_{\max}}\,(M_{\max} - M_{\min})!\,(\mathcal{F} - M_{\max} - M_{\min} + 1)!} \times \cdot \frac{\prod_{k=1}^{M_{\min}-1}(u - k + 1)}{\prod_{j=1}^{M_{\min}-1}(M_{\max} - j)\prod_{q=2}^{M_{\min}}(\mathcal{F} - M_{\max} - M_{\min} + q)} \tag{B.4}$$

Finally, one can expand all of the factorials and products and simplify (B.4) further to:

$$E\{\mathbf{K}\} = \frac{M_{\min}\,M_{\max}}{\mathcal{F}}, \tag{B.5}$$

which conforms with (7.3) in Corollary 7.3.1 and completes the proof. □

## Appendix C

*Proof.* If $\mathbf{K}$ denotes the number of collisions in (7.2), then, sample space is given by

$$S = \{0, 1, \ldots, \min(\mathcal{F}_1, \mathcal{F}_2)\}.$$

For an arbitrary $k \in S$ recall that

$$\Pr(\mathbf{K} \leq k) = \sum_{i=0}^{k} p(i),$$

which causes $\Pr(\mathbf{K} \leq k)$ to be strictly increasing.[1] Therefore, one is allowed to write $\Pr(\mathbf{K} \leq k+1) = \Pr(\mathbf{K} \leq k) + p(k+1)$ for all $k$ satisfying $k < \min(\mathcal{F}_1, \mathcal{F}_2)$. The unit measure axiom necessitates $\Pr(\mathbf{K} \leq \min(\mathcal{F}_1, \mathcal{F}_2)) = 1$. Note that Definition 3 stipulates $L \in [\Pr(\mathbf{K} = 0), 1)$ and $\Pr(\mathbf{K} \leq k)$ can be defined in terms of intervals such as $\Pr(\mathbf{K} \leq k) \in [p(0), 1)$ for $0 \leq k < \min(\mathcal{F}_1, \mathcal{F}_2)$. Along with the property of being strictly increasing, this causes the set $P$ actually to form a strict order for a given $S$ as $(P, <)$ where:

$$P = \{\Pr(\mathbf{K} \leq k) |\ 0 \leq k < \min(\mathcal{F}_1, \mathcal{F}_2)\}. \tag{C.1}$$

Therefore, for any given $L$ satisfying $L \in [\Pr(\mathbf{K} = 0), 1)$, there always exists a unique pair $(k, k+1)$ in $P$ corresponding to $k_\epsilon$ and this completes the proof. □

[1] Note that $\Pr(\mathbf{K} \leq k)$ is strictly increasing rather than only increasing due to non–zero probabilities for finite $\mathcal{F}$, as stated in Chapter 7.3. The only exception for this statement is a probability mass function (PMF) (or probability density function (PDF)) of $\delta(\cdot)$ form. This case will not be considered here due to the reasons explained in Footnote 7.

## ABOUT THE AUTHOR

Serhan YARKAN received both his B.S. and M.Sc. degrees in Computer Science from Istanbul University, Istanbul, Türkiye in 2001 and 2003, respectively. He joined the University of South Florida as a Ph.D. student at Electrical Engineering in August 2005. His research interests are cognitive radio, wireless propagation channel modeling, cross–layer adaptation and optimization, and interference management in next generation wireless networks.